6-5-2019 2:00 PM

Investigating the Role of ATRX in Glutamatergic Hippocampal Neurons

Renee Tamming
The University of Western Ontario

Supervisor
Berube, Nathalie G.
The University of Western Ontario

Graduate Program in Biochemistry
A thesis submitted in partial fulfillment of the requirements for the degree in Doctor of Philosophy

Abstract

Mutations in *ATRX*, a Snf2-type chromatin remodeler, frequently lead to intellectual disability. However, the function of ATRX within the brain in cognition and synaptic transmission are incompletely understood. The aim of this study was to investigate the role of ATRX in the adult mouse brain. While complete loss of ATRX in the embryonic mouse brain results in perinatal lethality, mosaic expression of ATRX stunted growth and perturbed circulating IGF-1 levels. Mosaic expression of ATRX also impaired adult cognition, specifically recognition memory and spatial learning and memory. However, there were confounding factors that led me to a new model in which I deleted the gene in postnatal mouse glutamatergic neurons. Magnetic resonance imaging of these mice revealed increased hippocampal CA1 and CA3 layers, and behaviour analysis indicated deficiencies in hippocampal-dependent learning and memory in the contextual fear task, Morris water maze, and paired-associate learning task. These behavioural abnormalities were not present in the female counterparts. Transmission electron microscopy of male hippocampal CA1 synapses revealed decreased number of total and docked vesicles and increased cleft width and post-synaptic density size. Hippocampal RNA-sequencing followed by sex-interaction analysis of male and female knockout transcripts highlighted potential impairments in the synaptic vesicle cycle. miR-137, a known regulator of presynaptic vesicle cycle and plasticity, was upregulated in the male knockout hippocampi but downregulated in the female knockouts. These results demonstrate sexually-dimorphic regulation of miR-137 and learning and memory by ATRX in forebrain glutamatergic neurons, indicating potential miRNA-targeting therapies for cognitive disorders by *ATRX* mutations.

Keywords

ATRX, hippocampus, glutamatergic neurons, learning, memory, synaptic plasticity

Summary for Lay Audience

The ATRX gene is required for the ATRX protein which modifies how the genetic material, DNA, is packaged and regulated in brain cells. When there is no ATRX present in the cell, there is deregulation of many different genes. Mutations during development that decrease the function of ATRX result in an intellectual disability disorder known as ATR-X syndrome. This syndrome is characterized by intellectual disability, developmental delay, abnormalities in facial structure, and small brain size. Therefore, ATRX is important in our nervous system and loss is directly related to many mental health disorders. My project focuses on the role of ATRX in learning and memory. I hypothesize that ATRX plays a very important role in the control of genes required for learning and memory by altering expression of genes involved in this process. In order to look at the effects that ATRX has on epigenetics in the adult brain, I generated two mouse models that deletes ATRX in the brain – one in the whole brain, and one in areas important for learning and memory. These mice underwent various behaviour tests to determine if they were able to learn and remember different tasks. I found that the mutant mice were unable to form two distinct types of memories: spatial memories and fear memories. I also found that loss of ATRX causes abnormal brain size in areas required for learning and memory. Additionally, ATRX may be required to regulate a particular microRNA, which in turn can regulate many different genes involved in proper neuron function. In summary, my work demonstrates a role for ATRX in learning and memory, thereby providing another link between chromatin remodeling proteins and cognition.

Co-Authorship Statement

I participated in the design of all experiments presented in this thesis, performed data analysis, and prepared all written material, with the following exceptions:

In chapter two, Yan Jiang performed the Western blot for ATRX. Serum isolation and hormone analysis by ELISA, as well as skeletal stain and long bone measurements were performed by Jennifer Siu. Mouse husbandry was also conducted by Yan Jiang.

In chapter three, Yan Jiang performed the Western blot for ATRX. Magnetic resonance imaging was performed and analyzed at Mice Imaging Centre (MICe) by Jacob Ellegood and Lily Qiu. Luana Langlois traced the Golgi-stained neurons. Paired associate learning and visual-paired discrimination touchscreen assays were performed at Robarts Research Institute Neurobehaviour Core by Matt Cowan. Analysis of RNA sequencing was performed by Dr. Vanessa Dumeaux.

Acknowledgments

First and foremost I would like to thank Dr. Nathalie Bérubé for her amazing guidance – and patience – over the years. Obviously, without her I would not be where I am today as a scientist. I would also like to thank my advisory committee members, Drs. Fred Dick and Jane Rylett, for continuously providing support and feedback on my project, as well as other researchers at the Victoria Research Labs who have offered advice on my dissertation – and life in general.

To the members of the Bérubé lab – past and present – I would like to thank you all for your support over the past 5 and a bit years. Megan: You were my first and closest friend in grad school and thank you for helping me keep my sanity via after-work beers. And adding in Miguel – the three amigos going for lunch tacos was always a highlight. To my friends outside of grad school, thank you for putting up with my craziness and letting me vent occasionally, even though I was a little bit of a hermit this past year.

To my family (aunts and uncles included!), I love you so much and you guys have never once doubted I could do this. Even if I had to repeatedly tell you to stop asking about my thesis.

And finally, to my husband Mike: You are amazing and your unwavering support has helped me keep focused and determined to finally finish this so we can continue on with the next chapter of our lives.

Table of Contents

Abstract ii

Summary for Lay Audience iii

Co-Authorship Statement iii

Acknowledgments v

List of Tables x

List of Figures xi

List of Appendices xiii

List of Abbreviations xiv

Chapter 1 1

1 Introduction 1

1.1 Intellectual disability 1

1.2 Genes and pathways linked to ID 2

1.3 Chromatin dysregulation in ID 3

1.4 The *ATRX* ID gene 7

1.4.1 Structural analysis of ATRX 8

1.4.2 ATRX has multiple binding partners 9

1.4.3 The role of ATRX in cell division 10

1.4.4 ATRX and DNA replication 10

1.4.5 Gene regulation by ATRX 11

1.4.6 The role of ATRX in development 13

1.4.7 ATRX and cancer 14

1.4.8 Neurological roles of ATRX 15

1.5 Types of memory 16

1.6 The hippocampus in learning and memory 17

1.6.1 What do we know from lesion studies? 17

1.6.2 The hippocampus 22

1.6.3 The electrophysiological pathways of the hippocampus 23

1.7 Synaptic Plasticity 24

1.7.1 The synapse 27

1.7.2 Pre-synaptic structure and function 27

1.7.3 Post-synaptic structure and function 29

1.8 Thesis Overview 32

1.9 References 33

Chapter 2 61

2 Mosaic expression of *Atrx* in the mouse central nervous system causes memory deficits 61

2.1 Introduction 61

2.2 Materials and Methods 62

2.2.1 Animal care and husbandry 62

2.2.2 Immunofluorescence staining 63

2.2.3 Microscopy 64

2.2.4 Haematoxylin and eosin staining 64

2.2.5 RT-qPCR 64

2.2.6 ELISAs 64

2.2.7 Bone staining and measurements 65

2.2.8 Behaviour analysis 65

2.2.9 Statistical analyses 68

2.3 Results 68

2.3.1 Survival to adulthood depends on the extent of *Atrx* deletion in the CNS 68

2.3.2 Mosaic inactivation of *Atrx* in the CNS impedes normal body growth 69

2.3.3 Hindlimb-clasping phenotype in *Atrx*-cHet mice 71

2.3.4 *Atrx*-cHet mice have normal working memory but deficits in object recognition memory ... 71

2.3.5 *Atrx*-cHet mice display deficits in contextual fear and spatial memory ... 73

2.3.6 *Atrx*-cHet mice have normal motor endurance and motor memory ... 75

2.4 Discussion ... 75

2.5 References ... 81

Chapter 3 ... 86

3 *Atrx* deletion in neurons leads to sexually-dimorphic dysregulation of miR-137 and spatial learning and memory deficits ... 86

3.1 Introduction ... 86

3.2 Methods ... 88

3.2.1 Animal care and husbandry ... 88

3.2.2 Cortical cultures ... 89

3.2.3 Immunofluorescence staining ... 89

3.2.4 Reverse transcriptase real-time PCR (qRT-PCR) ... 90

3.2.5 Western blot analysis ... 91

3.2.6 Magnetic resonance imaging ... 91

3.2.7 MRI Registration and Analysis ... 92

3.2.8 Golgi staining and analysis ... 92

3.2.9 Open field test ... 93

3.2.10 Elevated plus maze ... 93

3.2.11 Y maze ... 93

3.2.12 Novel object recognition ... 94

3.2.13 Morris water maze ... 94

3.2.14 Contextual fear conditioning ... 94

3.2.15 Touchscreen assays ... 95

3.2.16 RNA sequencing and analysis ... 96

3.2.17 Transmission electron microscopy 97

3.2.18 Statistical analyses 98

3.1 Results 99

3.1.1 Generation and validation of mice with neuron-specific Atrx deletion.... 99

3.1.2 MRI analysis reveals anatomical abnormalities in the hippocampus of Atrx-cKO mice 99

3.1.3 Pre- and post-synaptic structural defects in Atrx-cKO male mice 102

3.1.4 Loss of ATRX in neurons leads to long-term spatial learning and memory deficits 106

3.1.5 Neuron-specific deletion of *Atrx* in female mice does not cause memory deficits 108

3.1.6 Impaired object location associative memory in the rodent version of the paired associate learning (dPAL) task. 110

3.1.7 RNA sequencing of the hippocampus reveals sex-specific transcriptional changes 112

3.2 Discussion 116

3.3 References 124

Chapter 4 135

4 General Discussion and Future Directions 135

4.1 Thesis Summary 135

4.2 The role of ATRX in cognition 136

4.3 Synaptic plasticity and ATRX 140

4.4 ATRX in gene regulation 142

4.5 ATRX and miR-137 144

4.6 Proposed model of ATRX function in the hippocampus 146

4.7 Concluding remarks 148

Appendices 156

List of Tables

Table 1-1 Paradigms used to test for cognitive impairment in mice..... 18

Table 4-1 Behaviour impairments in *Atrx*-cHet and *Atrx*-cKO mice..... 138

List of Figures

Figure 1-1 The anatomy of the hippocampus and the CA1 pyramidal neuron. 20

Figure 1-2 The structure of an excitatory synapse. 26

Figure 2-1 Mosaic pattern of ATRX expression in the brain of *Atrx*-cHet mice. 70

Figure 2-2 *Atrx*-cHet mice have reduced body weight and low circulating IGF-1. 72

Figure 2-3 *Atrx*-cHet mice exhibit hindlimb clasping but normal activity and anxiety levels. 74

Figure 2-4 Impaired novel object recognition and contextual fear memory in *Atrx*-cHet mice. 76

Figure 2-5 *Atrx*-cHet mice perform poorly in the Morris water-maze paradigm. 78

Figure 2-6 Normal motor memory and endurance but decreased grip strength in *Atrx*-cHet mice. 80

Figure 3-1 Validation of Atrx inactivation in pyramidal neurons of the forebrain. 100

Figure 3-2 MRI reveals altered morphology of Atrx-cKO hippocampi. 101

Figure 3-3 CA1 dendritic length and branching and the number of non-neuronal cells are not affected in Atrx-cKO mouse hippocampi. 103

Figure 3-4 Ultrastructural analysis of Atrx-cKO CA1 apical synapses reveals a reduced number of total or docked presynaptic vesicles, wider synaptic cleft and larger post-synaptic density. 105

Figure 3-5 The Atrx-cKO males displayed decreased anxiety in the open field test and elevated plus maze. 107

Figure 3-6 The *Atrx*-cKO mice exhibit impaired long-term spatial memory in the Morris water maze paradigm and in the contextual fear conditioning task. 109

Figure 3-7 Expression of Atrx in Atrx-cKO females..... 111

Figure 3-8 Atrx-cKO females have no change in anxiety. 113

Figure 3-9 No change in spatial learning or memory in Atrx-cKO females in the Morris water maze or contextual fear conditioning tasks..... 115

Figure 3-10 Atrx-cKO mice display deficits in spatial learning in the Paired-Associate Learning operant task..... 117

Figure 3-11 Transcriptional profiling reveals dysregulation of presynaptic vesicular genes possibly resulting from miR-137 overexpression. 119

Figure 3-12 Transcriptional profiling reveals dysregulation of presynaptic genes in Atrx-FoxG1 mice..... 123

Figure 4-1 Proposed model of ATRX function in the hippocampus 147

List of Appendices

Appendix A ATRX loss does not affect expression of major immediate early genes. 156

Appendix B Permission to reproduce previously published work..... 157

List of Abbreviations

ADD	ATRX-DNMT3A/B-DNMT3L
ADHD	attention deficit hyperactive disorder
ALT	alternative lengthening of telomeres
AMPA	α-amino-3-hydroxy-5-methyl-4-isoxazolepropionic acid
ASD	autism spectrum disorder
ATP	adenosine triphosphate
ATRX	alpha thalassemia mental retardation, X-linked
BAF	BRG1- or HBRM-associated factors
CA	cornu ammonis
Cadps2	calcium dependent secretion activator 2
CBP	CREB-binding protein
cDNA	complementary DNA
CpG	cysteine-guanine dinucleotides
CREB	cAMP response element binding protein
CT	computed tomography
CTCF	CCCTC-binding factor
DAXX	death-domain associated protein
DLG2	discs large homolog 2
DNA	deoxyribonucleic acid
DNMT	DNA methyltransferase
dsDNA	double-stranded DNA
E	embryonic day
EZH2	enhancer of zeste homolog 2
FACS	fluorescence-activated cell sorting
Glrb	glycine receptor beta
GluR1	glutamate receptor 1
H3K4Me0	unmethylated histone 3 lysine 4
H3K4me3	histone 3 lysine 4 trimethylation
H3K9me3	histone 3 lysine 9 trimethylation
HA	hemagglutinin
HAT	histone acetyl transferase

HBA	hemoglobin subunit alpha
HDAC	histone deactelyase
HMT	histone methyltransferase
HP1α	heterochromatin protein 1α
ICF	immunodeficiency, Centromere instability and Facial anomalies
ICR	imprinting control region
ID	intellectual disability
IEG	immediate early gene
JNK	c-Jun N-terminal kinase
kDa	kilodaltons
LTP	long-term potentiation
MAPK	mitogen-activated protein kinase
MECP2	methyl CpG binding protein 2
mPFC	medial prefrontal cortex
MRI	magnetic resonance imaging
mRNA	messenger ribonucleic acid
NSD1	nuclear receptor binding SET domain protein 1
PanNET	pancreatic neuroendocrine
PCH	pericentromeric heterochromatin
PI3K	phosphoinositide 3-kinase
PML-NB	promyelocytic nuclear body
PPF	paired-pulse facilitation
PTP	post-tetanus potentiation
Sgip1	SH3-containing GRB2-like protein 3-interacting protein 1
Shank2	SH3 And Multiple Ankyrin Repeat Domains 2
SWI/SNF	switching defective / sucrose non-fermenter
TET	ten-eleven translocation methylcytosine dioxygenase
XCI	X chromosome inactivation
XH2	X-linked helicase 2
αCaMKII	α-Ca^{2+}/calmodulin-dependent protein kinase II

Chapter 1

1 Introduction

1.1 Intellectual disability

Disorders of intellectual development vary from mild to profound and are classified by the World Health Organization International Classification of Disease, Version 11 (ID:6A00) by below average intellectual capabilities and adaptive functioning, at least two standard deviations below the mean. The most recent estimate of intellectual disability (ID) prevalence in Canada ranges from 1-3% (Ouellette-Kuntz et al., 2005). Patients with ID will require lifelong treatments and services and so the economic costs of ID are quite high with over 36% of ID patients in Canada incurring health-care related costs of $2610 or more per year which includes physician services, medications, continuing care, and hospitalizations (Lunsky, De Oliveira, Wilton, & Wodchis, 2019).

ID disorders can further be classified as syndromic if accompanied by other symptoms (e.g. Down Syndrome, Fragile-X Syndrome), or non-syndromic if other symptoms are absent. ID can be caused by environmental, genetic, or a combination of environmental and genetic factors. Environmental factors include exposure to drugs in utero (e.g. Fetal alcohol spectrum disorder) or postnatal exposure to lead (Lidsky & Schneider, 2003; West, Chen, & Pantazis, 1994). There are a number of single-gene disorders that result in ID, such as Fragile-X or Cornelia de Lange syndrome (Krantz et al., 2004; McConkie-Rosell et al., 1993), but genetic factors leading to ID can also include chromosomal abnormalities, such as trisomy 21 leading to Down syndrome or the presence of an extra X chromosome (XXY) resulting in Klinefelter's (Antonarakis, Lyle, Dermitzakis, Reymond, & Deutsch, 2004; Lanfranco, Kamischke, Zitzmann, & Nieschlag, 2004). In 2011, approximately 500 genes had been identified that contribute to intellectual disability, but by 2016 that number had grown to over 700 due to the advent of next-generation sequencing techniques, indicating a high prevalence of genetic contribution to intellectual disability (reviewed in van Bokhoven (2011), Vissers, Gilissen, and Veltman (2016)).

1.2 Genes and pathways linked to ID

The proteins coded by ID genes are thought to be linked by different pathways, with either shared functions, binding partners, or other complex interactions. Indeed, multiple pathways linked to cognition have started to emerge. One such pathway is the RAS-MAPK cell signaling pathway, where extracellular stimuli activate receptor tyrosine kinases, triggering downstream targets including Ras-guanine exchange factors that convert Ras-GDP to Ras-GTP to signal to the Mitogen-activated protein kinase (MAPK), Phosphoinositide 3-kinase (PI3K), and c-Jun N-terminal kinase (JNK) pathways (reviewed in Borrie, Brems, Legius, and Bagni (2017)). Mutations in many Ras-MAPK pathway genes result in ID disorders with overlapping symptoms, termed Rasopothies. These diseases include Neurofibromatosis Type 1, caused by mutations in a Ras-GAP, which normally acts to negatively regulate Ras (Wallace et al., 1990) as well as Legius syndrome by mutations in *SPRED1,* a negative regulator of Ras-activated BRAF and CRAF (Brems et al., 2007). Patients of Neurofibromatosis Type 1 have motor abnormalities, cognitive and executive function impairments, and an increased risk for autism-spectrum disorder (ASD) (Debrabant et al., 2014; Lehtonen, Howie, Trump, & Huson, 2013; Morris et al., 2016). Legius syndrome is typically milder compared to Neurofibromatosis, but still causes learning impairments, attention problems, and ADHD (Brems et al., 2012).

Another pathway often implicated in ID is the Rho-GTPase pathway. Rho-GTPases are signaling proteins necessary for cytoskeleton remodeling, a process critical for axonal outgrowth, dendritic branching, and synapse formation and maturation (Elston & Fujita, 2014; Kalil & Dent, 2014; McAllister, 2007). Rho-GTPases switch between their active form (bound to GTP) and inactive form (bound to GDP) by other regulatory proteins. Rho-GEFs catalyze the reaction between GDP to GTP, activating Rho-GTPases, whereas Rho-GAPs stimulate the hydrolysis of GTP to GDP, thus inactivating Rho-GTPases (Cook, Rossman, & Der, 2014; Moon, Zang, & Zheng, 2003). Many mutations within this pathway have been identified in ID disorders. For example, mutations in *OPHN1*, which codes for a Rho-GAP protein, are linked to mild X-linked ID, cerebellar hypoplasia, and lateral ventricle enlargement in humans and in animal models (Philip et al., 2003) (Billuart et al.,

1998; Khelfaoui et al., 2007). Furthermore, deletion of *Ophn1* in mice results in spine immaturity and impaired short-term plasticity (Khelfaoui et al., 2007). Mutations in *RAC1*, which codes for a small GTPase, have also been implicated in varying degrees of developmental delay and brain malformations (Reijnders et al., 2017). In animal models, Rac1 has been shown to be necessary for spine development and long-term synaptic plasticity (Bongmba, Martinez, Elhardt, Butler, & Tejada-Simon, 2011), reinforcing the notion that Rho-GTPases and their regulators are critical for proper cognitive function.

Mutations in epigenetic proteins have also been linked to ID, including writers, erasers, and readers of the histone code, DNA methyltransferases, and chromatin remodeling proteins. A 2016 study reported that of 650 genes related to ID, 68 were linked to the "chromatin" Gene Ontology category, a >2-fold enrichment against genome-wide background (Kochinke et al., 2016). This suggests that proper regulation of chromatin is vital to cognitive processes.

1.3 Chromatin dysregulation in ID

Chromatin is made up of DNA wrapped tightly around protein octamers called histones, allowing for compaction of genetic material within the cell. Epigenetic changes to either the DNA or histones can affect basic cellular processes such as replication, transcription, and repair. The most common type of epigenetic change to DNA is methylation, which is generally associated with transcriptional silencing at CpG islands (Kass, Pruss, & Wolffe, 1997) and is controlled by DNA methyltransferases and demethylation enzymes. However, this modification has also been shown at non-CpG islands to control expression of tissue- and cell-type specific genes (Lister et al., 2013). Histone modifications are more diverse, and include acetylation, methylation, ubiquitination, phosphorylation, and many others. These modifications can act to facilitate or repress transcription, depending on the type and combination. For instance, acetylation almost always results in activation of transcription, as it results in a net negative charge on the histone, repelling the negatively charged DNA and opening the chromatin to allow binding of transcriptional machinery (Lee, Hayes, Pruss, & Wolffe, 1993). Methylation of the histone tails can either be repressive or

activating, depending on the residue modified and the extent of methylation (mono-, di-, or tri-). Trimethylation of lysine 4 on histone 3 (H3K4me3) results in activation of transcription, whereas trimethylation of lysine 27 on histone 3 (H3K27me3) is an indicator of repressive chromatin, deposited by Enhancer of zeste homolog 2 (EZH2) and usually found in heterochromatic regions (Barski et al., 2007; Plath et al., 2003). Histones can also be replaced with variants of different properties – for instance, histone 3 has seven variants (H3.1, H3.2, H3.3, H3.4, H3.5, H3.X, and H3.Y). For all these DNA and histone epigenetic modifications, there are proteins that act as writers, erasers, and readers, many of which are vital for normal cognitive function.

Epigenetic "writers" are proteins that add DNA methylation or histone marks, including methylation, acetylation, phosphorylation, and ubiquitination. DNA methylation is carried out by DNA methytransferases (DNMTs), of which there are 3: DNMT1, DNMT3A, and DNMT3B. DNMT1 and DNMT3B are both highly expressed in the central nervous system (Feng, Chang, Li, & Fan, 2005), and *DNMT3B* mutations lead to Immunodeficiency, Centromere instability and Facial anomalies (ICF) syndrome, symptoms of which can include ID (Weemaes et al., 2013; Xu et al., 1999). Mutations in histone methyltransferases (HMTs) and histone acetyltransferases (HATs) can also lead to ID. Rubinstein-Taybi syndrome arises from mutations in HATs *CBP* or *EP300*, and is characterized by moderate to severe ID and craniofacial and skeletal abnormalities (Roelfsema et al., 2005). Mutations in *NSD1* and *EZH2*, both HMTs, lead to Sotos syndrome and Weaver syndrome respectively (Gibson et al., 2012; Kurotaki et al., 2002). These syndromes have a lot of symptomatic overlap, including intellectual disability and skeletal overgrowth. Interestingly, mouse models for syndromes arising from these "writer" proteins all result in impairments in spatial learning and memory, particularly in the Morris water maze and contextual fear tasks (Feng et al., 2010; Wood et al., 2005; Zhang et al., 2014). Furthermore, mouse models of ICF syndrome and Rubinstein-Taybi have impaired long-term potentiation in the hippocampus (Feng et al., 2010; Wood et al., 2005), indicating overlap between clinical features and molecular mechanisms of the syndromes.

“Erasers” remove the marks that the “writers” deposit, through DNA demethylation, or removal of histone modifications through processes including deacetylation and demethylation. The major class of DNA demethylases are the ten-eleven translocation methylcytosine dioxygenase (TET) family, and while no members have been identified in human intellectual disability disorders, mouse models have implicated *TET1* in learning and memory. *Tet1* expression is induced through neuronal activation and activates memory-related genes (Kaas et al., 2013), and deletion of *Tet1* resulted in impaired memory extinction and enhanced long-term depression in the hippocampus (Rudenko et al., 2013). Histone deacetylases (HDACs) can also be mutated in ID. A variant of the histone deacetylase gene *HDAC8* has been identified in a family presenting with intellectual disability, hypogonadism, short stature, and craniofacial abnormalities (Harakalova et al., 2012). Additionally, HDACs are often differentially regulated in other cognitive disorders, such as autism spectrum disorders and Huntington’s (Bardai et al., 2013; Pinto et al., 2014). Finally, mutations in histone demethylases are tightly linked to ID disorders. *KDM6A* mutations lead to Kabuki syndrome, *KDM1A* mutations result in KBG syndrome, and Claes-Jensen syndrome arises from mutations in *KDM5C*. Patients of these three syndromes all display intellectual disability and have craniofacial abnormalities, again demonstrating overlap between many of these disorders.

Proteins that act as readers of the histone code function by recognizing specific histone modifications and either interacting with other proteins to form transcriptionally activating or repressing complexes, or by modulating the chromatin by changing its structure by nucleosome remodeling (removing or replacing histone variants or displacing histones on chromatin). Methyl-CpG-binding protein 2 (MECP2) recognizes and binds methylated DNA, where it interacts with other proteins to either activate or repress expression of genes, as well as alter global chromatin organization (Agarwal et al., 2011; Chahrour et al., 2008). Mutations in *MECP2* result in Rett syndrome, an autism spectrum disorder of developmental regression accompanied by microcephaly, hypotonia, and craniofacial and skeletal abnormalities (Amir et al., 1999; Neul et al., 2010; Percy et al., 2010), and duplication of the *MECP2* gene in males causes severe ID (Van Esch et al., 2005),

indicating the importance of gene dosage to proper cognitive function. Nucleosome remodeling proteins have intrinsic ATPase activity in order to remove or replace histone variants. There are multiple subfamilies of chromatin remodeling proteins, including the switching defective / sucrose non-fermenter (SWI/SNF) family (known as the BRG1- or HBRM-associated factors (BAF) complex family in humans). Several members of this family have been implicated in ID, including *ARID1A*, *ARID1B*, *SMARCB1*, *SMARCA4* in Coffin-Siris syndrome, *SMARCA2* in Nicolaides-Baraitser syndrome, and *ARID2* in non-syndromic ID (Miyake, Tsurusaki, & Matsumoto, 2014; Santen et al., 2012; Shang et al., 2015). Another member of the SWI/SNF family is the alpha-thalassemia X-linked intellectual disability protein (ATRX), which has been linked to the eponymous ATR-X ID syndrome, non-syndromic ID.

A subset of DNA-binding proteins can alter the higher-order architecture of chromatin and loss-of-function of these proteins can lead to ID. Regulators of chromatin higher order chromatin architecture, such as CCCTC-binding factor (CTCF) and cohesin-complex genes, are involved in chromatin looping to bring distal transcriptional start sites and enhancers or repressors into proximity to control gene expression (Zuin et al., 2014). Exome sequencing of individuals with non-syndromic intellectual disability, microcephaly, and growth retardation revealed *de novo* mutations in *CTCF* (Bastaki et al., 2017; Gregor et al., 2013). Mice lacking CTCF in forebrain excitatory neurons exhibit impaired learning in the Morris water maze and decreased hippocampal long-term potentiation (Sams et al., 2016). Cornelia de Lange syndrome, characterized by intellectual disability and craniofacial abnormalities such as long eyebrows and short nose, arises from mutations affecting the cohesin complex, mainly *NIPBL*, *SMC1A*, and *SMC3* (Deardorff et al., 2007; Krantz et al., 2004). Deletion of *Smc3* in mouse neurons led to impaired dendritic pruning, an increase in immature cortical synapses, and anxiety-like behaviours (Fujita et al., 2017), demonstrating that maintenance of genomic architecture is critical for cognitive function.

1.4 The *ATRX* ID gene

An association between alpha-thalassemia and intellectual disability was first described in 1988 in three patients (Weatherall et al., 1981) with several more individuals reported eight years later (Higgs et al., 1989). These patients had severe intellectual disability, facial dysmorphism, genital abnormalities, and hemoglobin H inclusions stemming from reduced expression of the of the α-globin gene. A study published in 1991 examined cytogenetics of 13 patients with both alpha-thalassemia and intellectual disability and found that 8 patients had a deletion of the 16p13.3 band on chromosome 16, which corresponds to the alpha-globin cluster (Wilkie et al., 1991). However, five of these individuals without this deletion still displayed low levels of *HBA1* and *HBA2* mRNA, indicating that this phenotype resulted from a missing regulatory factor. Due to the absence of male-to-male inheritance of the non-deletion form of these ID cases, it was named alpha-thalassemia mental retardation, X-linked syndrome – now, alpha-thalassemia X-linked intellectual disability syndrome (OMIM #301040) (Wilkie et al., 1991).

ATR-X syndrome is characterized by moderate to profound intellectual disability in 95% of cases, delay of developmental milestones, facial anomalies (including a flat nasal bridge, upturned nose, and a tented upper lip), genital abnormalities in 80% of affected children, a wide range of skeletal abnormalities (including clinodactyly, brachydactyly and kyphosis), and seizures in a subset of patients (35%) (Gibbons & Higgs, 2000). Magnetic resonance imaging (MRI) / Computed tomography (CT) scanning revealed gross morphological abnormalities in ATR-X syndrome patients, including brain atrophy, white matter abnormalities, and delayed myelination (Wada et al., 2013). Carrier females are generally unaffected due to extremely skewed inactivation of the affected X chromosome (greater than 90:10) (Gibbons, Suthers, Wilkie, Buckle, & Higgs, 1992), however in rare cases there is non-skewed X-inactivation and presence of moderate intellectual disability (Wada, Sugie, Fukushima, & Saitoh, 2005). The exact cause of the skewed X-inactivation is unclear; however, there is evidence that ATRX is involved in X-chromosome inactivation (XCI). In mice with early embryonic *Atrx* deletion, skewed XCI appears after the earliest stages of embryogenesis, and ATRX only localizes to the inactive X-chromosome after

XCI has occurred (Baumann & De La Fuente, 2009; Muers et al., 2007), hinting that perhaps ATRX is not required for the initiation of XCI, but may be involved in its maintenance.

There are several other syndromes that arise from mutations in the *ATRX* gene, including Chudley-Lowry, Juberg-Marsidi, Carpenter-Waziri, Holmes-Gang, and Smith-Fineman-Myers syndromes, which now fall under the term "X-linked mental retardation-hypotonic facies syndrome" (OMIM#309580) (Abidi et al., 2005; Villard & Fontes, 2002); these syndromes lack the haematological symptoms of ATR-X syndrome. Additionally, ATRX has been implicated in non-syndromic ID, where patients display ID without any additional symptoms (Renieri et al., 2005). Next-generation sequencing of 986 patients with non-syndromic ID identified variants in ATRX as one of the most common causes, alongside its interacting partner methyl-CpG binding protein 2 (MeCP2) (Morgan et al., 2015). This reinforces the idea that ATRX is extremely important for normal cognitive function.

1.4.1 Structural analysis of ATRX

Linkage analysis originally mapped the mutations in ATR-X syndrome to Xq12-q21.31 (Gibbons et al., 1992). Gibbons, Picketts, Villard, and Higgs (1995) further resolved the location to Xq13.3 and discovered a variety of mutations underlying ATR-X syndrome in the *XH2* gene in patients, later renamed *ATRX*. Characterization of the full-length cDNA indicated that *ATRX* consists of 36 exons spanning 306 kb with two splice variants of 270 kDa and 265 kDa and shows sequence homology to the SWItching defective/Sucrose NonFermenter (SWI/SNF) subgroup of DNA-dependent ATPases (Picketts et al., 1996). These complexes regulate gene expression through nucleosome remodeling capabilities (N. Liu, Balliano, & Hayes, 2011; L. Tang, Nogales, & Ciferri, 2010). Similarly, it was reported that ATRX was able to disrupt DNA-histone interactions in an ATP-dependent manner and translocate along double stranded DNA (Y. Xue et al., 2003). ATRX also exhibits an ability to assemble and mobilize nucleosomes (Lewis, Elsaesser, Noh, Stadler, & Allis, 2010), further reinforcing the role of ATRX as a chromatin remodeling protein through its SWI/SNF domain.

Another important domain within the ATRX protein is the ADD domain, named after its sequence homology with DNMT3A/B and DNMT3L (Aapola et al., 2000). This domain confers ATRX with its ability to localize to chromatin. The ADD domain was shown to mediate binding to naked dsDNA (Cardoso et al., 2000) and heterochromatin by recognition of the specific histone marks H3K9Me3/H3K4Me0 (Dhayalan et al., 2011; Eustermann et al., 2011; Iwase et al., 2011). The majority of *ATRX* patient mutations occur within the ADD (50%) and SWI/SNF (30%) domains (Gibbons et al., 2008), indicating the importance of these conserved domains.

1.4.2 ATRX has multiple binding partners

Interactors of ATRX include heterochromatin protein 1 α (HP1 α), methyl CpG binding protein 2 (MeCP2), cohesin complex (specifically SMC1 and SMC3), death-domain associated protein (DAXX) with the histone variant H3.3. HP1α is found in areas of dense heterochromatin, such as the centromeres and telomeres, but can also be found at euchromatin regions where its binding is associated with gene repression (Eissenberg & Elgin, 2000). ATRX can directly bind HP1α through its PxVxL binding motif , which aids its tethering to pericentromeric heterochromatin (PCH) and aids in repression of these regions (Eustermann et al., 2011; Kourmouli, Sun, van der Sar, Singh, & Brown, 2005; Lechner, Schultz, Negorev, Maul, & Rauscher, 2005).

ATRX was shown to bind MeCP2 at heterochromatin through its C-terminal domain, and a subset of mutations that occur in Rett syndrome (caused by *MeCP2* mutations) disrupt the ATRX-MeCP2 interaction (Nan et al., 2007). ATRX and MeCP2 bind imprinting control regions (ICR) alongside CTCF and cohesin (Kernohan et al., 2010). MeCP2 is required for ATRX localization at ICRs, where ATRX regulates positioning of nucleosomes to facilitate CTCF chromatin binding (Kernohan, Vernimmen, Gloor, & Berube, 2014).

Finally, ATRX also complexes with DAXX, a protein with roles in both suppression and activation of apoptosis (Salomoni & Khelifi, 2006). This interaction with DAXX serves

two major purposes: to localize ATRX to promyelocytic nuclear bodies (PML-NBs) (Y. Xue et al., 2003), and to act as a histone chaperone complex to deposit the histone variant H3.3 at pericentromeric heterochromatin, telomeres, and a subset of G-rich genes in the brain (Levy, Kernohan, Jiang, & Berube, 2015; Lewis et al., 2010). The finding that ATRX and DAXX deposit H3.3 at repressive heterochromatic regions was unexpected, given that H3.3 is generally a marker of active chromatin (Ahmad & Henikoff, 2002). While ATRX can bind H3.3 in its tail domain, this interaction is not required for histone deposition (Wong et al., 2010). Instead, DAXX binds H3.3 in its globular domain while ATRX recognizes heterochromatic histone signatures and localizes the ATRX-DAXX-H3.3 complex on chromatin (Lewis et al., 2010).

1.4.3 The role of ATRX in cell division

The initial study that investigated the cellular localization of ATRX found that it was associated with pericentromeric heterochromatin during both interphase and mitosis (McDowell et al., 1999). Bérubé, Smeenk, and Picketts (2000) demonstrated that ATRX is phosphorylated in a cell-cycle dependent manner: during interphase, ATRX is mainly associated with the nuclear matrix, however at the onset of mitosis it is phosphorylated and associates with condensed chromatin, suggesting different roles for ATRX in interphase and mitosis. Indeed, ATRX plays a vital role in mitosis, specifically in the proper congregation and segregation of sister chromatids (Ritchie et al., 2008). ATRX-depleted HeLa cells exhibited a prolonged prometaphase-to-metaphase transition and defective sister chromatid cohesion and congression; these mitotic defects were also shown *in vivo* in neuroprogenitors of the embryonic mouse forebrain (Ritchie et al., 2008). Similar results were observed when ATRX was deleted in mouse oocytes, leading to abnormal chromosome morphology and segregation defects during meiosis II (Baumann, Viveiros, & De La Fuente, 2010).

1.4.4 ATRX and DNA replication

The role for ATRX in DNA replication is thought to involve notoriously difficult to replicate regions of chromatin, particularly tandem repeats such as those found at telomeres

or pericentromeric heterochromatin. These repetitive regions can form structured DNA configurations such as G-quadruplexes, which can act as barriers to processes including replication (Rizzo et al., 2009). ATRX binds to G-quadruplexes *in vitro* (Law et al., 2010), and is required to prevent these structures through the deposition of H3.3 (Clynes & Gibbons, 2013; Clynes et al., 2015). Indeed, loss of ATRX in mouse embryonic stem cells (ESCs) or embryonic mouse brain results in an increased DNA damage response and telomere dysfunction which is exacerbated by G-quadruplex stabilization (Clynes et al., 2014; Watson et al., 2013; Wong et al., 2010). Leung et al. (2013) demonstrated that ATRX binds to sites of DNA damage, and that loss of ATRX results in defective replication checkpoints and replication restart. More recently it was discovered that ATRX is required at heterochromatic regions for protection of the stalled replication fork, where it prevents MRE11-dependent degradation of stalled forks due to lack of RAD51 protection (Huh et al., 2016).

1.4.5 Gene regulation by ATRX

Homology to the SWI/SNF family of proteins was the first indicator that ATRX might be involved in gene regulation (Gibbons et al., 1995). The presence of the ADD domain provided additional evidence: not only does ATRX contain a PHD zinc finger which recognizes histone H3 tails (Gibbons et al., 1997; Sanchez & Zhou, 2011), it also has sequence similarity to DNMT3A/B and DNMT3L, methyltransferases which repress transcription through DNA methylation (Bachman, Rountree, & Baylin, 2001). While there is evidence of altered DNA methylation patterns in ATRX patient blood samples (Gibbons & Higgs, 2000; Schenkel et al., 2017), the direct link between methylation and ATRX has not yet been identified.

In addition to structural data, there is also evidence of transcriptional control by ATRX through its binding partners. In Drosophila, the ATRX homologue is made up of two distinct proteins: dXNP which is similar to the SWI/SNF domain of ATRX, and dADD, which shares homology with the ADD domain. dXNP is required for HP1α deposition at PCH, and functions to silence these regions (Bassett, Cooper, Ragab, & Travers, 2008;

Emelyanov, Konev, Vershilova, & Fyodorov, 2010). However, it appears that dXNP dosage is vital for this repression, as overexpression of dXNP also causes de-repression at PCH (Schneiderman, Sakai, Goldstein, & Ahmad, 2009). dATRX and dADD also localize HP1α at telomeres and loss of either of the ATRX homologues results in increased expression of transposons found in Drosophila telomeres (Chavez et al., 2017). The complex formed by ATRX, cohesin, CTCF, and MeCP2 is found at imprinting control regions (ICR), specifically binding the unmethylated allele to facilitate intra-chromatin looping and post-natal repression of these genes essential for development (Kernohan et al., 2010; Kernohan et al., 2014). This three-dimensional structure can either mediate enhancer-promoter interactions, or isolate a promoter from an enhancer, resulting in activation or repression of gene expression, respectively (Zuin et al., 2014).

The contribution to gene expression by the ATRX/DAXX/H3.3 complex appears to be different. ATRX can repress genes by interacting with other transcription factors at promoter sites, and DAXX can impede this by sequestering ATRX into PML-NBs (J. Tang et al., 2004; Valadez-Graham et al., 2012). Additionally, there is evidence that the ATRX-DAXX complex represses viral gene expression in models of Herpes-Simplex virus, Epstein-Barr virus, and Adenovirus 5 infection (Lukashchuk & Everett, 2010; Schreiner et al., 2013; Tsai, Thikmyanova, Wojcechowskyj, Delecluse, & Lieberman, 2011). Goldberg et al. (2010) demonstrated that ATRX deposits H3.3 at telomeres, and is required for the suppression of telomeric RNA, which was counterintuitive as H3.3 is normally associated with active chromatin. Shortly after, it was demonstrated that ATRX occupies G-rich tandem repeats across the genome (Law et al., 2010). This binding was required for H3.3 deposition to resolve G-quadruplexes and facilitate transcription by RNA polymerase II (Levy et al., 2015). ATRX was also demonstrated to deposit H3.3 within the plant genome to affect gene expression (Duc et al., 2017). Similar to its interaction with MeCP2 in post-natal repression of imprinted alleles, ATRX is also required at the constitutively silenced imprinted allele to deposit H3.3 to maintain repression (Voon et al., 2015).

In the testes, ATRX binds the androgen receptor at promoters to facilitate expression of androgen-responsive genes (Bagheri-Fam et al., 2011). Finally, ATRX can also recruit DNMTs in the mouse brain, resulting in increased DNA methylation and repression of genes (Shioda et al., 2018). Altogether, evidence supports that ATRX can act as either an activator or repressor of gene expression through multiple mechanisms.

1.4.6 The role of ATRX in development

We know that mutations in ATRX result in severe developmental abnormalities such as intellectual disability, craniofacial abnormalities (e.g. microcephaly, wideset eyes), hypotonia, seizures, and underdeveloped testes (Weatherall et al., 1981), indicating that ATRX plays a critical role during development. *In situ* hybridization of the *Atrx* gene on mouse embryo sections showed diffuse expression early in development, however expression becomes more specific - particularly in the olfactory bulb, hippocampus, cortex, and cerebellum - in late-development and postnatal stages (Gecz et al., 1994; Stayton et al., 1994), suggesting a role for ATRX in brain development. Transgenic mice that overexpress ATRX displayed growth retardation, neural tube defects, and increased prevalence of embryonic lethality, with disorganization of the ventricular zone (Berube et al., 2002). The mice that survived until birth exhibited perinatal lethality, seizures, craniofacial abnormalities, and abnormal behaviour. Conditional inactivation of *Atrx* at the 8-16 cell stage of embryogenesis resulted in defective extraembryonic trophoblast development at approximately embryonic day 9.5 (E9.5) and termination of the embryo (Garrick et al., 2006), which may explain why there are no ‘null’ mutations that result in ATR-X syndrome. This finding also prompted the necessity for conditional knockouts of ATRX to study its effect in various tissues.

Many studies investigating ATRX in development have focused on the brain, due to the prevalence of severe-to-profound intellectual disability in ATR-X syndrome patients. In the first study that characterized loss of ATRX in the embryonic mouse forebrain, it was discovered that the cortex was significantly smaller due to increased apoptosis of new neurons, even though proliferation remained normal (Berube et al., 2005). Investigation of

neuroprogenitors in the ventricular zone displayed increased incidence of chromosomal abnormalities including micronuclei and misaligned chromosomes (Ritchie et al., 2008), and increased p53-dependent apoptosis (Seah et al., 2008). Deletion of ATRX in the forebrain and anterior pituitary caused reduced growth, shortened lifespan, kyphosis of the spine, loss of trabecular bone content and subcutaneous fat, and decreased circulating thyroxine and insulin-like growth factor 1 (Watson et al., 2013), highlighting the importance of ATRX in mouse development.

Conditional deletion of ATRX in testes leads to proliferative defects, delayed spermatogenesis, and seminiferous tubule defects (Bagheri-Fam et al., 2011). In muscle, deletion of ATRX delays S phase, resulting in accumulation of p53 and loss of genomic integrity (Huh et al., 2012). However, the muscles are able to “catch up” in growth by prolonging myoblast proliferation (Huh, Young, Yan, Price-O'Dea, & Picketts, 2017). Deletion in the retina results in defective interneuron differentiation and impaired visual function (Medina et al., 2009). Interestingly, even though ATR-X syndrome patients typically have short stature and craniofacial abnormalities, deletion of ATRX in chondrocytes had no effect on growth rate, body size, or bone length (Solomon, Li, Berube, & Beier, 2009).

1.4.7 ATRX and cancer

Recently it was discovered that somatic mutations in ATRX are linked to cancer, which has caused the field of ATRX research to explode in popularity. Approximately 90% of cancer types utilize telomerase reactivation to lengthen telomere ends and evade programmed cell death, however the remaining cancer types rely on alternative lengthening of telomeres (ALT), or homologous recombination between telomeres to extend these sequences. Mutations in *ATRX* were originally described in pancreatic neuroendocrine tumors (PanNETs) which utilize ALT in order to achieve replicative immortality (Heaphy et al., 2011), and have since been identified in paediatric glioblastomas, oligodendrogliomas, and medulloblastomas among others (Jiao et al., 2012; Kannan et al., 2012; X. Y. Liu et al., 2012; Schwartzentruber et al., 2012). The molecular mechanisms

behind ALT are largely unknown, however, it has been linked to high levels of genomic instability, likely resulting in homologous recombination and lengthening of the telomeres. It has been hypothesized that ATRX is required at telomeres in order to resolve G-quadruplexes for proper replication, and loss of ATRX causes stalling of replication forks, triggering homologous recombination (Clynes et al., 2015; O'Sullivan et al., 2014). Although deletion of ATRX causes telomere dysfunction, it is not enough on its own to drive ALT-like phenotypes (Lovejoy et al., 2012). Therefore, other factors must be required to trigger the ALT pathway after ATRX loss, such as p53. Dual mutations of *Atrx*/*p53* in mice rescues apoptosis, but results in increased genomic instability (Seah et al., 2008; Watson et al., 2013); additionally, mutations in *ATRX* are often concurrent with mutations in *TP53* in human tumours (X. Y. Liu et al., 2012; Schwartzentruber et al., 2012). These studies reinforce the idea that ATRX is critical for genomic integrity and telomere maintenance.

1.4.8 Neurological roles of ATRX

Due to the prevalence of ATRX mutations in ID, research has focused on the role of ATRX in the nervous system. Many of these studies have concentrated on neurodevelopment, investigating ATRX in neuroprogenitors, and how loss leads to DNA replication stress, genomic instability, telomere dysfunction, and p53-dependent apoptosis (Ritchie et al., 2008; Seah et al., 2008; Watson et al., 2013), however the postnatal role of ATRX in the brain is largely unknown. Mice were generated that lacked exon 2 of the ATRX gene ($ATRX^{\Delta E2}$) (Nogami et al., 2011) to mimic a human variant of ATR-X syndrome called Chudley-Lowry syndrome, characterized by mild ID (Abidi et al., 2005; Guerrini et al., 2000). Deletion of exon 2 resulted in a reduction of ATRX protein levels by approximately 80% with no obvious morphological changes to the hippocampus or cortex, though the overall brain size was decreased proportional to body weight (Nogami et al., 2011; Shioda et al., 2011). Mutant mice displayed defective working memory, novel object recognition, and impaired spatial memory in the Barnes maze and contextual fear task but not Morris water maze when tested 24 hours post training (Nogami et al., 2011; Shioda et al., 2011). These behaviours were linked to decreased α-amino-3-hydroxy-5-methyl-4-

isoxazolepropionic acid (AMPA) receptor-mediated long-term potentiation (LTP), with decreased phosphorylation of α-Ca^{2+}/calmodulin-dependent protein kinase II (CaMKII) and AMPA receptor subunit glutamate receptor 1 (GluR1) in the hippocampus (Nogami et al., 2011). Conversely, in the medial prefrontal cortex (mPFC), increased autophosphorylation of αCaMKII was associated with increased phosphorylation of downstream Rac1-related proteins, resulting in abnormal dendritic spine morphology (Shioda et al., 2011). These studies highlight that ATRX depletion could potentially result in different outcomes in different areas of the brain. Moreover, it is not clear from these studies whether depletion of ATRX protein in neurons or glial cells is responsible for the observed defects.

Transcriptional profiling of the $ATRX^{\Delta E2}$ hippocampus via microarray revealed increased expression of the imprinted *Xlr3b* gene. The associated increased XLR3B protein levels were shown to sequester *Camk2a* mRNA and thus inhibit its transport to dendritic spines (Shioda et al., 2018). The *Xlr3b* gene sequence is extremely GC-rich, and the authors found that ATRX recognizes G-quadruplexes upstream of the gene and recruits DNMT1/DNMT3a to repress gene expression. Treatment of the $ATRX^{\Delta E2}$ mice with a G-quadruplex stabilizer resulted in repression of the *Xlr3b* gene and reversal of impairments seen in the novel object recognition task, passive avoidance task, and Y maze. However, ATRX can also recognize and prevent G-quadruplex structures through deposition of H3.3 at a subset of G-rich genes in the brain, including the autism-related gene *Nlgn4*, thereby activating transcription (Levy et al., 2015). Therefore, ATRX may act as a repressor or activator of neuronal genes depending on chromatin environment and its binding partners.

1.5 Types of memory

Humans with ID disorders often have varying levels of memory impairments, and in different types of memory. *Mus musculus*, the common house mouse, is an excellent model to study memory due to its largely conserved molecular mechanisms regulating cognition compared to humans. Many behavioural paradigms have been developed to test different types of memory in rodents and a description of the tests performed in this dissertation can

be found in Table 1-1. There are three main types of memory: working memory, short-term memory, and long-term memory. Working memory involves the storage and manipulation of information over extremely short periods of time, for example “carrying” digits when mentally adding numbers together (reviewed in Goldman-Rakic (1995), D'Esposito and Postle (2015)). In mouse models, working memory is tested using the Y-maze spontaneous alternation task and is dependent on the prefrontal cortex, hippocampus, and basal forebrain (Aggleton, Hunt, & Rawlins, 1986; Curtis & D'Esposito, 2003; Givens & Olton, 1994).

Short-term memory is used for storage but not manipulation of information over a short period of time, although there is controversy on whether this lasts hours, days, or weeks, whereas long-term memory involves indefinite storage of knowledge (reviewed in Cowan (2008)). However, there are multiple different subtypes of short- and long-term memory that depend on different regions of the brain. For example, recognition memory is the ability to recognize certain objects, people, or events that have been previously encountered. This type of memory is dependent on the prefrontal cortex and medial temporal lobe, which includes the hippocampus (Brown & Aggleton, 2001; Slotnick, Moo, Segal, & Hart, 2003). In mice, recognition memory is tested using the novel object recognition task, which requires a mouse to discern between an object it has been previously exposed to and a novel object (Antunes & Biala, 2012). Spatial memory records information about one’s spatial environment and is typically encoded through the hippocampus (Bird & Burgess, 2008). In mice, this can be tested using paradigms such as the Morris water maze, contextual fear conditioning task, and the paired-associate learning task (Kim, Heath, Kent, Bussey, & Saksida, 2015; McEchron, Bouwmeester, Tseng, Weiss, & Disterhoft, 1998; Vorhees & Williams, 2006).

1.6 The hippocampus in learning and memory

1.6.1 What do we know from lesion studies?

The ability to learn and remember spatial locations is an essential behaviour for survival. To study differential contributions to spatial learning and memory by various brain

Paradigm	Behaviour(s) tested
Open field test	General activity, anxiety
Elevated plus maze	Anxiety
Y maze	Working memory
Novel object recognition	Recognition memory
Morris water maze	Spatial learning and memory
Contextual fear conditioning	Spatial memory, fear memory
Paired-associate learning task	Spatial learning

Table 1-1 Paradigms used to test for cognitive impairment in mice

structures, lesion studies have been used in both humans and rodents. The first human lesion study, and possibly one of the most famous psychiatric studies, is patient H.M., who suffered from tonic-clonic seizures early in life. To remedy this, he underwent a bilateral medial temporal lobectomy, removing the hippocampus and surrounding structures. While this was partially successful in controlling seizures, patient H.M. started to suffer from severe anterograde amnesia, or inability to form new memories (Scoville & Milner, 1957). However, since almost the entire medial temporal lobe was bilaterally removed, it was not entirely conclusive as to what structure was responsible for the memory loss. Almost 30 years later, Zola-Morgan, Squire, and Amaral (1986) described the case of patient R.B., who had bilateral lesions of the CA1 region of the hippocampus that extended fully rostro-caudal. This patient displayed severe anterograde amnesia (inability to form new memories), and no other cognitive signs, indicating that the amnesia stems directly from the hippocampal lesions. Additionally, magnetic resonance imaging (MRI) revealed shrunken and atrophic hippocampi in four patients with severe, non-syndromic memory impairment (Squire, Amaral, & Press, 1990). Lesion studies in monkeys determined that the perirhinal and parahippocampal cortices also result in amnesia-related impairments in behaviour (Zola-Morgan, Squire, Amaral, & Suzuki, 1989).

Lesion studies in rodents have also linked the hippocampus to spatial learning and memory. Loss of hippocampal function in rats leads to impairment in the Morris water maze (Sutherland & McDonald, 1990), spatial alternation task (Aggleton et al., 1986), and radial arm maze (Becker & Olton, 1980). Therefore, the hippocampus is vital for formation of memories in humans and is linked to spatial learning and memory in animal models.

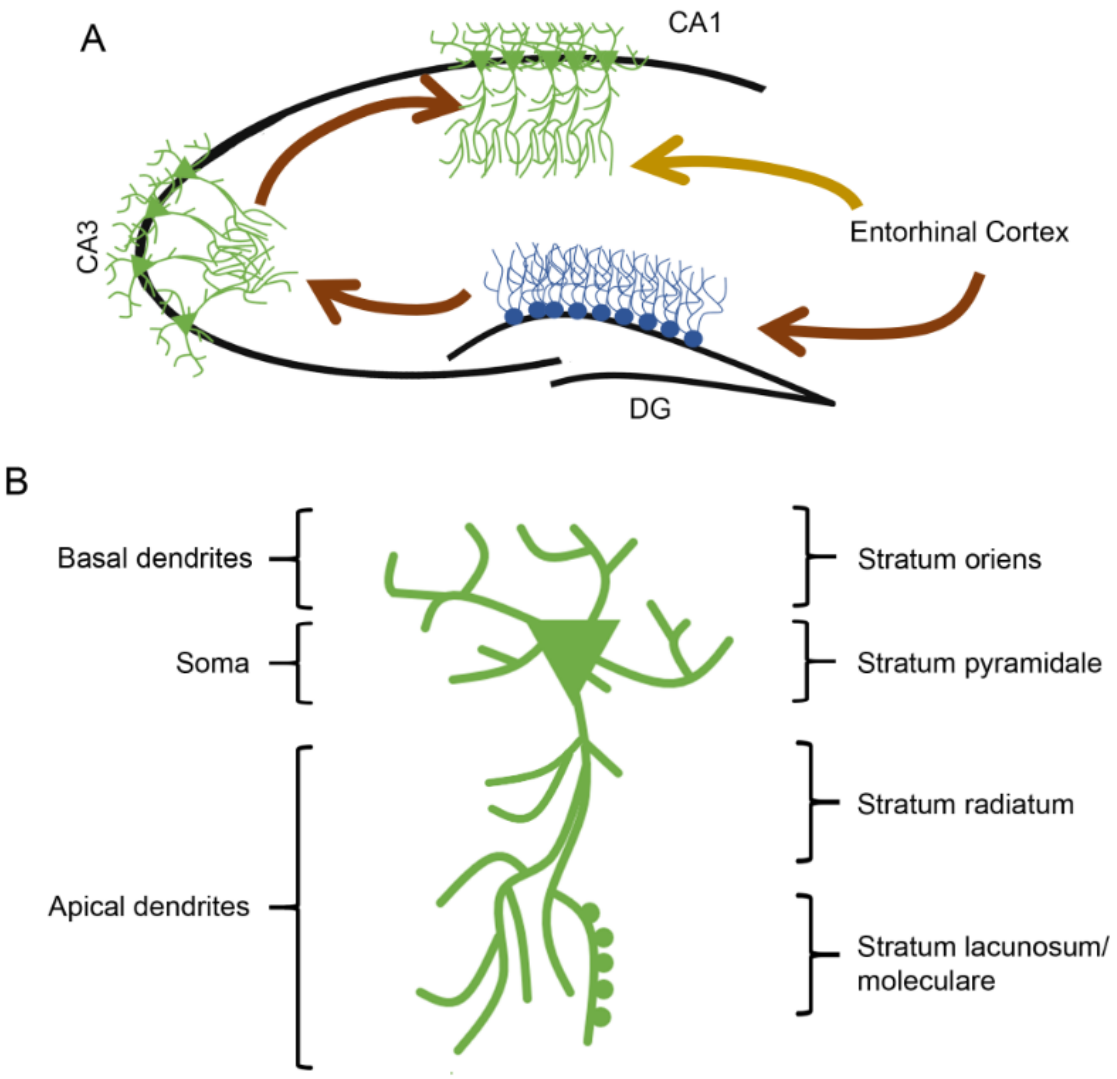

Figure 1-1 The anatomy of the hippocampus and the CA1 pyramidal neuron.

(A) The hippocampus consists of the Cornu Ammonis (CA) 1, 2, and 3 and dentate gyrus (DG). The CA regions are formed by densely packed pyramidal neurons (green) and the main signaling body of the DG is the granule cell (blue). Two main electrophysiological pathways converge on the hippocampus, both originating from the entorhinal cortex. The trisynaptic loop (brown) starts in the entorhinal cortex, where it travels through the DG to the CA3, then to the proximal dendrites of the CA1 for further processing. The

temporoammonic pathway (yellow) is a direct route from the entorhinal cortex to the distal dendrites of the CA1. (B) A pyramidal neuron consists of a triangular cell body called the soma. Dendrites protrude from the base (basal dendrites) or apex (apical dendrites). On these dendrites are small spinous processes where the synapse occurs. The CA1 is divided into four regions: stratum oriens, pryamidale, radiatum, and lacunosum/moleculare.

1.6.2 The hippocampus

The hippocampus is in the medial temporal lobe of the human brain and is a common structure in both humans and mice. It contains two major subregions: the hippocampus proper (or Ammon's horn, *Cornu Ammonis*) and the dentate gyrus (Figure 1-1A). The abbreviation "CA" is used for subdividing the hippocampus proper in to CA1, CA2, CA3, and CA4 (Amaral & Witter, 1989). The CA regions can be visualized in the brain as a region of densely packed neurons forming a sideways "U" shape. One end of the "U" is inserted into the dentate gyrus, is called the dentate hilus in rodents (Knowles, 1992). The CA3 is the curve of the "U", and the CA1 is the dorsal section of the hippocampus. The CA2 region is very small and located between the CA1 and CA3. The CA1-CA3 regions have distinct layers, or strata: oriens (containing the basal dendritic projections), pyramidal (containing the densely packed cell bodies), radiatum (the layer containing proximal apical dendrites), and lacunosum-moleculare (the layer containing distal apical dendrites) (Amaral & Witter, 1989). The CA3 contains an additional layer, the stratum lucidum, between the pyramidal and radiatum strata, and is composed mainly of mossy fiber axons and interneurons. The dentate gyrus is one of three areas of the brain responsible for adult neurogenesis (Kuhn, Dickinson-Anson, & Gage, 1996). It forms a "V"-like structure around the CA3 and consists of three layers: the molecular layer (receiving axonal input from other areas such as the entorhinal cortex), the granular layer (containing granule cells which project to the CA3 neurons), and polymorphic layer (containing mossy cells which project to the molecular layer) (Amaral, Scharfman, & Lavenex, 2007).

Pyramidal neurons are perhaps the most well-characterized cell type of the hippocampus. They are the principle excitatory neurons, receiving input from other regions, such as the CA3 pyramidal neurons from the dentate gyrus, or the CA1 neurons from the CA3. As their name suggests, the soma of pyramidal neurons is triangular with one long apical dendrite emerging from the apex, and many smaller basal dendrites emerging from the base (Figure 1-1B) (DeFelipe & Farinas, 1992). Along these dendrites are the dendritic spines, which are the main location at which synapses occur (reviewed in Nimchinsky, Sabatini, and Svoboda (2002)). A subset of pyramidal neurons are known as place cells that only

fire when an animal enters a specific location (O'Keefe & Dostrovsky, 1971), and the presence of place cells further reinforces the importance of the hippocampus in spatial cognition.

Interneurons are also found within the hippocampus and are largely inhibitory, working to regulate pyramidal cell activity. Non-neuronal cells also reside in the hippocampus and include astrocytes which aid in clearing neurotransmitters from the synaptic cleft and cross the blood-brain-barrier to provide nutrients for neurons and remove waste. Oligodendrocytes are the other major non-neuronal cell in the hippocampus and are responsible for myelination of pyramidal cell axons. Microglia are also present and act as the primary immune defense in the central nervous system.

1.6.3 The electrophysiological pathways of the hippocampus

There are two major pathways that have been implicated in the formation of spatial memories in mice: the trisynaptic loop and the temporoammonic pathway (Figure 1-1A). The trisynaptic loop is an indirect pathway in which information is passed from the entorhinal cortex (EC) to the CA1 via the dentate gyrus and CA3, known as the perforant pathway. The entorhinal cortex consists of 6 layers, of which layer II projects to the dentate gyrus granule cells (Ruth, Collier, & Routtenberg, 1982; van Groen, Miettinen, & Kadish, 2003), however there is some evidence that layers IV-VI may also project to the DG (van Groen et al., 2003; Witter & Amaral, 1991). In humans, the EC layer II neurons are preferentially affected by Alzheimer’s disease, indicating its importance in memory formation (Hyman, Van Hoesen, Kromer, & Damasio, 1986; Morys, Sadowski, Barcikowska, Maciejewska, & Narkiewicz, 1994). The entorhinal cortex can be further subdivided into medial and lateral entorhinal cortex (MEC and LEC, respectively). The LEC generally processes non-spatial information and projects to the outer 1/3 of the DG, whereas the MEC processes spatial information and projects to the middle 1/3 of the dentate gyrus (Hjorth-Simonsen, 1972; Mayeaux & Johnston, 2004; Naber, Caballero-Bleda, Jorritsma-Byham, & Witter, 1997; Sargolini et al., 2006).

The DG, after receiving input from the EC, projects this information to the suprapyramidal stratum lucidum of the CA3 region through the unmyelinated mossy fibres of the granule cells (Gaarskjaer, 1978). Unlike the perforant pathway, all granule cells from the DG generate mossy fibres that extend through the whole CA3 (i.e. no specific area of the DG projects to a specific area of the CA3). The Schaffer collateral pathway connects the CA3 to the CA1 and is the most often-studied in relation to learning and memory. The distal CA3 connects the proximal CA1 while the proximal CA3 connects the distal CA1 (Ishizuka, Weber, & Amaral, 1990; Laurberg, 1979), however, all synapses occur within the stratum radiatum and stratum oriens layers (Raisman, Cowan, & Powell, 1966). These synapses are largely glutamatergic and dependent on N-methyl-D-aspartic acid (NMDA) receptor activation indicating the presence of excitatory synapses (Collingridge, Kehl, & McLennan, 1983). Activation of the Schaffer-collateral pathway induces LTP, a long-lasting increase in synapse strength (Larson, Wong, & Lynch, 1986), and loss of LTP along this pathway results in impaired spatial learning and memory in mice (Brucato et al., 1996; C. M. Chen et al., 2017; Grant et al., 1992; Wang et al., 2017). Therefore, the Schaffer-collateral pathway is very important for proper formation of spatial memories.

The temporoammonic pathway is a direct input to the CA1 stratum lacunosum moleculare from the entorhinal cortex layer 3 neurons (Steward, 1976). Similar to the Schaffer-collaterals, this pathway exhibits NMDA receptor-dependent LTP (Aksoy-Aksel & Manahan-Vaughan, 2015; Remondes & Schuman, 2003) and is heavily implicated in long-term spatial learning and memory (Brun et al., 2008; Vago & Kesner, 2008). The reason for this overlap between the trisynaptic loop and temporoammonic pathway is not fully understood. Brun et al. (2002) cut off input to the CA1 from the CA3 and noted normal spatial recognition memory but impaired recall or navigation, indicating two functionally separate circuits.

1.7 Synaptic Plasticity

Synaptic plasticity is based on the idea that synaptic transmission will get stronger following repetitive stimulation and weaker following decreased activity, and is one of the

most important correlates of learning and memory (Hughes, 1958). The synaptic changes can be defined as short-term or long-term depending on how long they persist. Short-term synaptic plasticity lasts between a few milliseconds to several minutes, and is most often characterized using paired-pulse facilitation where identical stimuli are delivered within a short interval (Katz & Miledi, 1968). This results in either enhancement or depression of the second stimulus response depending on numerous factors including number of docked vesicles (Dobrunz & Stevens, 1997).

Long-term synaptic plasticity was first proposed in 1949 by a model known as Hebbian plasticity: that synaptic efficiency increases when a post-synaptic neuron is persistently stimulated by a pre-synaptic terminal (Hebb, 1949). Long-term synaptic plasticity can further be classified as either long-term potentiation (LTP) or long-term depression (LTD). Bliss and Gardner-Medwin (1973) demonstrated that repeated activation of a neuron resulted in a potentiation of synaptic strength that lasted for hours or even days, and they named this phenomenon LTP. There are three main properties of LTP: cooperativity, associativity, and input specificity (Nicoll, Kauer, & Malenka, 1988). Cooperativity is described as the critical number of activated synapses required to induce LTP. Associativity dictates that if weak stimulation does not induce LTP at a dendritic spine, then concurrent strong stimulation of a neighbouring spine on the same post-synaptic neuron will result in LTP. Finally, input specificity is the finding that LTP is only elicited at the active synapse, and not other synapses. After activation of LTP, the signal needs to be maintained. This is achieved through new protein synthesis at dendritic spines (Reymann & Frey, 2007; Sutton & Schuman, 2006) and transcription in the nucleus (Zhou et al., 2006).

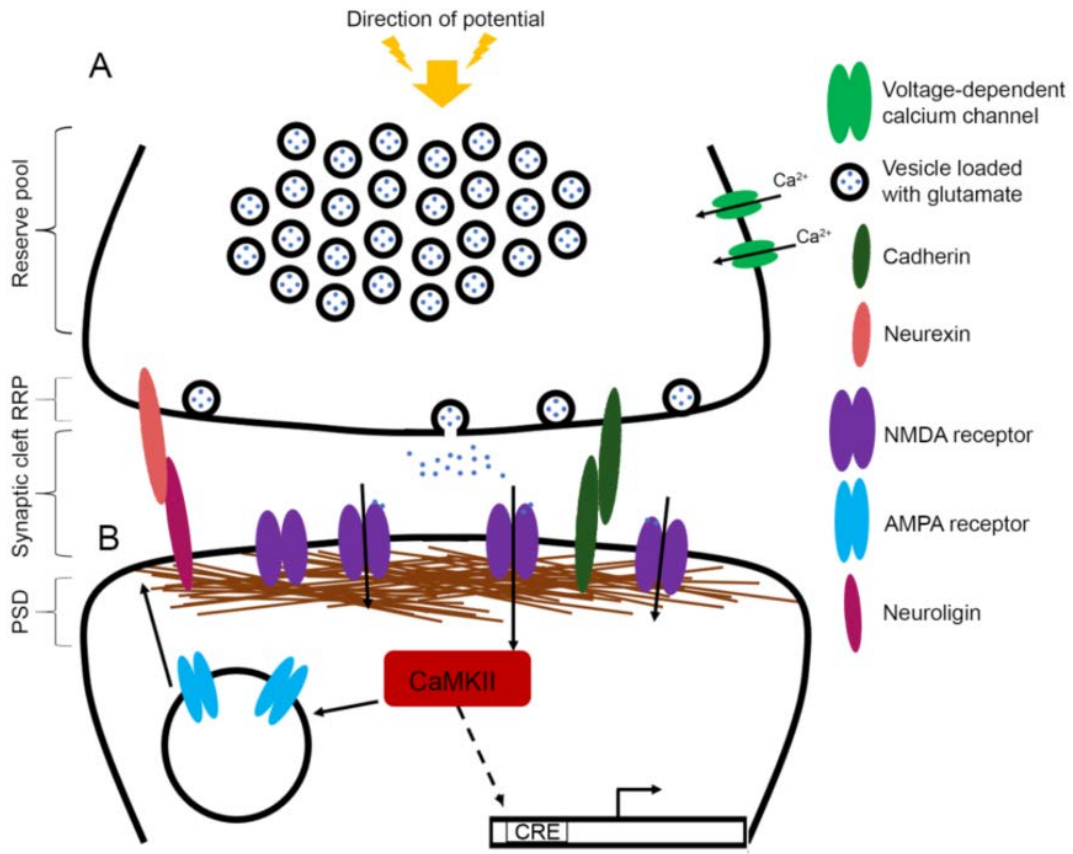

Figure 1-2 The structure of an excitatory synapse.

(A) The presynaptic structure. Vesicles are localized in either the reserve pool or readily releasable pool (RRP). Calcium influx occurs through voltage-dependent calcium channels, triggering exocytosis of glutamate. Neurexins and cadherins can be found as cell adhesion molecules. (B) The postsynaptic structure. Glutamate activates the NMDA receptor which causes autophosphorylation of CaMKII, which triggers mobility of AMPA receptors to the postsynaptic density in addition to a signaling cascade ultimately ending in activation of gene expression.

Long-term depression is less well-studied in comparison to LTP but results in a weakening of the synapse. The establishment of LTD demonstrated that synaptic signaling can control synaptic strength in a bidirectional manner (Dudek & Bear, 1992; Mulkey & Malenka, 1992). Unlike LTP, which requires a calcium influx beyond a certain threshold (Malenka & Nicoll, 1993), LTD requires low-frequency stimulation that results in a small increase of intracellular calcium (Cummings, Mulkey, Nicoll, & Malenka, 1996), which results in increased activation of protein phosphatases, exocytosis of neurotransmitter receptors, and shrinkage of dendritic spines (Heynen, Quinlan, Bae, & Bear, 2000; Morishita et al., 2001; Nagerl, Eberhorn, Cambridge, & Bonhoeffer, 2004).

1.7.1 The synapse

There are two main types of synapses: asymmetric, where the post-synaptic density (PSD) is larger than the pre-synaptic density, and symmetric, where the PSD is roughly the same thickness than the pre-synaptic density (Tao et al., 2018). Excitatory synapses are generally asymmetric, and are axo-dendritic with round vesicles, whereas inhibitory are usually symmetric, axo-somatic, and have flat vesicles (Colonnier, 1968; Gray, 1969). Most excitatory synapses occur on dendritic spines within the stratum radiatum and stratum oriens of the CA1 hippocampus, while inhibitory synapses are generally found on the dendritic shaft or cell body in this region (Megias, Emri, Freund, & Gulyas, 2001). Within the stratum lacunosum, however, asymmetric synapses can also be found on shafts, and symmetric synapses can be found on spines (Megias et al., 2001). However, while there are differences in the appearance and location of asymmetric and symmetric synapses, the structure of their pre-synapse and post-synapse is largely the same (Figure 1-2) (Gray, 1969).

1.7.2 Pre-synaptic structure and function

The pre-synaptic neuron is responsible for neurotransmitter release from the axonal terminal into the synaptic cleft at the active zone (AZ) (Figure 1-2A). The active zone is aligned with the PSD of the post-synaptic neuron, with the synaptic cleft spanning approximately 15-30 nm (Landis, Hall, Weinstein, & Reese, 1988). This alignment is

possible through many different types of cell adhesion molecules which include cadherins, protocadherins, and neurexins (Frank & Kemler, 2002; Missler & Sudhof, 1998; Shapiro & Colman, 1999; Yagi & Takeichi, 2000). All these adhesion molecules have similar protein motifs: an extracellular domain that binds PSD adhesion molecules or extracellular matrix, a single transmembrane domain, and an intracellular domain that binds the cytoskeleton or scaffolding proteins along the AZ (Gottardi & Gumbiner, 2001; Hung & Sheng, 2002).

The two main functions of the AZ are to allow calcium ion (Ca^{2+}) entry and to release neurotransmitters within a fraction of a millisecond (Heidelberger, Heinemann, Neher, & Matthews, 1994). Voltage-dependent calcium channels (VDCC) open in response to an action potential, allowing for calcium influx (Augustine, Charlton, & Smith, 1987). This increase in cytoplasmic calcium activates soluble N-ethylmaleimade-sensitive factor attachment protein receptor (SNARE) complex proteins, facilitating vesicular-membrane fusion and release of neurotransmitter. Synaptotagmins are a family of calcium-sensitive proteins that localize to secretory vesicles and membranes, but synaptotagmin-1 (Syt1) is the main calcium sensor in forebrain neurons (Geppert et al., 1994). Syt1 can bind to SNAREs through a Ca^{2+} binding domain; this interaction is functionally important, yet the significance is still unknown (Bai & Chapman, 2004; Bowen, Weninger, Ernst, Chu, & Brunger, 2005; Pang, Shin, Meyer, Rosenmund, & Sudhof, 2006). Syt1 induces vesicular clustering at the synapse (Arac et al., 2006), and reducing the binding affinity of the Syt1 Ca^{2+} domain decreased the amount of neurotransmitter released (Fernandez-Chacon et al., 2001), indicating the importance of Syt1 in Ca^{2+}-mediated exocytosis.

The complexin family has also been implicated in Ca^{2+}-dependent neurotransmitter release, however, studies have shown contrasting roles in vesicular fusion. Loss of complexin-1 (Cplx1) and complexin-2 (Cplx2) in neurons resulted in reduced Ca^{2+}-triggered neurotransmitter release, however, overexpression of Cplx1 at synaptic terminals also decreased neurotransmitter release, indicating a requirement for balance in Cplx1 expression (Ono et al., 1998; Reim et al., 2001; Tokumaru et al., 2001). Cplx1 binds

SNARE proteins and clamps the SNARE/vesicle complex to the pre-synaptic membrane (Giraudo, Eng, Melia, & Rothman, 2006; M. Xue et al., 2007). Upon Ca^{2+} influx, Syt1 displaces Cplx1 on the SNARE complex allowing for fusion of the vesicle to the pre-synaptic membrane and release of neurotransmitter into the synaptic cleft (Schaub, Lu, Doneske, Shin, & McNew, 2006; J. Tang et al., 2006).

Since long-term memory depends on synthesis of new proteins (Sutton & Schuman, 2006), microRNAs (miRNA) can provide another layer of regulation of synaptic plasticity. These non-coding RNA bind to messenger RNA 3' untranslated regions (UTR) to promote degradation of the transcript or to block translation (Bagga et al., 2005; Humphreys, Westman, Martin, & Preiss, 2005). Indeed, LTP causes altered transcription of many miRNA, which in turn have diverse targets across the transcriptome (Joilin et al., 2014). A subset of miRNAs have been shown to act within the synaptic terminal to control neurotransmitter release and regulate presynaptic potential by targeting transporters or synaptic vesicle machinery (Siegert et al., 2015; Verma, Augustine, Ammar, Tashiro, & Cohen, 2015). miRNA regulation of synaptic plasticity translates to cognitive effects, as behaviour in the Morris water maze, novel object recognition, and contextual fear task is affected in miRNA loss-of-function models(Hansen, Sakamoto, Wayman, Impey, & Obrietan, 2010; Siegert et al., 2015)

1.7.3 Post-synaptic structure and function

The postsynaptic neuron is responsible for receiving neurotransmitter and turning it into a signaling cascade. Most of this process occurs within a structure called the post-synaptic density (PSD), an electron-dense thickening at the postsynaptic membrane (Figure 1-2B) (Gray, 1959; Palay, 1956). The PSD consists of many scaffolding proteins that anchor neurotransmitter receptors, cell adhesion molecules, and signaling complexes. The main scaffolding protein is PSD-95 which comprises approximately 2.3% of the total PSD mass, and can interact with a variety of proteins through its PDZ motif (X. Chen et al., 2005). Mice lacking PSD-95 have impaired spatial learning and altered LTP and LTD, indicating the importance of PSD-95 in NMDAR-dependent signaling (Migaud et al., 1998).

The postsynaptic membrane shares many cell adhesion molecule classes with the presynaptic membrane, such as cadherins and protocadherins, however there are some that are specific to the postsynapse. For example, neuroligins are a class of four proteins (Neuroligin-1 through -4) only found on post-synaptic membranes and bind to neurexins to align the synaptic cleft (Ichtchenko et al., 1995; Ichtchenko, Nguyen, & Sudhof, 1996). Neuroligins are typically synapse specific, with neuroligin-1 found at excitatory, neuroligin-2 and -4 at inhibitory, and neuroligin-3 at both (Budreck & Scheiffele, 2007; Hoon et al., 2011; Song, Ichtchenko, Sudhof, & Brose, 1999; Varoqueaux, Jamain, & Brose, 2004). Their cytoplasmic domain contains a PDZ motif to recruit PSD-95 and other scaffolding proteins (Kornau, Schenker, Kennedy, & Seeburg, 1995). Other cell adhesion molecules include synaptic cell adhesion molecules (synCAMs) which act across the cleft to increase active synapse numbers, and neural cell adhesion molecules (NCAMs) which promote assembly of cytoskeletal scaffolds (Sytnyk, Leshchyns'ka, Nikonenko, & Schachner, 2006).

Other proteins anchored to the PSD include neurotransmitter receptors. The two main classes in excitatory neurons are NMDAR and AMPAR. NMDARs allow calcium influx in response to synaptic depolarization, and can trigger either LTP or LTD (Sheng & Kim, 2002). They are formed by a tetramer of four subunits GluN1-3. NDMAR require two GluN1 with either two GluN2 or a GluN2/GluN3 combination (Monyer et al., 1992; Schorge & Colquhoun, 2003). Intracellular domains of these subunits bind CaMKII and calmodulin, allowing for fast activation of these proteins upon Ca^{2+} influx (Ehlers, Zhang, Bernhadt, & Huganir, 1996; Strack & Colbran, 1998). AMPAR can be found at the synaptic membrane, but are most often found packaged in vesicles ready to be trafficked to the membrane upon depolarization (Bredt & Nicoll, 2003; Hayashi et al., 2000). Like NMDAR, AMPAR are tetrameric and heteromeric complexes and it can contain a combination of subunits GluR1-4 (or GluRA-D in some nomenclature). GluR2 is usually found in all conformations of the receptor, as it confers Ca^{2+} permeability (Isaac, Ashby, & McBain, 2007), and the majority of AMPAR found in hippocampal pyramidal neurons contain two GluR1 and two GluR2 (Wenthold, Petralia, Blahos, & Niedzielski, 1996).

Early LTP (E-LTP) induction requires NMDAR activation and an increase in intracellular Ca^{2+} (Huber, Mauk, & Kelly, 1995). Upon Ca^{2+} influx, CaMKII activates via autophosphorylation (Fukunaga, Muller, & Miyamoto, 1995). This is a critical step, since mice expressing mutant CaMKII display a drastic reduction in LTP (Giese, Fedorov, Filipkowski, & Silva, 1998; Silva et al., 1992). Activation of CaMKII results in phosphorylation of many downstream proteins and signaling cascades. CaMKII phosphorylates AMPAR to increase its conductance as well as allow for trafficking of the receptor to the synaptic membrane (Derkach, Barria, & Soderling, 1999; Hayashi et al., 2000). Phosphorylation of synGAP, a Ras/Rap GTPase-activating protein, by CaMKII causes activation of Ras, critical for AMPAR trafficking (Araki, Zeng, Zhang, & Huganir, 2015; Zhu, Qin, Zhao, Van Aelst, & Malinow, 2002). CaMKII also targets Rho guanine exchange factors (GEFs) which in turn activate Rho GTPases such as Rac1 and RhoA (Herring & Nicoll, 2016). These GTPases are involved in actin cytoskeletal remodeling in dendritic spines (Murakoshi, Wang, & Yasuda, 2011; Penzes, Cahill, Jones, & Srivastava, 2008). The roles of CaMKII in E-LTP are summarized in Figure 1-2.

Late LTP (L-LTP) is dependent on gene expression changes and *de novo* protein synthesis and requires activation of PKA and its downstream targets CREB and MAPK (Frey, Huang, & Kandel, 1993; Huang & Kandel, 1994; Nguyen, Abel, & Kandel, 1994). Adenylate cyclase (AC) is induced by Ca^{2+} influx and catalyzes adenosine triphosphate (ATP) into cyclic adenosine monophosphate (cAMP) (Eliot, Dudai, Kandel, & Abrams, 1989). cAMP binds and activates protein kinase A (PKA) which phosphorylates CRE-binding protein (CREB), resulting in activation of cAMP-response element (CRE) related genes (Nguyen & Woo, 2003). PKA also activates the mitogen-activated protein kinase (MAPK) pathway, causing MAPK to translocate to the nucleus where it is involved in activating transcription factors including CREB (Boglari, Erhardt, Cooper, & Szeberenyi, 1998; Thomson, Mahadevan, & Clayton, 1999; Vossler et al., 1997).

A large number of genes contain the CRE recognition site, including immediate early genes (IEGs), which are activated quickly and transiently following post-synaptic stimulation.

Zif268 (or Egr1) is included in this class as a secondary transcription factor for other genes involved in synaptic plasticity (James, Conway, & Morris, 2005; Veyrac, Besnard, Caboche, Davis, & Laroche, 2014). Arc is another IEG where upon transcription, Arc mRNA is translocated to the active spine for local translation (Moga et al., 2004; Steward, Wallace, Lyford, & Worley, 1998) where the protein regulates structural changes via actin polymerization (Bramham et al., 2010). Taken together, evidence indicates that E-LTP requires modification of existing proteins and L-LTP requires *de novo* transcription and translation, but there is still much unknown about the molecular and cellular mechanisms underlying memory formation.

1.8 Thesis Overview

The overall aim of this work was to identify the role of ATRX in learning and memory and determine a mechanism by which ATRX regulates cognition. At the beginning of this study, there had been no models investigating ATRX loss specifically in the adult central nervous system, and most ATRX research had focused on the role of ATRX in development, not in adult mice. Since mutations in ATRX cause intellectual disability in humans, and there is evidence that ATRX regulates gene expression in the brain, I hypothesized that ATRX is required for learning and memory processes by controlling expression of genes involved in synaptic transmission. To identify the role of ATRX in cognition we utilized two different mouse models of ATRX loss in the brain: *Atrx*-cHet displayed mosaic expression of ATRX in neural and glial precursors and *Atrx*-cKO had no ATRX expression in glutamatergic neurons of the mouse forebrain. Remarkably, we found the *Atrx*-cHet had endocrine defects in addition to profound intellectual impairment in many different paradigms (Tamming et al., 2017). However, due to confounding effects we opted to use the *Atrx*-cKO mice for further studies

I found both gross and ultrastructural morphology changes in the *Atrx*-cKO hippocampus. The hippocampal CA1 stratum radiatum and stratum lacunosum moleculare were significantly increased in size. However, these increases could not be explained by increased dendritic branching of the neurons nor increased glial or microglial cell

infiltration. At the ultrastructural level, I observed an increased number of docked and total presynaptic vesicles and an increase in postsynaptic density size which are associated with hippocampal-dependent impairments in learning and memory in the Morris water maze, contextual fear conditioning, and paired-associate learning task. However, *Atrx*-cKO female mice did not display any behavioural impairments, indicating a sexually-dimorphic effect of ATRX loss in glutamatergic neurons. RNA sequencing revealed sex-specific alterations in synaptic transcript expression which were correlated to miR-137 expression. We propose a model whereby ATRX directly or indirectly regulates miR-137 resulting in repression of synaptic target genes, altered synaptic ultrastructure, and impaired spatial learning and memory. Taken together, the findings presented here identify a novel function for ATRX in the regulation of cognition and provide insight into how defects in ATRX function lead to intellectual disability.

1.9 References

Aapola, U., Kawasaki, K., Scott, H. S., Ollila, J., Vihinen, M., Heino, M., . . . Peterson, P. (2000). Isolation and initial characterization of a novel zinc finger gene, DNMT3L, on 21q22.3, related to the cytosine-5-methyltransferase 3 gene family. *Genomics, 65*(3), 293-298. doi: 10.1006/geno.2000.6168

Abidi, F. E., Cardoso, C., Lossi, A. M., Lowry, R. B., Depetris, D., Mattei, M. G., . . . Schwartz, C. E. (2005). Mutation in the 5' alternatively spliced region of the XNP/ATR-X gene causes Chudley-Lowry syndrome. *Eur J Hum Genet, 13*(2), 176-183. doi: 10.1038/sj.ejhg.5201303

Agarwal, N., Becker, A., Jost, K. L., Haase, S., Thakur, B. K., Brero, A., . . . Cardoso, M. C. (2011). MeCP2 Rett mutations affect large scale chromatin organization. *Hum Mol Genet, 20*(21), 4187-4195. doi: 10.1093/hmg/ddr346

Aggleton, J. P., Hunt, P. R., & Rawlins, J. N. (1986). The effects of hippocampal lesions upon spatial and non-spatial tests of working memory. *Behav Brain Res, 19*(2), 133-146.

Ahmad, K., & Henikoff, S. (2002). The histone variant H3.3 marks active chromatin by replication-independent nucleosome assembly. *Mol Cell, 9*(6), 1191-1200.

Aksoy-Aksel, A., & Manahan-Vaughan, D. (2015). Synaptic strength at the temporoammonic input to the hippocampal CA1 region in vivo is regulated by

NMDA receptors, metabotropic glutamate receptors and voltage-gated calcium channels. *Neuroscience, 309*, 191-199. doi: 10.1016/j.neuroscience.2015.03.014

Amaral, D. G., Scharfman, H. E., & Lavenex, P. (2007). The dentate gyrus: fundamental neuroanatomical organization (dentate gyrus for dummies). *Prog Brain Res, 163*, 3-22. doi: 10.1016/S0079-6123(07)63001-5

Amaral, D. G., & Witter, M. P. (1989). The three-dimensional organization of the hippocampal formation: a review of anatomical data. *Neuroscience, 31*(3), 571-591.

Amir, R. E., Van den Veyver, I. B., Wan, M., Tran, C. Q., Francke, U., & Zoghbi, H. Y. (1999). Rett syndrome is caused by mutations in X-linked MECP2, encoding methyl-CpG-binding protein 2. *Nat Genet, 23*(2), 185-188. doi: 10.1038/13810

Antonarakis, S. E., Lyle, R., Dermitzakis, E. T., Reymond, A., & Deutsch, S. (2004). Chromosome 21 and down syndrome: from genomics to pathophysiology. *Nat Rev Genet, 5*(10), 725-738. doi: 10.1038/nrg1448

Antunes, M., & Biala, G. (2012). The novel object recognition memory: neurobiology, test procedure, and its modifications. *Cogn Process, 13*(2), 93-110. doi: 10.1007/s10339-011-0430-z

Arac, D., Chen, X., Khant, H. A., Ubach, J., Ludtke, S. J., Kikkawa, M., . . . Rizo, J. (2006). Close membrane-membrane proximity induced by Ca(2+)-dependent multivalent binding of synaptotagmin-1 to phospholipids. *Nat Struct Mol Biol, 13*(3), 209-217. doi: 10.1038/nsmb1056

Araki, Y., Zeng, M., Zhang, M., & Huganir, R. L. (2015). Rapid dispersion of SynGAP from synaptic spines triggers AMPA receptor insertion and spine enlargement during LTP. *Neuron, 85*(1), 173-189. doi: 10.1016/j.neuron.2014.12.023

Augustine, G. J., Charlton, M. P., & Smith, S. J. (1987). Calcium action in synaptic transmitter release. *Annu Rev Neurosci, 10*, 633-693. doi: 10.1146/annurev.ne.10.030187.003221

Bachman, K. E., Rountree, M. R., & Baylin, S. B. (2001). Dnmt3a and Dnmt3b are transcriptional repressors that exhibit unique localization properties to heterochromatin. *J Biol Chem, 276*(34), 32282-32287. doi: 10.1074/jbc.M104661200

Bagga, S., Bracht, J., Hunter, S., Massirer, K., Holtz, J., Eachus, R., & Pasquinelli, A. E. (2005). Regulation by let-7 and lin-4 miRNAs results in target mRNA degradation. *Cell, 122*(4), 553-563. doi: 10.1016/j.cell.2005.07.031

Bagheri-Fam, S., Argentaro, A., Svingen, T., Combes, A. N., Sinclair, A. H., Koopman, P., & Harley, V. R. (2011). Defective survival of proliferating Sertoli cells and androgen receptor function in a mouse model of the ATR-X syndrome. *Hum Mol Genet, 20*(11), 2213-2224. doi: 10.1093/hmg/ddr109

Bai, J., & Chapman, E. R. (2004). The C2 domains of synaptotagmin--partners in exocytosis. *Trends Biochem Sci, 29*(3), 143-151. doi: 10.1016/j.tibs.2004.01.008

Bardai, F. H., Verma, P., Smith, C., Rawat, V., Wang, L., & D'Mello, S. R. (2013). Disassociation of histone deacetylase-3 from normal huntingtin underlies mutant huntingtin neurotoxicity. *J Neurosci, 33*(29), 11833-11838. doi: 10.1523/JNEUROSCI.5831-12.2013

Barski, A., Cuddapah, S., Cui, K., Roh, T. Y., Schones, D. E., Wang, Z., . . . Zhao, K. (2007). High-resolution profiling of histone methylations in the human genome. *Cell, 129*(4), 823-837. doi: 10.1016/j.cell.2007.05.009

Bassett, A. R., Cooper, S. E., Ragab, A., & Travers, A. A. (2008). The chromatin remodelling factor dATRX is involved in heterochromatin formation. *PLoS One, 3*(5), e2099. doi: 10.1371/journal.pone.0002099

Bastaki, F., Nair, P., Mohamed, M., Malik, E. M., Helmi, M., Al-Ali, M. T., & Hamzeh, A. R. (2017). Identification of a novel CTCF mutation responsible for syndromic intellectual disability - a case report. *BMC Med Genet, 18*(1), 68. doi: 10.1186/s12881-017-0429-0

Baumann, C., & De La Fuente, R. (2009). ATRX marks the inactive X chromosome (Xi) in somatic cells and during imprinted X chromosome inactivation in trophoblast stem cells. *Chromosoma, 118*(2), 209-222. doi: 10.1007/s00412-008-0189-x

Baumann, C., Viveiros, M. M., & De La Fuente, R. (2010). Loss of maternal ATRX results in centromere instability and aneuploidy in the mammalian oocyte and pre-implantation embryo. *PLoS Genet, 6*(9), e1001137. doi: 10.1371/journal.pgen.1001137

Becker, J. T., & Olton, D. S. (1980). Object discrimination by rats: the role of frontal and hippocampal systems in retention and reversal. *Physiol Behav, 24*(1), 33-38.

Berube, N. G., Jagla, M., Smeenk, C., De Repentigny, Y., Kothary, R., & Picketts, D. J. (2002). Neurodevelopmental defects resulting from ATRX overexpression in transgenic mice. *Hum Mol Genet, 11*(3), 253-261.

Berube, N. G., Mangelsdorf, M., Jagla, M., Vanderluit, J., Garrick, D., Gibbons, R. J., . . . Picketts, D. J. (2005). The chromatin-remodeling protein ATRX is critical for

neuronal survival during corticogenesis. *J Clin Invest, 115*(2), 258-267. doi: 10.1172/JCI22329

Bérubé, N. G., Smeenk, C. A., & Picketts, D. J. (2000). Cell cycle-dependent phosphorylation of the ATRX protein correlates with changes in nuclear matrix and chromatin association. *Hum Mol Genet, 9*(4), 539-547.

Billuart, P., Bienvenu, T., Ronce, N., des Portes, V., Vinet, M. C., Zemni, R., . . . Chelly, J. (1998). Oligophrenin 1 encodes a rho-GAP protein involved in X-linked mental retardation. *Pathol Biol (Paris), 46*(9), 678.

Bird, C. M., & Burgess, N. (2008). The hippocampus and memory: insights from spatial processing. *Nat Rev Neurosci, 9*(3), 182-194. doi: 10.1038/nrn2335

Bliss, T. V., & Gardner-Medwin, A. R. (1973). Long-lasting potentiation of synaptic transmission in the dentate area of the unanaestetized rabbit following stimulation of the perforant path. *J Physiol, 232*(2), 357-374.

Boglari, G., Erhardt, P., Cooper, G. M., & Szeberenyi, J. (1998). Intact Ras function is required for sustained activation and nuclear translocation of extracellular signal-regulated kinases in nerve growth factor-stimulated PC12 cells. *Eur J Cell Biol, 75*(1), 54-58. doi: 10.1016/S0171-9335(98)80046-0

Bongmba, O. Y., Martinez, L. A., Elhardt, M. E., Butler, K., & Tejada-Simon, M. V. (2011). Modulation of dendritic spines and synaptic function by Rac1: a possible link to Fragile X syndrome pathology. *Brain Res, 1399*, 79-95. doi: 10.1016/j.brainres.2011.05.020

Borrie, S. C., Brems, H., Legius, E., & Bagni, C. (2017). Cognitive Dysfunctions in Intellectual Disabilities: The Contributions of the Ras-MAPK and PI3K-AKT-mTOR Pathways. *Annu Rev Genomics Hum Genet, 18*, 115-142. doi: 10.1146/annurev-genom-091416-035332

Bowen, M. E., Weninger, K., Ernst, J., Chu, S., & Brunger, A. T. (2005). Single-molecule studies of synaptotagmin and complexin binding to the SNARE complex. *Biophys J, 89*(1), 690-702. doi: 10.1529/biophysj.104.054064

Bramham, C. R., Alme, M. N., Bittins, M., Kuipers, S. D., Nair, R. R., Pai, B., . . . Wibrand, K. (2010). The Arc of synaptic memory. *Exp Brain Res, 200*(2), 125-140. doi: 10.1007/s00221-009-1959-2

Bredt, D. S., & Nicoll, R. A. (2003). AMPA receptor trafficking at excitatory synapses. *Neuron, 40*(2), 361-379.

Brems, H., Chmara, M., Sahbatou, M., Denayer, E., Taniguchi, K., Kato, R., . . . Legius, E. (2007). Germline loss-of-function mutations in SPRED1 cause a

neurofibromatosis 1-like phenotype. *Nat Genet, 39*(9), 1120-1126. doi: 10.1038/ng2113

Brems, H., Pasmant, E., Van Minkelen, R., Wimmer, K., Upadhyaya, M., Legius, E., & Messiaen, L. (2012). Review and update of SPRED1 mutations causing Legius syndrome. *Hum Mutat, 33*(11), 1538-1546. doi: 10.1002/humu.22152

Brown, M. W., & Aggleton, J. P. (2001). Recognition memory: what are the roles of the perirhinal cortex and hippocampus? *Nat Rev Neurosci, 2*(1), 51-61. doi: 10.1038/35049064

Brucato, F. H., Levin, E. D., Mott, D. D., Lewis, D. V., Wilson, W. A., & Swartzwelder, H. S. (1996). Hippocampal long-term potentiation and spatial learning in the rat: effects of GABAB receptor blockade. *Neuroscience, 74*(2), 331-339.

Brun, V. H., Leutgeb, S., Wu, H. Q., Schwarcz, R., Witter, M. P., Moser, E. I., & Moser, M. B. (2008). Impaired spatial representation in CA1 after lesion of direct input from entorhinal cortex. *Neuron, 57*(2), 290-302. doi: 10.1016/j.neuron.2007.11.034

Brun, V. H., Otnass, M. K., Molden, S., Steffenach, H. A., Witter, M. P., Moser, M. B., & Moser, E. I. (2002). Place cells and place recognition maintained by direct entorhinal-hippocampal circuitry. *Science, 296*(5576), 2243-2246. doi: 10.1126/science.1071089

Budreck, E. C., & Scheiffele, P. (2007). Neuroligin-3 is a neuronal adhesion protein at GABAergic and glutamatergic synapses. *Eur J Neurosci, 26*(7), 1738-1748. doi: 10.1111/j.1460-9568.2007.05842.x

Cardoso, C., Lutz, Y., Mignon, C., Compe, E., Depetris, D., Mattei, M. G., . . . Colleaux, L. (2000). ATR-X mutations cause impaired nuclear location and altered DNA binding properties of the XNP/ATR-X protein. *J Med Genet, 37*(10), 746-751.

Chahrour, M., Jung, S. Y., Shaw, C., Zhou, X., Wong, S. T., Qin, J., & Zoghbi, H. Y. (2008). MeCP2, a key contributor to neurological disease, activates and represses transcription. *Science, 320*(5880), 1224-1229. doi: 10.1126/science.1153252

Chavez, J., Murillo-Maldonado, J. M., Bahena, V., Cruz, A. K., Castaneda-Sortibran, A., Rodriguez-Arnaiz, R., . . . Valadez-Graham, V. (2017). dAdd1 and dXNP prevent genome instability by maintaining HP1a localization at Drosophila telomeres. *Chromosoma, 126*(6), 697-712. doi: 10.1007/s00412-017-0634-9

Chen, C. M., Orefice, L. L., Chiu, S. L., LeGates, T. A., Hattar, S., Huganir, R. L., . . . Kuruvilla, R. (2017). Wnt5a is essential for hippocampal dendritic maintenance and spatial learning and memory in adult mice. *Proc Natl Acad Sci U S A, 114*(4), E619-E628. doi: 10.1073/pnas.1615792114

Chen, X., Vinade, L., Leapman, R. D., Petersen, J. D., Nakagawa, T., Phillips, T. M., . . . Reese, T. S. (2005). Mass of the postsynaptic density and enumeration of three key molecules. *Proc Natl Acad Sci U S A, 102*(32), 11551-11556. doi: 10.1073/pnas.0505359102

Clynes, D., & Gibbons, R. J. (2013). ATRX and the replication of structured DNA. *Curr Opin Genet Dev, 23*(3), 289-294. doi: 10.1016/j.gde.2013.01.005

Clynes, D., Jelinska, C., Xella, B., Ayyub, H., Scott, C., Mitson, M., . . . Gibbons, R. J. (2015). Suppression of the alternative lengthening of telomere pathway by the chromatin remodelling factor ATRX. *Nat Commun, 6*, 7538. doi: 10.1038/ncomms8538

Clynes, D., Jelinska, C., Xella, B., Ayyub, H., Taylor, S., Mitson, M., . . . Gibbons, R. J. (2014). ATRX dysfunction induces replication defects in primary mouse cells. *PLoS One, 9*(3), e92915. doi: 10.1371/journal.pone.0092915

Collingridge, G. L., Kehl, S. J., & McLennan, H. (1983). Excitatory amino acids in synaptic transmission in the Schaffer collateral-commissural pathway of the rat hippocampus. *J Physiol, 334*, 33-46.

Colonnier, M. (1968). Synaptic patterns on different cell types in the different laminae of the cat visual cortex. An electron microscope study. *Brain Res, 9*(2), 268-287.

Cook, D. R., Rossman, K. L., & Der, C. J. (2014). Rho guanine nucleotide exchange factors: regulators of Rho GTPase activity in development and disease. *Oncogene, 33*(31), 4021-4035. doi: 10.1038/onc.2013.362

Cowan, N. (2008). What are the differences between long-term, short-term, and working memory? *Prog Brain Res, 169*, 323-338. doi: 10.1016/S0079-6123(07)00020-9

Cummings, J. A., Mulkey, R. M., Nicoll, R. A., & Malenka, R. C. (1996). Ca2+ signaling requirements for long-term depression in the hippocampus. *Neuron, 16*(4), 825-833.

Curtis, C. E., & D'Esposito, M. (2003). Persistent activity in the prefrontal cortex during working memory. *Trends Cogn Sci, 7*(9), 415-423.

D'Esposito, M., & Postle, B. R. (2015). The cognitive neuroscience of working memory. *Annu Rev Psychol, 66*, 115-142. doi: 10.1146/annurev-psych-010814-015031

Deardorff, M. A., Kaur, M., Yaeger, D., Rampuria, A., Korolev, S., Pie, J., . . . Krantz, I. D. (2007). Mutations in cohesin complex members SMC3 and SMC1A cause a mild variant of cornelia de Lange syndrome with predominant mental retardation. *Am J Hum Genet, 80*(3), 485-494. doi: 10.1086/511888

Debrabant, J., Plasschaert, E., Caeyenberghs, K., Vingerhoets, G., Legius, E., Janssens, S., & Van Waelvelde, H. (2014). Deficient motor timing in children with neurofibromatosis type 1. *Res Dev Disabil, 35*(11), 3131-3138. doi: 10.1016/j.ridd.2014.07.059

DeFelipe, J., & Farinas, I. (1992). The pyramidal neuron of the cerebral cortex: morphological and chemical characteristics of the synaptic inputs. *Prog Neurobiol, 39*(6), 563-607.

Derkach, V., Barria, A., & Soderling, T. R. (1999). Ca2+/calmodulin-kinase II enhances channel conductance of alpha-amino-3-hydroxy-5-methyl-4-isoxazolepropionate type glutamate receptors. *Proc Natl Acad Sci U S A, 96*(6), 3269-3274.

Dhayalan, A., Tamas, R., Bock, I., Tattermusch, A., Dimitrova, E., Kudithipudi, S., . . . Jeltsch, A. (2011). The ATRX-ADD domain binds to H3 tail peptides and reads the combined methylation state of K4 and K9. *Hum Mol Genet, 20*(11), 2195-2203. doi: 10.1093/hmg/ddr107

Dobrunz, L. E., & Stevens, C. F. (1997). Heterogeneity of release probability, facilitation, and depletion at central synapses. *Neuron, 18*(6), 995-1008.

Duc, C., Benoit, M., Detourne, G., Simon, L., Poulet, A., Jung, M., . . . Probst, A. V. (2017). Arabidopsis ATRX Modulates H3.3 Occupancy and Fine-Tunes Gene Expression. *Plant Cell, 29*(7), 1773-1793. doi: 10.1105/tpc.16.00877

Dudek, S. M., & Bear, M. F. (1992). Homosynaptic long-term depression in area CA1 of hippocampus and effects of N-methyl-D-aspartate receptor blockade. *Proc Natl Acad Sci U S A, 89*(10), 4363-4367.

Ehlers, M. D., Zhang, S., Bernhadt, J. P., & Huganir, R. L. (1996). Inactivation of NMDA receptors by direct interaction of calmodulin with the NR1 subunit. *Cell, 84*(5), 745-755.

Eissenberg, J. C., & Elgin, S. C. (2000). The HP1 protein family: getting a grip on chromatin. *Curr Opin Genet Dev, 10*(2), 204-210.

Eliot, L. S., Dudai, Y., Kandel, E. R., & Abrams, T. W. (1989). Ca2+/calmodulin sensitivity may be common to all forms of neural adenylate cyclase. *Proc Natl Acad Sci U S A, 86*(23), 9564-9568.

Elston, G. N., & Fujita, I. (2014). Pyramidal cell development: postnatal spinogenesis, dendritic growth, axon growth, and electrophysiology. *Front Neuroanat, 8*, 78. doi: 10.3389/fnana.2014.00078

Emelyanov, A. V., Konev, A. Y., Vershilova, E., & Fyodorov, D. V. (2010). Protein complex of Drosophila ATRX/XNP and HP1a is required for the formation of

pericentric beta-heterochromatin in vivo. *J Biol Chem, 285*(20), 15027-15037. doi: 10.1074/jbc.M109.064790

Eustermann, S., Yang, J. C., Law, M. J., Amos, R., Chapman, L. M., Jelinska, C., . . . Neuhaus, D. (2011). Combinatorial readout of histone H3 modifications specifies localization of ATRX to heterochromatin. *Nat Struct Mol Biol, 18*(7), 777-782. doi: 10.1038/nsmb.2070

Feng, J., Chang, H., Li, E., & Fan, G. (2005). Dynamic expression of de novo DNA methyltransferases Dnmt3a and Dnmt3b in the central nervous system. *J Neurosci Res, 79*(6), 734-746. doi: 10.1002/jnr.20404

Feng, J., Zhou, Y., Campbell, S. L., Le, T., Li, E., Sweatt, J. D., . . . Fan, G. (2010). Dnmt1 and Dnmt3a maintain DNA methylation and regulate synaptic function in adult forebrain neurons. *Nat Neurosci, 13*(4), 423-430. doi: 10.1038/nn.2514

Fernandez-Chacon, R., Konigstorfer, A., Gerber, S. H., Garcia, J., Matos, M. F., Stevens, C. F., . . . Sudhof, T. C. (2001). Synaptotagmin I functions as a calcium regulator of release probability. *Nature, 410*(6824), 41-49. doi: 10.1038/35065004

Frank, M., & Kemler, R. (2002). Protocadherins. *Curr Opin Cell Biol, 14*(5), 557-562.

Frey, U., Huang, Y. Y., & Kandel, E. R. (1993). Effects of cAMP simulate a late stage of LTP in hippocampal CA1 neurons. *Science, 260*(5114), 1661-1664.

Fujita, Y., Masuda, K., Bando, M., Nakato, R., Katou, Y., Tanaka, T., . . . Yamashita, T. (2017). Decreased cohesin in the brain leads to defective synapse development and anxiety-related behavior. *J Exp Med, 214*(5), 1431-1452. doi: 10.1084/jem.20161517

Fukunaga, K., Muller, D., & Miyamoto, E. (1995). Increased phosphorylation of Ca2+/calmodulin-dependent protein kinase II and its endogenous substrates in the induction of long-term potentiation. *J Biol Chem, 270*(11), 6119-6124.

Gaarskjaer, F. B. (1978). Organization of the mossy fiber system of the rat studied in extended hippocampi. I. Terminal area related to number of granule and pyramidal cells. *J Comp Neurol, 178*(1), 49-72. doi: 10.1002/cne.901780104

Garrick, D., Sharpe, J. A., Arkell, R., Dobbie, L., Smith, A. J., Wood, W. G., . . . Gibbons, R. J. (2006). Loss of Atrx affects trophoblast development and the pattern of X-inactivation in extraembryonic tissues. *PLoS Genet, 2*(4), e58. doi: 10.1371/journal.pgen.0020058

Gecz, J., Pollard, H., Consalez, G., Villard, L., Stayton, C., Millasseau, P., . . . Fontes, M. (1994). Cloning and expression of the murine homologue of a putative human X-

linked nuclear protein gene closely linked to PGK1 in Xq13.3. *Hum Mol Genet, 3*(1), 39-44.

Geppert, M., Goda, Y., Hammer, R. E., Li, C., Rosahl, T. W., Stevens, C. F., & Sudhof, T. C. (1994). Synaptotagmin I: a major Ca2+ sensor for transmitter release at a central synapse. *Cell, 79*(4), 717-727.

Gibbons, R. J., Bachoo, S., Picketts, D. J., Aftimos, S., Asenbauer, B., Bergoffen, J., . . . Higgs, D. R. (1997). Mutations in transcriptional regulator ATRX establish the functional significance of a PHD-like domain. *Nat Genet, 17*(2), 146-148. doi: 10.1038/ng1097-146

Gibbons, R. J., & Higgs, D. R. (2000). Molecular-clinical spectrum of the ATR-X syndrome. *Am J Med Genet, 97*(3), 204-212. doi: 10.1002/1096-8628(200023)97:3<204::AID-AJMG1038>3.0.CO;2-X

Gibbons, R. J., Picketts, D. J., Villard, L., & Higgs, D. R. (1995). Mutations in a putative global transcriptional regulator cause X-linked mental retardation with alpha-thalassemia (ATR-X syndrome). *Cell, 80*(6), 837-845.

Gibbons, R. J., Suthers, G. K., Wilkie, A. O., Buckle, V. J., & Higgs, D. R. (1992). X-linked alpha-thalassemia/mental retardation (ATR-X) syndrome: localization to Xq12-q21.31 by X inactivation and linkage analysis. *Am J Hum Genet, 51*(5), 1136-1149.

Gibbons, R. J., Wada, T., Fisher, C. A., Malik, N., Mitson, M. J., Steensma, D. P., . . . Traeger-Synodinos, J. (2008). Mutations in the chromatin-associated protein ATRX. *Hum Mutat, 29*(6), 796-802. doi: 10.1002/humu.20734

Gibson, W. T., Hood, R. L., Zhan, S. H., Bulman, D. E., Fejes, A. P., Moore, R., . . . Jones, S. J. (2012). Mutations in EZH2 cause Weaver syndrome. *Am J Hum Genet, 90*(1), 110-118. doi: 10.1016/j.ajhg.2011.11.018

Giese, K. P., Fedorov, N. B., Filipkowski, R. K., & Silva, A. J. (1998). Autophosphorylation at Thr286 of the alpha calcium-calmodulin kinase II in LTP and learning. *Science, 279*(5352), 870-873.

Giraudo, C. G., Eng, W. S., Melia, T. J., & Rothman, J. E. (2006). A clamping mechanism involved in SNARE-dependent exocytosis. *Science, 313*(5787), 676-680. doi: 10.1126/science.1129450

Givens, B., & Olton, D. S. (1994). Local modulation of basal forebrain: effects on working and reference memory. *J Neurosci, 14*(6), 3578-3587.

Goldberg, A. D., Banaszynski, L. A., Noh, K. M., Lewis, P. W., Elsaesser, S. J., Stadler, S., . . . Allis, C. D. (2010). Distinct factors control histone variant H3.3 localization at specific genomic regions. *Cell, 140*(5), 678-691. doi: 10.1016/j.cell.2010.01.003

Goldman-Rakic, P. S. (1995). Cellular basis of working memory. *Neuron, 14*(3), 477-485.

Gottardi, C. J., & Gumbiner, B. M. (2001). Adhesion signaling: how beta-catenin interacts with its partners. *Curr Biol, 11*(19), R792-794.

Grant, S. G., O'Dell, T. J., Karl, K. A., Stein, P. L., Soriano, P., & Kandel, E. R. (1992). Impaired long-term potentiation, spatial learning, and hippocampal development in fyn mutant mice. *Science, 258*(5090), 1903-1910.

Gray, E. G. (1959). Electron microscopy of synaptic contacts on dendrite spines of the cerebral cortex. *Nature, 183*(4675), 1592-1593.

Gray, E. G. (1969). Electron microscopy of excitatory and inhibitory synapses: a brief review. *Prog Brain Res, 31*, 141-155. doi: 10.1016/S0079-6123(08)63235-5

Gregor, A., Oti, M., Kouwenhoven, E. N., Hoyer, J., Sticht, H., Ekici, A. B., . . . Zweier, C. (2013). De novo mutations in the genome organizer CTCF cause intellectual disability. *Am J Hum Genet, 93*(1), 124-131. doi: 10.1016/j.ajhg.2013.05.007

Guerrini, R., Shanahan, J. L., Carrozzo, R., Bonanni, P., Higgs, D. R., & Gibbons, R. J. (2000). A nonsense mutation of the ATRX gene causing mild mental retardation and epilepsy. *Ann Neurol, 47*(1), 117-121.

Hansen, K. F., Sakamoto, K., Wayman, G. A., Impey, S., & Obrietan, K. (2010). Transgenic miR132 alters neuronal spine density and impairs novel object recognition memory. *PLoS One, 5*(11), e15497. doi: 10.1371/journal.pone.0015497

Harakalova, M., van den Boogaard, M. J., Sinke, R., van Lieshout, S., van Tuil, M. C., Duran, K., . . . Ploos van Amstel, H. K. (2012). X-exome sequencing identifies a HDAC8 variant in a large pedigree with X-linked intellectual disability, truncal obesity, gynaecomastia, hypogonadism and unusual face. *J Med Genet, 49*(8), 539-543. doi: 10.1136/jmedgenet-2012-100921

Hayashi, Y., Shi, S. H., Esteban, J. A., Piccini, A., Poncer, J. C., & Malinow, R. (2000). Driving AMPA receptors into synapses by LTP and CaMKII: requirement for GluR1 and PDZ domain interaction. *Science, 287*(5461), 2262-2267.

Heaphy, C. M., de Wilde, R. F., Jiao, Y., Klein, A. P., Edil, B. H., Shi, C., . . . Meeker, A. K. (2011). Altered telomeres in tumors with ATRX and DAXX mutations. *Science, 333*(6041), 425. doi: 10.1126/science.1207313

Hebb, D. O. (1949). *Organization of Behavior*. New York: Wiley & Sons.

Heidelberger, R., Heinemann, C., Neher, E., & Matthews, G. (1994). Calcium dependence of the rate of exocytosis in a synaptic terminal. *Nature, 371*(6497), 513-515. doi: 10.1038/371513a0

Herring, B. E., & Nicoll, R. A. (2016). Kalirin and Trio proteins serve critical roles in excitatory synaptic transmission and LTP. *Proc Natl Acad Sci U S A, 113*(8), 2264-2269. doi: 10.1073/pnas.1600179113

Heynen, A. J., Quinlan, E. M., Bae, D. C., & Bear, M. F. (2000). Bidirectional, activity-dependent regulation of glutamate receptors in the adult hippocampus in vivo. *Neuron, 28*(2), 527-536.

Higgs, D. R., Vickers, M. A., Wilkie, A. O., Pretorius, I. M., Jarman, A. P., & Weatherall, D. J. (1989). A review of the molecular genetics of the human alpha-globin gene cluster. *Blood, 73*(5), 1081-1104.

Hjorth-Simonsen, A. (1972). Projection of the lateral part of the entorhinal area to the hippocampus and fascia dentata. *J Comp Neurol, 146*(2), 219-232. doi: 10.1002/cne.901460206

Hoon, M., Soykan, T., Falkenburger, B., Hammer, M., Patrizi, A., Schmidt, K. F., . . . Varoqueaux, F. (2011). Neuroligin-4 is localized to glycinergic postsynapses and regulates inhibition in the retina. *Proc Natl Acad Sci U S A, 108*(7), 3053-3058. doi: 10.1073/pnas.1006946108

Huang, Y. Y., & Kandel, E. R. (1994). Recruitment of long-lasting and protein kinase A-dependent long-term potentiation in the CA1 region of hippocampus requires repeated tetanization. *Learn Mem, 1*(1), 74-82.

Huber, K. M., Mauk, M. D., & Kelly, P. T. (1995). Distinct LTP induction mechanisms: contribution of NMDA receptors and voltage-dependent calcium channels. *J Neurophysiol, 73*(1), 270-279. doi: 10.1152/jn.1995.73.1.270

Hughes, J. R. (1958). Post-tetanic potentiation. *Physiol Rev, 38*(1), 91-113. doi: 10.1152/physrev.1958.38.1.91

Huh, M. S., Ivanochko, D., Hashem, L. E., Curtin, M., Delorme, M., Goodall, E., . . . Picketts, D. J. (2016). Stalled replication forks within heterochromatin require ATRX for protection. *Cell Death Dis, 7*, e2220. doi: 10.1038/cddis.2016.121

Huh, M. S., Price O'Dea, T., Ouazia, D., McKay, B. C., Parise, G., Parks, R. J., . . . Picketts, D. J. (2012). Compromised genomic integrity impedes muscle growth after Atrx inactivation. *J Clin Invest, 122*(12), 4412-4423. doi: 10.1172/JCI63765

Huh, M. S., Young, K. G., Yan, K., Price-O'Dea, T., & Picketts, D. J. (2017). Recovery from impaired muscle growth arises from prolonged postnatal accretion of myonuclei in Atrx mutant mice. *PLoS One, 12*(11), e0186989. doi: 10.1371/journal.pone.0186989

Humphreys, D. T., Westman, B. J., Martin, D. I., & Preiss, T. (2005). MicroRNAs control translation initiation by inhibiting eukaryotic initiation factor 4E/cap and poly(A) tail function. *Proc Natl Acad Sci U S A, 102*(47), 16961-16966. doi: 10.1073/pnas.0506482102

Hung, A. Y., & Sheng, M. (2002). PDZ domains: structural modules for protein complex assembly. *J Biol Chem, 277*(8), 5699-5702. doi: 10.1074/jbc.R100065200

Hyman, B. T., Van Hoesen, G. W., Kromer, L. J., & Damasio, A. R. (1986). Perforant pathway changes and the memory impairment of Alzheimer's disease. *Ann Neurol, 20*(4), 472-481. doi: 10.1002/ana.410200406

Ichtchenko, K., Hata, Y., Nguyen, T., Ullrich, B., Missler, M., Moomaw, C., & Sudhof, T. C. (1995). Neuroligin 1: a splice site-specific ligand for beta-neurexins. *Cell, 81*(3), 435-443.

Ichtchenko, K., Nguyen, T., & Sudhof, T. C. (1996). Structures, alternative splicing, and neurexin binding of multiple neuroligins. *J Biol Chem, 271*(5), 2676-2682.

Isaac, J. T., Ashby, M. C., & McBain, C. J. (2007). The role of the GluR2 subunit in AMPA receptor function and synaptic plasticity. *Neuron, 54*(6), 859-871. doi: 10.1016/j.neuron.2007.06.001

Ishizuka, N., Weber, J., & Amaral, D. G. (1990). Organization of intrahippocampal projections originating from CA3 pyramidal cells in the rat. *J Comp Neurol, 295*(4), 580-623. doi: 10.1002/cne.902950407

Iwase, S., Xiang, B., Ghosh, S., Ren, T., Lewis, P. W., Cochrane, J. C., . . . Shi, Y. (2011). ATRX ADD domain links an atypical histone methylation recognition mechanism to human mental-retardation syndrome. *Nat Struct Mol Biol, 18*(7), 769-776. doi: 10.1038/nsmb.2062

James, A. B., Conway, A. M., & Morris, B. J. (2005). Genomic profiling of the neuronal target genes of the plasticity-related transcription factor -- Zif268. *J Neurochem, 95*(3), 796-810. doi: 10.1111/j.1471-4159.2005.03400.x

Jiao, Y., Killela, P. J., Reitman, Z. J., Rasheed, A. B., Heaphy, C. M., de Wilde, R. F., . . . Yan, H. (2012). Frequent ATRX, CIC, FUBP1 and IDH1 mutations refine the classification of malignant gliomas. *Oncotarget, 3*(7), 709-722. doi: 10.18632/oncotarget.588

Joilin, G., Guevremont, D., Ryan, B., Claudianos, C., Cristino, A. S., Abraham, W. C., & Williams, J. M. (2014). Rapid regulation of microRNA following induction of long-term potentiation in vivo. *Front Mol Neurosci, 7,* 98. doi: 10.3389/fnmol.2014.00098

Kaas, G. A., Zhong, C., Eason, D. E., Ross, D. L., Vachhani, R. V., Ming, G. L., . . . Sweatt, J. D. (2013). TET1 controls CNS 5-methylcytosine hydroxylation, active DNA demethylation, gene transcription, and memory formation. *Neuron, 79*(6), 1086-1093. doi: 10.1016/j.neuron.2013.08.032

Kalil, K., & Dent, E. W. (2014). Branch management: mechanisms of axon branching in the developing vertebrate CNS. *Nat Rev Neurosci, 15*(1), 7-18. doi: 10.1038/nrn3650

Kannan, K., Inagaki, A., Silber, J., Gorovets, D., Zhang, J., Kastenhuber, E. R., . . . Huse, J. T. (2012). Whole-exome sequencing identifies ATRX mutation as a key molecular determinant in lower-grade glioma. *Oncotarget, 3*(10), 1194-1203. doi: 10.18632/oncotarget.689

Kass, S. U., Pruss, D., & Wolffe, A. P. (1997). How does DNA methylation repress transcription? *Trends Genet, 13*(11), 444-449.

Katz, B., & Miledi, R. (1968). The role of calcium in neuromuscular facilitation. *J Physiol, 195*(2), 481-492.

Kernohan, K. D., Jiang, Y., Tremblay, D. C., Bonvissuto, A. C., Eubanks, J. H., Mann, M. R., & Berube, N. G. (2010). ATRX partners with cohesin and MeCP2 and contributes to developmental silencing of imprinted genes in the brain. *Dev Cell, 18*(2), 191-202. doi: 10.1016/j.devcel.2009.12.017

Kernohan, K. D., Vernimmen, D., Gloor, G. B., & Berube, N. G. (2014). Analysis of neonatal brain lacking ATRX or MeCP2 reveals changes in nucleosome density, CTCF binding and chromatin looping. *Nucleic Acids Res, 42*(13), 8356-8368. doi: 10.1093/nar/gku564

Khelfaoui, M., Denis, C., van Galen, E., de Bock, F., Schmitt, A., Houbron, C., . . . Billuart, P. (2007). Loss of X-linked mental retardation gene oligophrenin1 in mice impairs spatial memory and leads to ventricular enlargement and dendritic spine immaturity. *J Neurosci, 27*(35), 9439-9450. doi: 10.1523/JNEUROSCI.2029-07.2007

Kim, C. H., Heath, C. J., Kent, B. A., Bussey, T. J., & Saksida, L. M. (2015). The role of the dorsal hippocampus in two versions of the touchscreen automated paired associates learning (PAL) task for mice. *Psychopharmacology (Berl), 232*(21-22), 3899-3910. doi: 10.1007/s00213-015-3949-3

Knowles, W. D. (1992). Normal anatomy and neurophysiology of the hippocampal formation. *J Clin Neurophysiol, 9*(2), 252-263.

Kochinke, K., Zweier, C., Nijhof, B., Fenckova, M., Cizek, P., Honti, F., . . . Schenck, A. (2016). Systematic Phenomics Analysis Deconvolutes Genes Mutated in Intellectual Disability into Biologically Coherent Modules. *Am J Hum Genet, 98*(1), 149-164. doi: 10.1016/j.ajhg.2015.11.024

Kornau, H. C., Schenker, L. T., Kennedy, M. B., & Seeburg, P. H. (1995). Domain interaction between NMDA receptor subunits and the postsynaptic density protein PSD-95. *Science, 269*(5231), 1737-1740.

Kourmouli, N., Sun, Y. M., van der Sar, S., Singh, P. B., & Brown, J. P. (2005). Epigenetic regulation of mammalian pericentric heterochromatin in vivo by HP1. *Biochem Biophys Res Commun, 337*(3), 901-907. doi: 10.1016/j.bbrc.2005.09.132

Krantz, I. D., McCallum, J., DeScipio, C., Kaur, M., Gillis, L. A., Yaeger, D., . . . Jackson, L. G. (2004). Cornelia de Lange syndrome is caused by mutations in NIPBL, the human homolog of Drosophila melanogaster Nipped-B. *Nat Genet, 36*(6), 631-635. doi: 10.1038/ng1364

Kuhn, H. G., Dickinson-Anson, H., & Gage, F. H. (1996). Neurogenesis in the dentate gyrus of the adult rat: age-related decrease of neuronal progenitor proliferation. *J Neurosci, 16*(6), 2027-2033.

Kurotaki, N., Imaizumi, K., Harada, N., Masuno, M., Kondoh, T., Nagai, T., . . . Matsumoto, N. (2002). Haploinsufficiency of NSD1 causes Sotos syndrome. *Nat Genet, 30*(4), 365-366. doi: 10.1038/ng863

Landis, D. M., Hall, A. K., Weinstein, L. A., & Reese, T. S. (1988). The organization of cytoplasm at the presynaptic active zone of a central nervous system synapse. *Neuron, 1*(3), 201-209.

Lanfranco, F., Kamischke, A., Zitzmann, M., & Nieschlag, E. (2004). Klinefelter's syndrome. *Lancet, 364*(9430), 273-283. doi: 10.1016/S0140-6736(04)16678-6

Larson, J., Wong, D., & Lynch, G. (1986). Patterned stimulation at the theta frequency is optimal for the induction of hippocampal long-term potentiation. *Brain Res, 368*(2), 347-350.

Laurberg, S. (1979). Commissural and intrinsic connections of the rat hippocampus. *J Comp Neurol, 184*(4), 685-708. doi: 10.1002/cne.901840405

Law, M. J., Lower, K. M., Voon, H. P., Hughes, J. R., Garrick, D., Viprakasit, V., . . . Gibbons, R. J. (2010). ATR-X syndrome protein targets tandem repeats and

influences allele-specific expression in a size-dependent manner. *Cell, 143*(3), 367-378. doi: 10.1016/j.cell.2010.09.023

Lechner, M. S., Schultz, D. C., Negorev, D., Maul, G. G., & Rauscher, F. J., 3rd. (2005). The mammalian heterochromatin protein 1 binds diverse nuclear proteins through a common motif that targets the chromoshadow domain. *Biochem Biophys Res Commun, 331*(4), 929-937. doi: 10.1016/j.bbrc.2005.04.016

Lee, D. Y., Hayes, J. J., Pruss, D., & Wolffe, A. P. (1993). A positive role for histone acetylation in transcription factor access to nucleosomal DNA. *Cell, 72*(1), 73-84.

Lehtonen, A., Howie, E., Trump, D., & Huson, S. M. (2013). Behaviour in children with neurofibromatosis type 1: cognition, executive function, attention, emotion, and social competence. *Dev Med Child Neurol, 55*(2), 111-125. doi: 10.1111/j.1469-8749.2012.04399.x

Leung, J. W., Ghosal, G., Wang, W., Shen, X., Wang, J., Li, L., & Chen, J. (2013). Alpha thalassemia/mental retardation syndrome X-linked gene product ATRX is required for proper replication restart and cellular resistance to replication stress. *J Biol Chem, 288*(9), 6342-6350. doi: 10.1074/jbc.M112.411603

Levy, M. A., Kernohan, K. D., Jiang, Y., & Berube, N. G. (2015). ATRX promotes gene expression by facilitating transcriptional elongation through guanine-rich coding regions. *Hum Mol Genet, 24*(7), 1824-1835. doi: 10.1093/hmg/ddu596

Lewis, P. W., Elsaesser, S. J., Noh, K. M., Stadler, S. C., & Allis, C. D. (2010). Daxx is an H3.3-specific histone chaperone and cooperates with ATRX in replication-independent chromatin assembly at telomeres. *Proc Natl Acad Sci U S A, 107*(32), 14075-14080. doi: 10.1073/pnas.1008850107

Lidsky, T. I., & Schneider, J. S. (2003). Lead neurotoxicity in children: basic mechanisms and clinical correlates. *Brain, 126*(Pt 1), 5-19.

Lister, R., Mukamel, E. A., Nery, J. R., Urich, M., Puddifoot, C. A., Johnson, N. D., . . . Ecker, J. R. (2013). Global epigenomic reconfiguration during mammalian brain development. *Science, 341*(6146), 1237905. doi: 10.1126/science.1237905

Liu, N., Balliano, A., & Hayes, J. J. (2011). Mechanism(s) of SWI/SNF-induced nucleosome mobilization. *Chembiochem, 12*(2), 196-204. doi: 10.1002/cbic.201000455

Liu, X. Y., Gerges, N., Korshunov, A., Sabha, N., Khuong-Quang, D. A., Fontebasso, A. M., . . . Jabado, N. (2012). Frequent ATRX mutations and loss of expression in adult diffuse astrocytic tumors carrying IDH1/IDH2 and TP53 mutations. *Acta Neuropathol, 124*(5), 615-625. doi: 10.1007/s00401-012-1031-3

Lovejoy, C. A., Li, W., Reisenweber, S., Thongthip, S., Bruno, J., de Lange, T., . . . Consortium, A. L. T. Starr Cancer. (2012). Loss of ATRX, genome instability, and an altered DNA damage response are hallmarks of the alternative lengthening of telomeres pathway. *PLoS Genet, 8*(7), e1002772. doi: 10.1371/journal.pgen.1002772

Lukashchuk, V., & Everett, R. D. (2010). Regulation of ICP0-null mutant herpes simplex virus type 1 infection by ND10 components ATRX and hDaxx. *J Virol, 84*(8), 4026-4040. doi: 10.1128/JVI.02597-09

Lunsky, Y., De Oliveira, C., Wilton, A., & Wodchis, W. (2019). High health care costs among adults with intellectual and developmental disabilities: a population-based study. *J Intellect Disabil Res, 63*(2), 124-137. doi: 10.1111/jir.12554

Malenka, R. C., & Nicoll, R. A. (1993). NMDA-receptor-dependent synaptic plasticity: multiple forms and mechanisms. *Trends Neurosci, 16*(12), 521-527.

Mayeaux, D. J., & Johnston, R. E. (2004). Discrimination of social odors and their locations: role of lateral entorhinal area. *Physiol Behav, 82*(4), 653-662. doi: 10.1016/j.physbeh.2004.06.002

McAllister, A. K. (2007). Dynamic aspects of CNS synapse formation. *Annu Rev Neurosci, 30*, 425-450. doi: 10.1146/annurev.neuro.29.051605.112830

McConkie-Rosell, A., Lachiewicz, A. M., Spiridigliozzi, G. A., Tarleton, J., Schoenwald, S., Phelan, M. C., . . . Brown, W. T. (1993). Evidence that methylation of the FMR-I locus is responsible for variable phenotypic expression of the fragile X syndrome. *Am J Hum Genet, 53*(4), 800-809.

McDowell, T. L., Gibbons, R. J., Sutherland, H., O'Rourke, D. M., Bickmore, W. A., Pombo, A., . . . Higgs, D. R. (1999). Localization of a putative transcriptional regulator (ATRX) at pericentromeric heterochromatin and the short arms of acrocentric chromosomes. *Proc Natl Acad Sci U S A, 96*(24), 13983-13988.

McEchron, M. D., Bouwmeester, H., Tseng, W., Weiss, C., & Disterhoft, J. F. (1998). Hippocampectomy disrupts auditory trace fear conditioning and contextual fear conditioning in the rat. *Hippocampus, 8*(6), 638-646. doi: 10.1002/(SICI)1098-1063(1998)8:6<638::AID-HIPO6>3.0.CO;2-Q

Medina, C. F., Mazerolle, C., Wang, Y., Berube, N. G., Coupland, S., Gibbons, R. J., . . . Picketts, D. J. (2009). Altered visual function and interneuron survival in Atrx knockout mice: inference for the human syndrome. *Hum Mol Genet, 18*(5), 966-977. doi: 10.1093/hmg/ddn424

Megias, M., Emri, Z., Freund, T. F., & Gulyas, A. I. (2001). Total number and distribution of inhibitory and excitatory synapses on hippocampal CA1 pyramidal cells. *Neuroscience, 102*(3), 527-540.

Migaud, M., Charlesworth, P., Dempster, M., Webster, L. C., Watabe, A. M., Makhinson, M., . . . Grant, S. G. (1998). Enhanced long-term potentiation and impaired learning in mice with mutant postsynaptic density-95 protein. *Nature, 396*(6710), 433-439. doi: 10.1038/24790

Missler, M., & Sudhof, T. C. (1998). Neurexins: three genes and 1001 products. *Trends Genet, 14*(1), 20-26. doi: 10.1016/S0168-9525(97)01324-3

Miyake, N., Tsurusaki, Y., & Matsumoto, N. (2014). Numerous BAF complex genes are mutated in Coffin-Siris syndrome. *Am J Med Genet C Semin Med Genet, 166C*(3), 257-261. doi: 10.1002/ajmg.c.31406

Moga, D. E., Calhoun, M. E., Chowdhury, A., Worley, P., Morrison, J. H., & Shapiro, M. L. (2004). Activity-regulated cytoskeletal-associated protein is localized to recently activated excitatory synapses. *Neuroscience, 125*(1), 7-11. doi: 10.1016/j.neuroscience.2004.02.004

Monyer, H., Sprengel, R., Schoepfer, R., Herb, A., Higuchi, M., Lomeli, H., . . . Seeburg, P. H. (1992). Heteromeric NMDA receptors: molecular and functional distinction of subtypes. *Science, 256*(5060), 1217-1221.

Moon, S. Y., Zang, H., & Zheng, Y. (2003). Characterization of a brain-specific Rho GTPase-activating protein, p200RhoGAP. *J Biol Chem, 278*(6), 4151-4159. doi: 10.1074/jbc.M207789200

Morgan, A., Gandin, I., Belcaro, C., Palumbo, P., Palumbo, O., Biamino, E., . . . Vozzi, D. (2015). Target sequencing approach intended to discover new mutations in non-syndromic intellectual disability. *Mutat Res, 781*, 32-36. doi: 10.1016/j.mrfmmm.2015.09.002

Morishita, W., Connor, J. H., Xia, H., Quinlan, E. M., Shenolikar, S., & Malenka, R. C. (2001). Regulation of synaptic strength by protein phosphatase 1. *Neuron, 32*(6), 1133-1148.

Morris, S. M., Acosta, M. T., Garg, S., Green, J., Huson, S., Legius, E., . . . Constantino, J. N. (2016). Disease Burden and Symptom Structure of Autism in Neurofibromatosis Type 1: A Study of the International NF1-ASD Consortium Team (INFACT). *JAMA Psychiatry, 73*(12), 1276-1284. doi: 10.1001/jamapsychiatry.2016.2600

Morys, J., Sadowski, M., Barcikowska, M., Maciejewska, B., & Narkiewicz, O. (1994). The second layer neurones of the entorhinal cortex and the perforant path in

physiological ageing and Alzheimer's disease. *Acta Neurobiol Exp (Wars), 54*(1), 47-53.

Muers, M. R., Sharpe, J. A., Garrick, D., Sloane-Stanley, J., Nolan, P. M., Hacker, T., . . . Gibbons, R. J. (2007). Defining the cause of skewed X-chromosome inactivation in X-linked mental retardation by use of a mouse model. *Am J Hum Genet, 80*(6), 1138-1149. doi: 10.1086/518369

Mulkey, R. M., & Malenka, R. C. (1992). Mechanisms underlying induction of homosynaptic long-term depression in area CA1 of the hippocampus. *Neuron, 9*(5), 967-975.

Murakoshi, H., Wang, H., & Yasuda, R. (2011). Local, persistent activation of Rho GTPases during plasticity of single dendritic spines. *Nature, 472*(7341), 100-104. doi: 10.1038/nature09823

Naber, P. A., Caballero-Bleda, M., Jorritsma-Byham, B., & Witter, M. P. (1997). Parallel input to the hippocampal memory system through peri- and postrhinal cortices. *Neuroreport, 8*(11), 2617-2621.

Nagerl, U. V., Eberhorn, N., Cambridge, S. B., & Bonhoeffer, T. (2004). Bidirectional activity-dependent morphological plasticity in hippocampal neurons. *Neuron, 44*(5), 759-767. doi: 10.1016/j.neuron.2004.11.016

Nan, X., Hou, J., Maclean, A., Nasir, J., Lafuente, M. J., Shu, X., . . . Bird, A. (2007). Interaction between chromatin proteins MECP2 and ATRX is disrupted by mutations that cause inherited mental retardation. *Proc Natl Acad Sci U S A, 104*(8), 2709-2714. doi: 10.1073/pnas.0608056104

Neul, J. L., Kaufmann, W. E., Glaze, D. G., Christodoulou, J., Clarke, A. J., Bahi-Buisson, N., . . . RettSearch, Consortium. (2010). Rett syndrome: revised diagnostic criteria and nomenclature. *Ann Neurol, 68*(6), 944-950. doi: 10.1002/ana.22124

Nguyen, P. V., Abel, T., & Kandel, E. R. (1994). Requirement of a critical period of transcription for induction of a late phase of LTP. *Science, 265*(5175), 1104-1107.

Nguyen, P. V., & Woo, N. H. (2003). Regulation of hippocampal synaptic plasticity by cyclic AMP-dependent protein kinases. *Prog Neurobiol, 71*(6), 401-437. doi: 10.1016/j.pneurobio.2003.12.003

Nicoll, R. A., Kauer, J. A., & Malenka, R. C. (1988). The current excitement in long-term potentiation. *Neuron, 1*(2), 97-103.

Nimchinsky, E. A., Sabatini, B. L., & Svoboda, K. (2002). Structure and function of dendritic spines. *Annu Rev Physiol, 64*, 313-353. doi: 10.1146/annurev.physiol.64.081501.160008

Nogami, T., Beppu, H., Tokoro, T., Moriguchi, S., Shioda, N., Fukunaga, K., . . . Kitajima, I. (2011). Reduced expression of the ATRX gene, a chromatin-remodeling factor, causes hippocampal dysfunction in mice. *Hippocampus, 21*(6), 678-687. doi: 10.1002/hipo.20782

O'Keefe, J., & Dostrovsky, J. (1971). The hippocampus as a spatial map. Preliminary evidence from unit activity in the freely-moving rat. *Brain Res, 34*(1), 171-175.

O'Sullivan, R. J., Arnoult, N., Lackner, D. H., Oganesian, L., Haggblom, C., Corpet, A., . . . Karlseder, J. (2014). Rapid induction of alternative lengthening of telomeres by depletion of the histone chaperone ASF1. *Nat Struct Mol Biol, 21*(2), 167-174. doi: 10.1038/nsmb.2754

Ono, S., Baux, G., Sekiguchi, M., Fossier, P., Morel, N. F., Nihonmatsu, I., . . . Takahashi, M. (1998). Regulatory roles of complexins in neurotransmitter release from mature presynaptic nerve terminals. *Eur J Neurosci, 10*(6), 2143-2152.

Ouellette-Kuntz, H., Garcin, N., Lewis, M. E., Minnes, P., Martin, C., & Holden, J. J. (2005). Addressing health disparities through promoting equity for individuals with intellectual disability. *Can J Public Health, 96 Suppl 2*, S8-22.

Palay, S. L. (1956). Synapses in the central nervous system. *J Biophys Biochem Cytol, 2*(4 Suppl), 193-202.

Pang, Z. P., Shin, O. H., Meyer, A. C., Rosenmund, C., & Sudhof, T. C. (2006). A gain-of-function mutation in synaptotagmin-1 reveals a critical role of Ca2+-dependent soluble N-ethylmaleimide-sensitive factor attachment protein receptor complex binding in synaptic exocytosis. *J Neurosci, 26*(48), 12556-12565. doi: 10.1523/JNEUROSCI.3804-06.2006

Penzes, P., Cahill, M. E., Jones, K. A., & Srivastava, D. P. (2008). Convergent CaMK and RacGEF signals control dendritic structure and function. *Trends Cell Biol, 18*(9), 405-413. doi: 10.1016/j.tcb.2008.07.002

Percy, A. K., Neul, J. L., Glaze, D. G., Motil, K. J., Skinner, S. A., Khwaja, O., . . . Barnes, K. (2010). Rett syndrome diagnostic criteria: lessons from the Natural History Study. *Ann Neurol, 68*(6), 951-955. doi: 10.1002/ana.22154

Philip, N., Chabrol, B., Lossi, A. M., Cardoso, C., Guerrini, R., Dobyns, W. B., . . . Villard, L. (2003). Mutations in the oligophrenin-1 gene (OPHN1) cause X linked congenital cerebellar hypoplasia. *J Med Genet, 40*(6), 441-446.

Picketts, D. J., Higgs, D. R., Bachoo, S., Blake, D. J., Quarrell, O. W., & Gibbons, R. J. (1996). ATRX encodes a novel member of the SNF2 family of proteins: mutations

point to a common mechanism underlying the ATR-X syndrome. *Hum Mol Genet, 5*(12), 1899-1907.

Pinto, D., Delaby, E., Merico, D., Barbosa, M., Merikangas, A., Klei, L., . . . Scherer, S. W. (2014). Convergence of genes and cellular pathways dysregulated in autism spectrum disorders. *Am J Hum Genet, 94*(5), 677-694. doi: 10.1016/j.ajhg.2014.03.018

Plath, K., Fang, J., Mlynarczyk-Evans, S. K., Cao, R., Worringer, K. A., Wang, H., . . . Zhang, Y. (2003). Role of histone H3 lysine 27 methylation in X inactivation. *Science, 300*(5616), 131-135. doi: 10.1126/science.1084274

Raisman, G., Cowan, W. M., & Powell, T. P. (1966). An experimental analysis of the efferent projection of the hippocampus. *Brain, 89*(1), 83-108.

Reijnders, M. R. F., Ansor, N. M., Kousi, M., Yue, W. W., Tan, P. L., Clarkson, K., . . . Banka, S. (2017). RAC1 Missense Mutations in Developmental Disorders with Diverse Phenotypes. *Am J Hum Genet, 101*(3), 466-477. doi: 10.1016/j.ajhg.2017.08.007

Reim, K., Mansour, M., Varoqueaux, F., McMahon, H. T., Sudhof, T. C., Brose, N., & Rosenmund, C. (2001). Complexins regulate a late step in Ca2+-dependent neurotransmitter release. *Cell, 104*(1), 71-81.

Remondes, M., & Schuman, E. M. (2003). Molecular mechanisms contributing to long-lasting synaptic plasticity at the temporoammonic-CA1 synapse. *Learn Mem, 10*(4), 247-252. doi: 10.1101/lm.59103

Renieri, A., Pescucci, C., Longo, I., Ariani, F., Mari, F., & Meloni, I. (2005). Non-syndromic X-linked mental retardation: from a molecular to a clinical point of view. *J Cell Physiol, 204*(1), 8-20. doi: 10.1002/jcp.20296

Reymann, K. G., & Frey, J. U. (2007). The late maintenance of hippocampal LTP: requirements, phases, 'synaptic tagging', 'late-associativity' and implications. *Neuropharmacology, 52*(1), 24-40. doi: 10.1016/j.neuropharm.2006.07.026

Ritchie, K., Seah, C., Moulin, J., Isaac, C., Dick, F., & Berube, N. G. (2008). Loss of ATRX leads to chromosome cohesion and congression defects. *J Cell Biol, 180*(2), 315-324. doi: 10.1083/jcb.200706083

Rizzo, A., Salvati, E., Porru, M., D'Angelo, C., Stevens, M. F., D'Incalci, M., . . . Biroccio, A. (2009). Stabilization of quadruplex DNA perturbs telomere replication leading to the activation of an ATR-dependent ATM signaling pathway. *Nucleic Acids Res, 37*(16), 5353-5364. doi: 10.1093/nar/gkp582

Roelfsema, J. H., White, S. J., Ariyurek, Y., Bartholdi, D., Niedrist, D., Papadia, F., . . . Peters, D. J. (2005). Genetic heterogeneity in Rubinstein-Taybi syndrome: mutations in both the CBP and EP300 genes cause disease. *Am J Hum Genet, 76*(4), 572-580. doi: 10.1086/429130

Rudenko, A., Dawlaty, M. M., Seo, J., Cheng, A. W., Meng, J., Le, T., . . . Tsai, L. H. (2013). Tet1 is critical for neuronal activity-regulated gene expression and memory extinction. *Neuron, 79*(6), 1109-1122. doi: 10.1016/j.neuron.2013.08.003

Ruth, R. E., Collier, T. J., & Routtenberg, A. (1982). Topography between the entorhinal cortex and the dentate septotemporal axis in rats: I. Medial and intermediate entorhinal projecting cells. *J Comp Neurol, 209*(1), 69-78. doi: 10.1002/cne.902090107

Salomoni, P., & Khelifi, A. F. (2006). Daxx: death or survival protein? *Trends Cell Biol, 16*(2), 97-104. doi: 10.1016/j.tcb.2005.12.002

Sams, D. S., Nardone, S., Getselter, D., Raz, D., Tal, M., Rayi, P. R., . . . Elliott, E. (2016). Neuronal CTCF Is Necessary for Basal and Experience-Dependent Gene Regulation, Memory Formation, and Genomic Structure of BDNF and Arc. *Cell Rep, 17*(9), 2418-2430. doi: 10.1016/j.celrep.2016.11.004

Sanchez, R., & Zhou, M. M. (2011). The PHD finger: a versatile epigenome reader. *Trends Biochem Sci, 36*(7), 364-372. doi: 10.1016/j.tibs.2011.03.005

Santen, G. W., Aten, E., Sun, Y., Almomani, R., Gilissen, C., Nielsen, M., . . . Kriek, M. (2012). Mutations in SWI/SNF chromatin remodeling complex gene ARID1B cause Coffin-Siris syndrome. *Nat Genet, 44*(4), 379-380. doi: 10.1038/ng.2217

Sargolini, F., Fyhn, M., Hafting, T., McNaughton, B. L., Witter, M. P., Moser, M. B., & Moser, E. I. (2006). Conjunctive representation of position, direction, and velocity in entorhinal cortex. *Science, 312*(5774), 758-762. doi: 10.1126/science.1125572

Schaub, J. R., Lu, X., Doneske, B., Shin, Y. K., & McNew, J. A. (2006). Hemifusion arrest by complexin is relieved by Ca2+-synaptotagmin I. *Nat Struct Mol Biol, 13*(8), 748-750. doi: 10.1038/nsmb1124

Schenkel, L. C., Kernohan, K. D., McBride, A., Reina, D., Hodge, A., Ainsworth, P. J., . . . Sadikovic, B. (2017). Identification of epigenetic signature associated with alpha thalassemia/mental retardation X-linked syndrome. *Epigenetics Chromatin, 10*, 10. doi: 10.1186/s13072-017-0118-4

Schneiderman, J. I., Sakai, A., Goldstein, S., & Ahmad, K. (2009). The XNP remodeler targets dynamic chromatin in Drosophila. *Proc Natl Acad Sci U S A, 106*(34), 14472-14477. doi: 10.1073/pnas.0905816106

Schorge, S., & Colquhoun, D. (2003). Studies of NMDA receptor function and stoichiometry with truncated and tandem subunits. *J Neurosci, 23*(4), 1151-1158.

Schreiner, S., Burck, C., Glass, M., Groitl, P., Wimmer, P., Kinkley, S., . . . Dobner, T. (2013). Control of human adenovirus type 5 gene expression by cellular Daxx/ATRX chromatin-associated complexes. *Nucleic Acids Res, 41*(6), 3532-3550. doi: 10.1093/nar/gkt064

Schwartzentruber, J., Korshunov, A., Liu, X. Y., Jones, D. T., Pfaff, E., Jacob, K., . . . Jabado, N. (2012). Driver mutations in histone H3.3 and chromatin remodelling genes in paediatric glioblastoma. *Nature, 482*(7384), 226-231. doi: 10.1038/nature10833

Scoville, W. B., & Milner, B. (1957). Loss of recent memory after bilateral hippocampal lesions. *J Neurol Neurosurg Psychiatry, 20*(1), 11-21.

Seah, C., Levy, M. A., Jiang, Y., Mokhtarzada, S., Higgs, D. R., Gibbons, R. J., & Berube, N. G. (2008). Neuronal death resulting from targeted disruption of the Snf2 protein ATRX is mediated by p53. *J Neurosci, 28*(47), 12570-12580. doi: 10.1523/JNEUROSCI.4048-08.2008

Shang, L., Cho, M. T., Retterer, K., Folk, L., Humberson, J., Rohena, L., . . . Chung, W. K. (2015). Mutations in ARID2 are associated with intellectual disabilities. *Neurogenetics, 16*(4), 307-314. doi: 10.1007/s10048-015-0454-0

Shapiro, L., & Colman, D. R. (1999). The diversity of cadherins and implications for a synaptic adhesive code in the CNS. *Neuron, 23*(3), 427-430.

Sheng, M., & Kim, M. J. (2002). Postsynaptic signaling and plasticity mechanisms. *Science, 298*(5594), 776-780. doi: 10.1126/science.1075333

Shioda, N., Beppu, H., Fukuda, T., Li, E., Kitajima, I., & Fukunaga, K. (2011). Aberrant calcium/calmodulin-dependent protein kinase II (CaMKII) activity is associated with abnormal dendritic spine morphology in the ATRX mutant mouse brain. *J Neurosci, 31*(1), 346-358. doi: 10.1523/JNEUROSCI.4816-10.2011

Shioda, N., Yabuki, Y., Yamaguchi, K., Onozato, M., Li, Y., Kurosawa, K., . . . Fukunaga, K. (2018). Targeting G-quadruplex DNA as cognitive function therapy for ATR-X syndrome. *Nat Med, 24*(6), 802-813. doi: 10.1038/s41591-018-0018-6

Siegert, S., Seo, J., Kwon, E. J., Rudenko, A., Cho, S., Wang, W., . . . Tsai, L. H. (2015). The schizophrenia risk gene product miR-137 alters presynaptic plasticity. *Nat Neurosci, 18*(7), 1008-1016. doi: 10.1038/nn.4023

Silva, A. J., Wang, Y., Paylor, R., Wehner, J. M., Stevens, C. F., & Tonegawa, S. (1992). Alpha calcium/calmodulin kinase II mutant mice: deficient long-term potentiation and impaired spatial learning. *Cold Spring Harb Symp Quant Biol, 57,* 527-539.

Slotnick, S. D., Moo, L. R., Segal, J. B., & Hart, J., Jr. (2003). Distinct prefrontal cortex activity associated with item memory and source memory for visual shapes. *Brain Res Cogn Brain Res, 17*(1), 75-82.

Solomon, L. A., Li, J. R., Berube, N. G., & Beier, F. (2009). Loss of ATRX in chondrocytes has minimal effects on skeletal development. *PLoS One, 4*(9), e7106. doi: 10.1371/journal.pone.0007106

Song, J. Y., Ichtchenko, K., Sudhof, T. C., & Brose, N. (1999). Neuroligin 1 is a postsynaptic cell-adhesion molecule of excitatory synapses. *Proc Natl Acad Sci U S A, 96*(3), 1100-1105.

Squire, L. R., Amaral, D. G., & Press, G. A. (1990). Magnetic resonance imaging of the hippocampal formation and mammillary nuclei distinguish medial temporal lobe and diencephalic amnesia. *J Neurosci, 10*(9), 3106-3117.

Stayton, C. L., Dabovic, B., Gulisano, M., Gecz, J., Broccoli, V., Giovanazzi, S., . . . et al. (1994). Cloning and characterization of a new human Xq13 gene, encoding a putative helicase. *Hum Mol Genet, 3*(11), 1957-1964.

Steward, O. (1976). Topographic organization of the projections from the entorhinal area to the hippocampal formation of the rat. *J Comp Neurol, 167*(3), 285-314. doi: 10.1002/cne.901670303

Steward, O., Wallace, C. S., Lyford, G. L., & Worley, P. F. (1998). Synaptic activation causes the mRNA for the IEG Arc to localize selectively near activated postsynaptic sites on dendrites. *Neuron, 21*(4), 741-751.

Strack, S., & Colbran, R. J. (1998). Autophosphorylation-dependent targeting of calcium/ calmodulin-dependent protein kinase II by the NR2B subunit of the N-methyl- D-aspartate receptor. *J Biol Chem, 273*(33), 20689-20692.

Sutherland, R. J., & McDonald, R. J. (1990). Hippocampus, amygdala, and memory deficits in rats. *Behav Brain Res, 37*(1), 57-79.

Sutton, M. A., & Schuman, E. M. (2006). Dendritic protein synthesis, synaptic plasticity, and memory. *Cell, 127*(1), 49-58. doi: 10.1016/j.cell.2006.09.014

Sytnyk, V., Leshchyns'ka, I., Nikonenko, A. G., & Schachner, M. (2006). NCAM promotes assembly and activity-dependent remodeling of the postsynaptic signaling complex. *J Cell Biol, 174*(7), 1071-1085. doi: 10.1083/jcb.200604145

Tamming, R. J., Siu, J. R., Jiang, Y., Prado, M. A., Beier, F., & Berube, N. G. (2017). Mosaic expression of Atrx in the mouse central nervous system causes memory deficits. *Dis Model Mech, 10*(2), 119-126. doi: 10.1242/dmm.027482

Tang, J., Maximov, A., Shin, O. H., Dai, H., Rizo, J., & Sudhof, T. C. (2006). A complexin/synaptotagmin 1 switch controls fast synaptic vesicle exocytosis. *Cell, 126*(6), 1175-1187. doi: 10.1016/j.cell.2006.08.030

Tang, J., Wu, S., Liu, H., Stratt, R., Barak, O. G., Shiekhattar, R., . . . Yang, X. (2004). A novel transcription regulatory complex containing death domain-associated protein and the ATR-X syndrome protein. *J Biol Chem, 279*(19), 20369-20377. doi: 10.1074/jbc.M401321200

Tang, L., Nogales, E., & Ciferri, C. (2010). Structure and function of SWI/SNF chromatin remodeling complexes and mechanistic implications for transcription. *Prog Biophys Mol Biol, 102*(2-3), 122-128. doi: 10.1016/j.pbiomolbio.2010.05.001

Tao, C. L., Liu, Y. T., Sun, R., Zhang, B., Qi, L., Shivakoti, S., . . . Bi, G. Q. (2018). Differentiation and Characterization of Excitatory and Inhibitory Synapses by Cryo-electron Tomography and Correlative Microscopy. *J Neurosci, 38*(6), 1493-1510. doi: 10.1523/JNEUROSCI.1548-17.2017

Thomson, S., Mahadevan, L. C., & Clayton, A. L. (1999). MAP kinase-mediated signalling to nucleosomes and immediate-early gene induction. *Semin Cell Dev Biol, 10*(2), 205-214. doi: 10.1006/scdb.1999.0302

Tokumaru, H., Umayahara, K., Pellegrini, L. L., Ishizuka, T., Saisu, H., Betz, H., . . . Abe, T. (2001). SNARE complex oligomerization by synaphin/complexin is essential for synaptic vesicle exocytosis. *Cell, 104*(3), 421-432.

Tsai, K., Thikmyanova, N., Wojcechowskyj, J. A., Delecluse, H. J., & Lieberman, P. M. (2011). EBV tegument protein BNRF1 disrupts DAXX-ATRX to activate viral early gene transcription. *PLoS Pathog, 7*(11), e1002376. doi: 10.1371/journal.ppat.1002376

Vago, D. R., & Kesner, R. P. (2008). Disruption of the direct perforant path input to the CA1 subregion of the dorsal hippocampus interferes with spatial working memory and novelty detection. *Behav Brain Res, 189*(2), 273-283. doi: 10.1016/j.bbr.2008.01.002

Valadez-Graham, V., Yoshioka, Y., Velazquez, O., Kawamori, A., Vazquez, M., Neumann, A., . . . Zurita, M. (2012). XNP/dATRX interacts with DREF in the chromatin to regulate gene expression. *Nucleic Acids Res, 40*(4), 1460-1474. doi: 10.1093/nar/gkr865

van Bokhoven, H. (2011). Genetic and epigenetic networks in intellectual disabilities. *Annu Rev Genet, 45*, 81-104. doi: 10.1146/annurev-genet-110410-132512

Van Esch, H., Bauters, M., Ignatius, J., Jansen, M., Raynaud, M., Hollanders, K., . . . Froyen, G. (2005). Duplication of the MECP2 region is a frequent cause of severe mental retardation and progressive neurological symptoms in males. *Am J Hum Genet, 77*(3), 442-453. doi: 10.1086/444549

van Groen, T., Miettinen, P., & Kadish, I. (2003). The entorhinal cortex of the mouse: organization of the projection to the hippocampal formation. *Hippocampus, 13*(1), 133-149. doi: 10.1002/hipo.10037

Varoqueaux, F., Jamain, S., & Brose, N. (2004). Neuroligin 2 is exclusively localized to inhibitory synapses. *Eur J Cell Biol, 83*(9), 449-456. doi: 10.1078/0171-9335-00410

Verma, P., Augustine, G. J., Ammar, M. R., Tashiro, A., & Cohen, S. M. (2015). A neuroprotective role for microRNA miR-1000 mediated by limiting glutamate excitotoxicity. *Nat Neurosci, 18*(3), 379-385. doi: 10.1038/nn.3935

Veyrac, A., Besnard, A., Caboche, J., Davis, S., & Laroche, S. (2014). The transcription factor Zif268/Egr1, brain plasticity, and memory. *Prog Mol Biol Transl Sci, 122*, 89-129. doi: 10.1016/B978-0-12-420170-5.00004-0

Villard, L., & Fontes, M. (2002). Alpha-thalassemia/mental retardation syndrome, X-Linked (ATR-X, MIM #301040, ATR-X/XNP/XH2 gene MIM #300032). *Eur J Hum Genet, 10*(4), 223-225. doi: 10.1038/sj.ejhg.5200800

Vissers, L. E., Gilissen, C., & Veltman, J. A. (2016). Genetic studies in intellectual disability and related disorders. *Nat Rev Genet, 17*(1), 9-18. doi: 10.1038/nrg3999

Voon, H. P., Hughes, J. R., Rode, C., De La Rosa-Velazquez, I. A., Jenuwein, T., Feil, R., . . . Gibbons, R. J. (2015). ATRX Plays a Key Role in Maintaining Silencing at Interstitial Heterochromatic Loci and Imprinted Genes. *Cell Rep, 11*(3), 405-418. doi: 10.1016/j.celrep.2015.03.036

Vorhees, C. V., & Williams, M. T. (2006). Morris water maze: procedures for assessing spatial and related forms of learning and memory. *Nat Protoc, 1*(2), 848-858. doi: 10.1038/nprot.2006.116

Vossler, M. R., Yao, H., York, R. D., Pan, M. G., Rim, C. S., & Stork, P. J. (1997). cAMP activates MAP kinase and Elk-1 through a B-Raf- and Rap1-dependent pathway. *Cell, 89*(1), 73-82.

Wada, T., Ban, H., Matsufuji, M., Okamoto, N., Enomoto, K., Kurosawa, K., & Aida, N. (2013). Neuroradiologic features in X-linked alpha-thalassemia/mental retardation syndrome. *AJNR Am J Neuroradiol, 34*(10), 2034-2038. doi: 10.3174/ajnr.A3560

Wada, T., Sugie, H., Fukushima, Y., & Saitoh, S. (2005). Non-skewed X-inactivation may cause mental retardation in a female carrier of X-linked alpha-thalassemia/mental retardation syndrome (ATR-X): X-inactivation study of nine female carriers of ATR-X. *Am J Med Genet A, 138*(1), 18-20. doi: 10.1002/ajmg.a.30901

Wallace, M. R., Marchuk, D. A., Andersen, L. B., Letcher, R., Odeh, H. M., Saulino, A. M., . . . et al. (1990). Type 1 neurofibromatosis gene: identification of a large transcript disrupted in three NF1 patients. *Science, 249*(4965), 181-186.

Wang, P., Mei, F., Hu, J., Zhu, M., Qi, H., Chen, X., . . . Yin, Y. (2017). PTENalpha Modulates CaMKII Signaling and Controls Contextual Fear Memory and Spatial Learning. *Cell Rep, 19*(12), 2627-2641. doi: 10.1016/j.celrep.2017.05.088

Watson, L. A., Solomon, L. A., Li, J. R., Jiang, Y., Edwards, M., Shin-ya, K., . . . Berube, N. G. (2013). Atrx deficiency induces telomere dysfunction, endocrine defects, and reduced life span. *J Clin Invest, 123*(5), 2049-2063. doi: 10.1172/JCI65634

Weatherall, D. J., Higgs, D. R., Bunch, C., Old, J. M., Hunt, D. M., Pressley, L., . . . Bebbington, D. (1981). Hemoglobin H disease and mental retardation: a new syndrome or a remarkable coincidence? *N Engl J Med, 305*(11), 607-612. doi: 10.1056/NEJM198109103051103

Weemaes, C. M., van Tol, M. J., Wang, J., van Ostaijen-ten Dam, M. M., van Eggermond, M. C., Thijssen, P. E., . . . van der Maarel, S. M. (2013). Heterogeneous clinical presentation in ICF syndrome: correlation with underlying gene defects. *Eur J Hum Genet, 21*(11), 1219-1225. doi: 10.1038/ejhg.2013.40

Wenthold, R. J., Petralia, R. S., Blahos, J., II, & Niedzielski, A. S. (1996). Evidence for multiple AMPA receptor complexes in hippocampal CA1/CA2 neurons. *J Neurosci, 16*(6), 1982-1989.

West, J. R., Chen, W. J., & Pantazis, N. J. (1994). Fetal alcohol syndrome: the vulnerability of the developing brain and possible mechanisms of damage. *Metab Brain Dis, 9*(4), 291-322.

Wilkie, A. O., Pembrey, M. E., Gibbons, R. J., Higgs, D. R., Porteous, M. E., Burn, J., & Winter, R. M. (1991). The non-deletion type of alpha thalassaemia/mental retardation: a recognisable dysmorphic syndrome with X linked inheritance. *J Med Genet, 28*(10), 724.

Witter, M. P., & Amaral, D. G. (1991). Entorhinal cortex of the monkey: V. Projections to the dentate gyrus, hippocampus, and subicular complex. *J Comp Neurol, 307*(3), 437-459. doi: 10.1002/cne.903070308

Wong, L. H., McGhie, J. D., Sim, M., Anderson, M. A., Ahn, S., Hannan, R. D., . . . Choo, K. H. (2010). ATRX interacts with H3.3 in maintaining telomere structural integrity in pluripotent embryonic stem cells. *Genome Res, 20*(3), 351-360. doi: 10.1101/gr.101477.109

Wood, M. A., Kaplan, M. P., Park, A., Blanchard, E. J., Oliveira, A. M., Lombardi, T. L., & Abel, T. (2005). Transgenic mice expressing a truncated form of CREB-binding protein (CBP) exhibit deficits in hippocampal synaptic plasticity and memory storage. *Learn Mem, 12*(2), 111-119. doi: 10.1101/lm.86605

Xu, G. L., Bestor, T. H., Bourc'his, D., Hsieh, C. L., Tommerup, N., Bugge, M., . . . Viegas-Pequignot, E. (1999). Chromosome instability and immunodeficiency syndrome caused by mutations in a DNA methyltransferase gene. *Nature, 402*(6758), 187-191. doi: 10.1038/46052

Xue, M., Reim, K., Chen, X., Chao, H. T., Deng, H., Rizo, J., . . . Rosenmund, C. (2007). Distinct domains of complexin I differentially regulate neurotransmitter release. *Nat Struct Mol Biol, 14*(10), 949-958. doi: 10.1038/nsmb1292

Xue, Y., Gibbons, R., Yan, Z., Yang, D., McDowell, T. L., Sechi, S., . . . Wang, W. (2003). The ATRX syndrome protein forms a chromatin-remodeling complex with Daxx and localizes in promyelocytic leukemia nuclear bodies. *Proc Natl Acad Sci U S A, 100*(19), 10635-10640. doi: 10.1073/pnas.1937626100

Yagi, T., & Takeichi, M. (2000). Cadherin superfamily genes: functions, genomic organization, and neurologic diversity. *Genes Dev, 14*(10), 1169-1180.

Zhang, J., Ji, F., Liu, Y., Lei, X., Li, H., Ji, G., . . . Jiao, J. (2014). Ezh2 regulates adult hippocampal neurogenesis and memory. *J Neurosci, 34*(15), 5184-5199. doi: 10.1523/JNEUROSCI.4129-13.2014

Zhou, Y., Wu, H., Li, S., Chen, Q., Cheng, X. W., Zheng, J., . . . Xiong, Z. Q. (2006). Requirement of TORC1 for late-phase long-term potentiation in the hippocampus. *PLoS One, 1*, e16. doi: 10.1371/journal.pone.0000016

Zhu, J. J., Qin, Y., Zhao, M., Van Aelst, L., & Malinow, R. (2002). Ras and Rap control AMPA receptor trafficking during synaptic plasticity. *Cell, 110*(4), 443-455.

Zola-Morgan, S., Squire, L. R., & Amaral, D. G. (1986). Human amnesia and the medial temporal region: enduring memory impairment following a bilateral lesion limited to field CA1 of the hippocampus. *J Neurosci, 6*(10), 2950-2967.

Zola-Morgan, S., Squire, L. R., Amaral, D. G., & Suzuki, W. A. (1989). Lesions of perirhinal and parahippocampal cortex that spare the amygdala and hippocampal formation produce severe memory impairment. *J Neurosci, 9*(12), 4355-4370.

Zuin, J., Dixon, J. R., van der Reijden, M. I., Ye, Z., Kolovos, P., Brouwer, R. W., . . . Wendt, K. S. (2014). Cohesin and CTCF differentially affect chromatin architecture and gene expression in human cells. *Proc Natl Acad Sci U S A, 111*(3), 996-1001. doi: 10.1073/pnas.1317788111

Chapter 2

2 Mosaic expression of *Atrx* in the mouse central nervous system causes memory deficits

The aim of the work outlined in this chapter was to determine the effects of ATRX loss in the mouse central nervous system (CNS) on learning and memory. This work has been published in Disease Models and Mechanisms in 2017 (doi: 10.1242/dmm.027482). My findings suggest that total loss of ATRX in the CNS in males during development is perinatal lethal, however mosaic expression of ATRX in females is viable. I found that mosaic expression of ATRX leads to endocrine effects and has a negative impact on learning and memory.

2.1 Introduction

Alpha thalassemia mental retardation, X-linked, or ATR-X syndrome, is an intellectual disability (ID) disorder that arises from mutations in the *ATRX* gene (OMIM 301040). This rare syndrome is characterized by severe developmental delay, hypotonia, mild α-thalassemia and moderate-to-severe ID (Gibbons et al., 1995). A recent study screened a cohort of nearly 1000 individuals with ID using targeted next-generation sequencing and identified ATRX variants as one of the most common causes of ID, reinforcing its importance in cognition (Grozeva et al., 2015). The ATRX protein is a SWI/SNF-type chromatin remodeller. The N-terminal region of the protein contains a histone reader domain that mediates interaction of the protein with histone H3 trimethylated at lysine 9 (H3K9me3) and unmethylated at lysine 4 (H3K4me0) (Dhayalan et al., 2011). A SWI/SNF2-type helicase domain is located in the C-terminal half of the protein and confers ATP-dependent chromatin remodelling activity (Aapola et al., 2000; Gibbons et al., 1997; Picketts et al., 1996). Several proteins have been shown to interact with ATRX, including MeCP2, HP1α, EZH2 and DAXX (Bérubé, Smeenk, & Picketts, 2000; Cardoso et al., 1998; Nan et al., 2007; Xue et al., 2003). DAXX is a histone chaperone for histone variant H3.3. In association with ATRX, DAXX deposits H3.3-containing nucleosomes at

telomeres and pericentromeric heterochromatin (Drane, Ouararhni, Depaux, Shuaib, & Hamiche, 2010; Lewis, Elsaesser, Noh, Stadler, & Allis, 2010).

Several studies have previously implicated ATRX in the regulation of gene expression through a variety of mechanisms. Chromatin immunoprecipitation (ChIP) sequencing for ATRX in human erythroblasts showed that the protein tends to bind GC-rich regions with high tendency to form G-quadruplexes. For example, ATRX was found to bind tandem repeats within the human α-globin gene cluster, and it was suggested that reduced expression of α- globin might be caused by replication-dependent mechanisms that would affect the expression of nearby genes (Law et al., 2010). The induction of replication stress was in fact detected in vivo upon inactivation of *Atrx* in either muscle or brain (Leung et al., 2013; Watson et al., 2013). More recently, our group demonstrated that loss of ATRX corresponds to decreased H3.3 incorporation and increased PolII occupancy in GC-rich gene bodies, including Neuroligin 4, an autism susceptibility gene (Levy, Kernohan, Jiang, & Berube, 2015).

Although the mechanisms by which ATRX modulates chromatin and genes is starting to be resolved, its function in neurons and cognitive processes is still obscure. To address this question, we generated mice with conditional inactivation of *Atrx* in the central nervous system (CNS) starting at early stages of neurogenesis. Although hemizygous male progeny died shortly after birth, heterozygous female mice (henceforth called *Atrx*-cHet), which exhibit mosaic expression of ATRX caused by random X-inactivation, survived to adulthood, allowing the investigation of neurobehavioural outcomes upon inactivation of *Atrx* in the brain.

2.2 Materials and Methods

2.2.1 Animal care and husbandry

Mice were exposed to a 12 h:12 h light–dark cycle and with water and chow ad libitum. The *Atrx*loxP mice have been described previously (Bérubé et al., 2005). *Atrx*^{loxP} mice (129svj) were mated with mice expressing Cre recombinase under the control of the Nestin

gene promoter (Bl6) (Tronche et al., 1999). The progeny include hemizygous male mice that produce no full-length ATRX protein in the CNS (*Atrx*f/y Cre+) and heterozygous female mice with approximately half the cells lacking ATRX protein as a result of the random pattern of X-inactivation (*Atrx*f/+ Cre+). Male and female littermate floxed mice lacking the Cre allele were used as controls. Genotyping of tail biopsies for the presence of the floxed and Cre alleles was performed as described previously (Bérubé et al., 2005; Seah et al., 2008). All procedures involving animals were conducted in accordance with the regulations of the Animals for Research Act of the province of Ontario and approved by the University of Western Ontario Animal Care and Use Committee (2017-048). Behavioural assessments started with less demanding tasks (grip force, open-field tests), followed by more demanding ones (Morris water maze). Experimenters followed ARRIVE guidelines: mouse groups were randomized, they were blind to the genotypes, and software-based analysis was used to score mouse performance in most of the tasks. All experiments were performed between 09.00 and 16.00 h.

2.2.2 Immunofluorescence staining

Mice were perfused and the brains fixed for 72 h with 4% paraformaldehyde in PBS and cryopreserved in 30% sucrose/PBS. Brains were flash frozen in Cryomatrix (Thermo Fisher Scientific) and sectioned as described previously (Ritchie, Watson, Davidson, Jiang, & Berube, 2014). For immunostaining, antigen retrieval was performed by incubating slides in 10 mM sodium citrate at 95°C for 10 min. Cooled slides were washed and incubated overnight in anti-ATRX rabbit polyclonal antibody (Santa Cruz Biotechnology, SC-15408; 1:200, H-300) (Watson et al., 2013) diluted in 0.3% Triton-X100 in PBS. Sections were washed and incubated with goat anti-rabbit Alexa Fluor 594 (Life Technologies) for 1 h. Sections were counterstained with DAPI and mounted with SlowFade Gold (Invitrogen). Cell counts were done in three control–KO littermate-matched pairs in a blinded manner.

2.2.3 Microscopy

All images were captured using an inverted microscope (DMI 6000b; Leica) with a digital camera (ORCA-ER; Hamamatsu). Openlab image software was used for manual image capture, and images were processed using the Volocity software (PerkinElmer).

2.2.4 Haematoxylin and eosin staining

Brain cryosections (8 μm thick) from 3-month-old mice were rehydrated in 70% ethanol for 2 min followed by tap water for 5 min. They were then placed in CAT Haematoxylin (Biocare) for 2 min, placed under running tap water for 1 min, and set in filtered Tasha's Bluing Solution (Biocare) for 30 s. The slides were placed under running tap water for 10 min and set in filtered Eosin Y (Fisher Scientific) for 2 min. Immediately afterwards, the cells were dehydrated in 70% ethanol for 30 s each, then 90% ethanol for 1 min and 100% ethanol for 2 min each. The slides were placed in xylene 3× for 5 min and mounted with Permount (Fisher Scientific) immediately after.

2.2.5 RT-qPCR

Total RNA was isolated from control and *Atrx*-cHet rostral cortex and hippocampus using the RNeasy Mini Kit (Qiagen) and reverse transcribed to cDNA using 1 μg RNA and SuperScript II Reverse Transcriptase (Invitrogen). cDNA was amplified in duplicate using primers in the following conditions: 95°C for 10 s, 55°C for 20 s and 72°C for 30 s for 35 cycles. Primers detected *Atrx* exons 17 and 18. Standard curves were generated for each primer pair. Primer efficiency (E) was calculated as $E=(10^{-1/slope}-1)\times 100\%$, where a desirable slope is −3.32 and $R2>0.990$. All data were corrected against β-actin.

2.2.6 ELISAs

Blood was collected from the inferior vena cava of P17 mice. One hundred microlitres of 0.5 M EDTA pH 7.0 per millilitre of blood collected was added to the blood sample and centrifuged at 21,000 g for 10 min at 4°C. Plasma supernatant was collected and kept frozen at −80°C. Plasma IGF-1 concentration was measured using a mouse IGF-1 ELISA kit

(R&D Systems, MG100). Plasma GH (Millipore, EZRMGH-45K) and T4 (Calbiotech, T4044T) were also measured by ELISA according to the manufacturers' instructions.

2.2.7 Bone staining and measurements

Skinned and eviscerated P17 mouse carcasses were fixed overnight in 95% ethanol and transferred to acetone overnight (Ulici et al., 2009). Fixed skeletons were stained in a 0.05% Alizarin Red, 0.015% Alcian Blue, 5% acetic acid in 70% ethanol solution for 7-14 days. Stained skeletons were cleaned in decreasing concentrations of potassium hydroxide (2, 1 and 0.5%) for several days and stored in 50:50 70% ethanol/glycerol solution. Alcian Blue and Alizarin Red-stained skeletons were imaged using an Olympus SP-57OUZ digital camera. The lengths of the tibia, femur and humerus, the width of the skull and the length of the foot from at least four different littermate pairs from both mouse models were imaged using the Zeiss Stereo Zoom Microscope Stemi SV6 and measured with a ruler accurate to 0.1 mm.

2.2.8 Behaviour analysis

2.2.8.1 Hindlimb clasping

Hindlimb clasping was measured by lifting mice up by the base of the tail. Clasping was scored on a scale of 0 (no clasping, limbs splayed) to 2 (clasping, wringing paws).

2.2.8.2 Grip force

Grip force, an indicator of muscular strength, was measured using a Grip Strength Meter (Columbus Instruments) (Solomon, Russell, Makar, Berube, & Beier, 2013). The meter was positioned horizontally, and the mice were held by the base of the tail and lowered towards the triangular pull bar. Once the mice had gripped the bar, the meter was calibrated, and the mice were gently pulled away from the apparatus. The force applied to the bar as the mice released it was recorded as peak tension (in Newtons). This test was repeated five times, with the highest and lowest value being removed for user error, and the remaining three values were averaged for the final grip strength.

2.2.8.3 Rotarod

For the Rotarod task, mice were placed on the Rotarod apparatus (San Diego Instruments) and rotation was increased from 5 to 35 rpm over 5 min. Latency to fall was recorded automatically. Ten trials were performed on the first day and four were performed on the second day. There was an inter-trial period of 10 min, during which the mice were placed in their home cage.

2.2.8.4 Treadmill

Training for the treadmill test occurred over 4 days (3 min day−1). On the first day, the incline was set to 5° and increased by 5° every day to a maximum of 20°. The initial speed was 8 m min−1, and the treadmill was accelerated by 1 m min−2. On the subsequent training days 2, 3 and 4, the initial speed was increased to 10, 11 and 12 m min−1, respectively, with constant acceleration. During testing on the fifth day, the initial speed was 12 m min−1 and accelerated to 20 m min−1 over the course of 15 min. Distance to exhaustion was measured, and the work performed (W, in joules) was calculated using the formula: W (J)=body weight (kg)×cos20°×9.8 (J kg−1×m)×distance (m).

2.2.8.5 Open field test

In the open-field test, locomotor activity was automatically recorded (AccuScan Instrument). The mice were placed in an arena with an area of 20 cm×20 cm with 30-cm-high walls. Mice were acclimated to the locomotor room for 10 min before testing. Locomotor activity was measured in 5 min intervals over 2 h, as previously described (Martyn et al., 2012).

2.2.8.6 Elevated plus maze

Animals were placed in the centre of the elevated plus maze (Med Associate) and their activity was recorded over 5 min. The total time spent in the open and closed arms was recorded using computer software (AnyMaze). The centre of the mouse body was used as an indicator of which zone they were in.

2.2.8.7 Y-maze

Spontaneous Y-maze alternation was measured using a symmetrical three-armed Y-maze as described (de Castro et al., 2009). Video tracking was performed using computer software (AnyMaze) and the order and number of entries into each arm recorded. Each mouse underwent one trial lasting 5 min. Spontaneous alternation was counted when a mouse entered all three arms in a row without visiting a previous arm.

2.2.8.8 Contextual fear conditioning

To measure contextual fear, mice were placed in a 20 cm×10 cm clear acrylic enclosure with a metal grid floor and one wall distinct from the others (stripes were drawn on one of the walls). The chamber was equipped with an electric shock generator. Videos were recorded using the AnyMaze video tracking software. On Day 1, mice were allowed to explore the enclosure freely, and at 150 s the mice were given a shock (2 mA, 180 V, 2 s). Shock sensitivity was confirmed by vocalization of the mice. Thirty seconds later the mice were returned to their home cage. After 24 h, the mice were placed back into the enclosure for 6 min and freezing time was measured in 30 s intervals. Freezing was defined as immobility lasting >0.5 s.

2.2.8.9 Novel object recognition

To test novel object recognition, mice were habituated with no objects in an open arena (40 cm×40 cm) for 5 min on both Day 1 and Day 2. On Day 3, mice were placed in the arena with two identical objects (A; a red plastic ball attached on top of a yellow cube base) and allowed to explore for 10 min. Video tracking was used (AnyMaze). To test short-term memory, 1.5 h after training the mice were placed back in the arena for 5 min with one previous object (A) and one novel object (B; a blue plastic pyramid attached on top of a green prism base). To test long-term memory, 24 h after training the mice were placed back in the arena for 5 min with one previous object (A) and one novel object (B). Recognition of previous and novel objects was expressed as the percentage of time spent with each

object compared with the total time interacting. Interaction with the object was defined as sniffing or touching the object, but not leaning against or standing on the object.

2.2.8.10 Morris water maze

The Morris water-maze test was conducted as described previously (Vorhees & Williams, 2006). Mice were given four trials (90 s) a day for 4 days consecutively, with a 15 min inter-trial period. The latency to find the platform was recorded using video-tracking software (AnyMaze). If the mice did not find the platform during the 90 s, they were gently guided onto the platform. On the 5th and the 12th day, the platform was removed and time spent in each quadrant of the maze recorded using the video software. The task was performed in a pool 1.5 m in diameter with 25°C water, and the platform was submerged 1 cm beneath the water surface. Spatial cues (shapes printed in black and white) were distributed around the pool. For the cued version of the Morris water maze, mice were subjected to four trials (90 s) per day for 7 days consecutively, with a 30 s inter-trial period. If the mouse did not find the platform after 90 s, it was gently guided onto the platform. The visible platform and the mouse starting location changed with each trial, so they were unique between trials. The platform was made visible by placing a red plastic cube on top of the platform, which was wiped with ethanol between each trial.

2.2.9 Statistical analyses

All data were analysed using GraphPad Prism software or SPSS, with Student's t-test (unpaired, two tailed) or one- or two-way ANOVA with Bonferroni or Benjamini–Hochburg correction where indicated. All results are depicted as means±s.e.m. unless indicated otherwise. Values of $P \leq 0.05$ were considered to indicate significance.

2.3 Results

2.3.1 Survival to adulthood depends on the extent of *Atrx* deletion in the CNS

Conditional inactivation of *Atrx* is required to elucidate its functions in specific tissues, because general inactivation of the gene is embryonic lethal (Garrick et al., 2006). We thus

generated mice with Cre recombinase-mediated deletion of *Atrx*-floxed alleles in the CNS using the Nestin-Cre driver line of mice. Hemizygous male mice (*Atrx*-cKO) died by postnatal day (P)1 (Figure 2-1A). Owing to random X-inactivation in females, *Atrx* is expressed from only one of the alleles in any specific cell, resulting in a mosaic pattern of expression in the brain of *Atrx*-cHet mice (e.g. if the floxed allele is the active allele, these cells are functionally null for *Atrx*; however, if the floxed allele is the silent one, cells are functionally wild type for *Atrx*). This was validated by RT-qPCR with *Atrx* primers in exon 17 and the excised exon 18, showing ~50% decreased *Atrx* expression in the cortex and hippocampus of *Atrx*-cHet mice compared with littermate controls (Figure 2-1B). Moreover, a mosaic pattern of ATRX protein expression was observed by immunofluorescence staining of the hippocampus and medial prefrontal cortex (Figure 2-1C,D). This was quantified in the medial prefrontal cortex in three pairs of control and cKO animals (Figure 2-1E). Haematoxylin and Eosin staining of control and *Atrx*-cHet brain sections did not reveal major histological alterations in the CA1, CA3 and mPFC regions (Figure 2-1F). These results demonstrated that inactivation of *Atrx* throughout the CNS was perinatal lethal but that *Atrx* deletion in approximately half of cells allowed survival of the female heterozygous mice to adulthood.

2.3.2 Mosaic inactivation of *Atrx* in the CNS impedes normal body growth

Atrx-cHet mice were weighed weekly for the first 24 postnatal weeks. The data showed that the *Atrx*-cHet mice weighed significantly less than control mice over this time period ($F=17.87$, $P=0.0003$; Figure 2-2A,B). Alcian Blue and Alizarin Red skeletal staining of P17 mice reveal that the *Atrx*-cHet skeletons were smaller than those of the control mice (Figure 2-2C). Tibia, femur and humerus bones were also measured and found to be significantly shorter in the *Atrx*-cHet mice compared with littermate controls (Figure 2-2D).

We previously reported that deletion of *Atrx* in the developing mouse forebrain and anterior

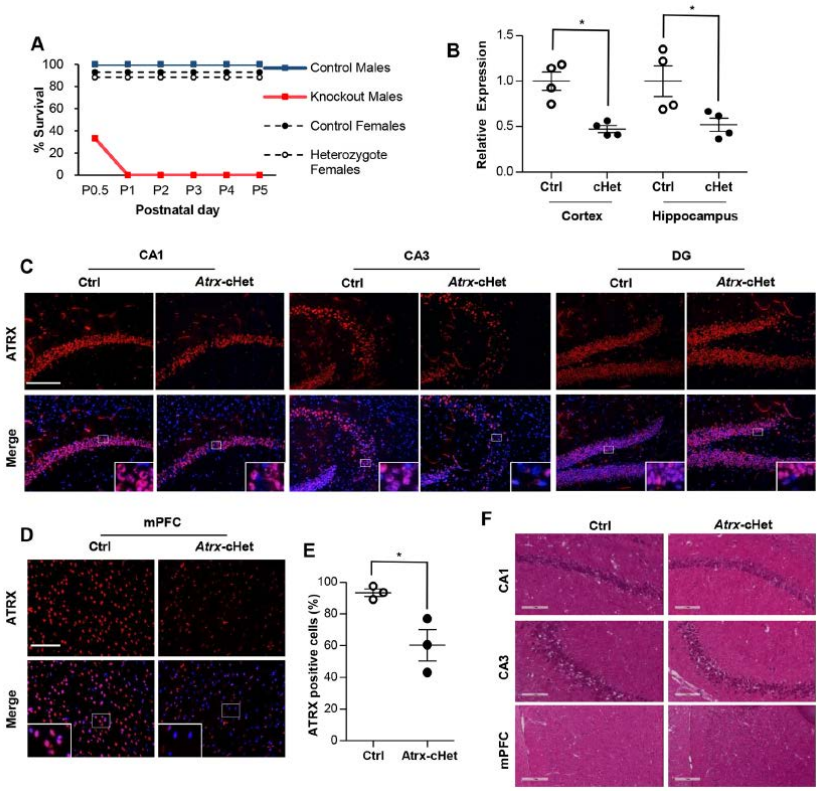

Figure 2-1 Mosaic pattern of ATRX expression in the brain of *Atrx*-cHet mice.

(A) Graph depicting the survival of control male mice (n=20), knockout male mice (n=6), control female mice (n=14) and heterozygote female mice (n=17) as the percentage survival at each time point. (B) RT-qPCR of Atrx (normalized to Gapdh expression) in the hippocampus and cortex of Atrx-cHet mice and littermate-matched controls (mean±s.e.m. of n=4 pairs, Student's two-tailed unpaired t-test). *P<0.05. (C)Immunofluorescence staining of ATRX (red) and DAPI (blue) in the hippocampus of control and Atrx-cHet mice. Scale bar: 100 μm.CA1, cornus ammoni 1; CA3, cornus ammoni 3; DG, dentate gyrus. (D) Immunofluorescence staining of ATRX (red) and DAPI (blue) in the medial prefrontal cortex (mPFC) of control and Atrx-cHet mice. Scale bar: 200 μm. (E) The percentage of ATRX-positive cells in the mPFC of control and Atrx-cHet mice (mean of three pairs±s.e.m., Student's two-tailed unpaired t-test). *P<0.05. (F) Haematoxylin and Eosin staining in the CA1, CA3 and mPFC of control and Atrx-cHet mice. Scale bar: 200 μm.

pituitary leads to low circulating concentrations of IGF-1 and thyroxine (T4) (Watson et al., 2013). Some evidence suggests that T4 regulates the prepubertal concentrations of insulin growth factor 1 (IGF-1), whereas after puberty this regulation is largely mediated by growth hormone (GH) (Xing et al., 2012). Given that the *Atrx*-cHet mice were smaller than control mice, we examined the concentrations of T4, IGF-1 and GH in the blood by enzyme-linked immunosorbent assays (ELISAs). We observed no significant difference in T4 and GH concentrations between P17 *Atrx*-cHet mice and control littermates. However, there was a large (80%) and significant decrease in IGF-1 concentrations (Figure 2-2E). Thus, the reduced body size of the *Atrx*-cHet mice was correlated with low circulating IGF-1 concentrations.

2.3.3 Hindlimb-clasping phenotype in *Atrx*-cHet mice

The *Atrx*-cHet mice displayed increased hindlimb clasping compared with control mice, with >90% exhibiting limb clasping by 3 months of age ($F=20.78$, $P<0.0001$; Figure 2-3A). In the open-field test, the distance travelled was not significantly different between control and *Atrx*-cHet mice, indicating that activity and locomotion were normal ($F=0.20$, $P=0.66$; Figure 2-3B). Anxiety levels were also normal, based on the time spent in the centre of the open-field apparatus ($F=0.84$, $P=0.44$; Figure 2-3C). Likewise, their performance in the elevated plus maze revealed no significant difference in the amount of time that control and *Atrx*-cHet mice spent in the open versus closed arms ($F=0.68$, $P=0.41$; Figure 2-3C,D).We concluded that the *Atrx*-cHet mice were not hyper- or hypo-active and did not exhibit excessive anxiety, but the increased level of hindlimb clasping behaviour was suggestive of neurological defects.

2.3.4 *Atrx*-cHet mice have normal working memory but deficits in object recognition memory

Given that ATRX mutations are linked to ID, we next evaluated memory in *Atrx*-cHet mice using various established paradigms. We first tested short-term working memory in the Y-maze task (de Castro et al., 2009). No difference was detected between control and *Atrx*-cHet mice in the percentage alternation or in the number of entries into the arms, suggesting

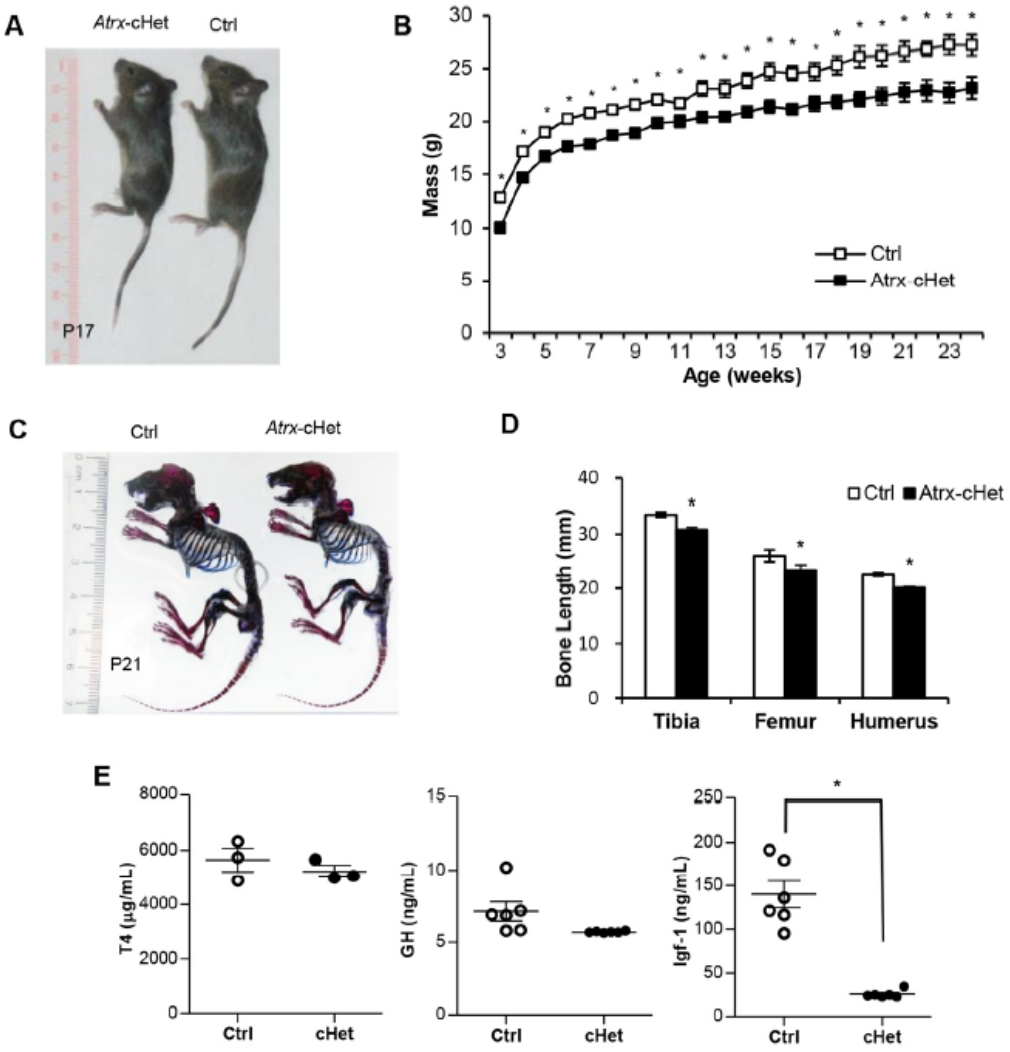

Figure 2-2 *Atrx*-cHet mice have reduced body weight and low circulating IGF-1.

(A) Atrx-cHet female mice are smaller than littermate-matched controls at P17. (B) Growth curve of mice from 3 to 24 weeks of age (n=13; *P<0.05). Data are represented as means±s.e.m., two-way repeated measures ANOVA with Benjamini–Hochburg posthoc test. (C) Skeletal stains of P21 control and Atrx-cHet mice showing cartilage (blue) and bone (red). (D) The lengths of long bones of Atrx-cHet mice (n=21) are decreased compared with control mice (n=19). (E) Circulating concentrations of T4, GH and IGF-1 in Atrx-cHet and control mice (n=3) at P17. Data are represented as means±s.e.m., Student's two-tailed, unpaired t-test. *P<0.05.

that working memory was normal in *Atrx*-cHet mice (t=0.05, P=0.96; Figure 2-4A). We then tested the *Atrx*-cHet mice in the spontaneous novel object recognition task that mainly involves the prefrontal cortex and hippocampus (Ennaceur & Delacour, 1988). In rodents, the natural tendency to seek out and explore novelty leads to a preference for the novel over the familiar object, indicating recognition memory of the familiar object (Bevins & Besheer, 2006). During the habituation period, both control and *Atrx*-cHet mice spent ~50% of the allotted time with each individual object (Figure 2-4B). In the course of the short-term memory test (1.5 h), control mice spent ~70% of their time with the novel object, whereas *Atrx*-cHet mice still spent ~50% of their time with each object, suggesting an inability to remember the familiar object (Figure 2-4B). Similar results were obtained in the long-term memory test (24 h). The total amount of time spent interacting with the objects was unchanged between control and *Atrx*-cHet mice during all three tests, ruling out visual or tactile impairment.

2.3.5 *Atrx*-cHet mice display deficits in contextual fear and spatial memory

To evaluate contextual fear memory, mice were placed in a box with distinctive black and white patterns on the sides for 3 min and shocked after 2.5 min. Twenty-four hours later, they were placed back into the same box with the same contextual cues, and the time spent freezing was measured at 30 s intervals. The data showed that the *Atrx*-cHet mice spent less time freezing than control mice (F=28.57, P<0.0001), and the total percentage of immobility time was significantly lower for *Atrx*-cHet mice, indicating impaired fear memory in these mice (t=5.35, P<0.0001; Figure 2-4C).

The Morris water maze was next used to evaluate hippocampus dependent spatial memory (Morris, 1984). During the 4 days of training, the *Atrx*-cHet mice took significantly more time finding the target platform while swimming a longer distance compared with control mice (latency F=31.44, P<0.0001; distance F=12.29, P<0.01; Figure 2-5A). The *Atrx*-cHet mice also swam more slowly than control mice (F=15.40, P<0.001; Figure 2-5A). During testing on the fifth day, the platform was removed and the time spent in each quadrant

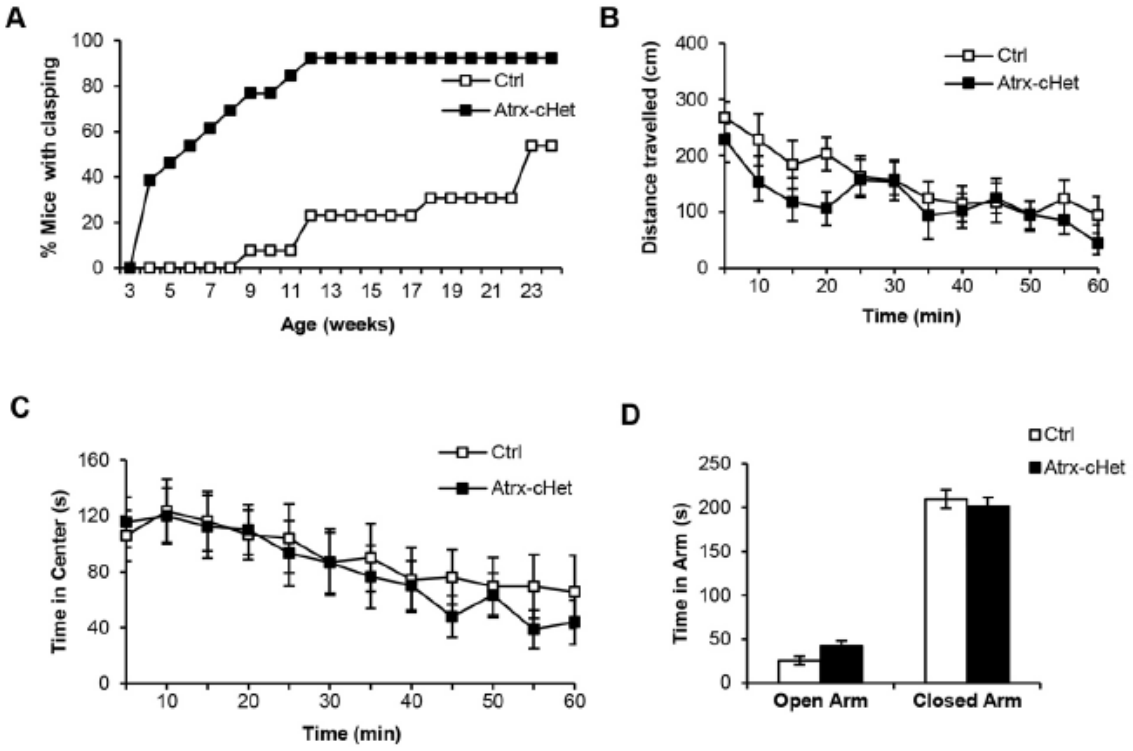

Figure 2-3 *Atrx*-cHet mice exhibit hindlimb clasping but normal activity and anxiety levels.

(A) Hindlimb clasping was evaluated in control (n=13) and Atrx-cHet (n=12) female mice and data plotted as the proportion of mice with hindlimb clasping from 3 to 25 weeks of age. (B,C) The open-field test showed no difference in distance travelled (B) and time spent in the centre (C) between control (n=11) and Atrx-cHet female mice (n=14). (D) Elevated plus maze test shows no difference in time spent in the open and closed arms in control (n=11) and Atrx-cHet (n=13) female mice. The data are represented as means±s.e.m. and a two-way ANOVA test was performed.

recorded as a measure of spatial memory. Whereas control mice spent significantly more time in the target quadrant than the left or opposite quadrant ($F=4.70$, $P<0.01$), *Atrx*-cHet mice showed no preference for the target quadrant ($F=0.75$, $P=0.53$; Figure 2-5B). The results suggested that spatial learning and memory might be impaired in the *Atrx*-cHet mice. The cued Morris water maze was used to determine whether motivational or sensorimotor defects contributed to the phenotype seen in the noncued version of the test. Whereas the control mice quickly learned to correlate the cue with the platform, the *Atrx*-cHet mice were unable to do so ($F=14.09$, $P<0.01$; Figure 2-5C). We noticed that the mice failed to show normal signs of aversion to water during this task, with a preference to be swimming rather than to climb on the platform during training, even jumping back into the water after being placed on the platform.

2.3.6 *Atrx*-cHet mice have normal motor endurance and motor memory

Given that the *Atrx*-cHet mice swam more slowly than control animals in the Morris water-maze task, we considered that perhaps the test was confounded by deficits in motor skills. To clarify this issue, we examined endurance and motor skills further in the mutant mice. We found that motor function and balance measured in the Rotarod task were not significantly different in *Atrx*-cHet mice during any of the trials ($F=3.02$, $P=0.09$; Fig. 6A). *Atrx*-cHet mice also performed similarly to control animals in the treadmill task ($t=0.34$, $P=0.73$; Fig. 6B). By contrast, *Atrx*-cHet mice exhibited decreased forelimb grip strength, normalized to body weight ($t=2.80$, $P<0.05$; Fig. 6C).

2.4 Discussion

This study demonstrates that deletion of *Atrx* in the CNS leads to endocrine defects and behavioural abnormalities. Specifically, we see impairments in spatial learning and memory in the Morris water maze, in contextual fear conditioning and in novel object recognition.

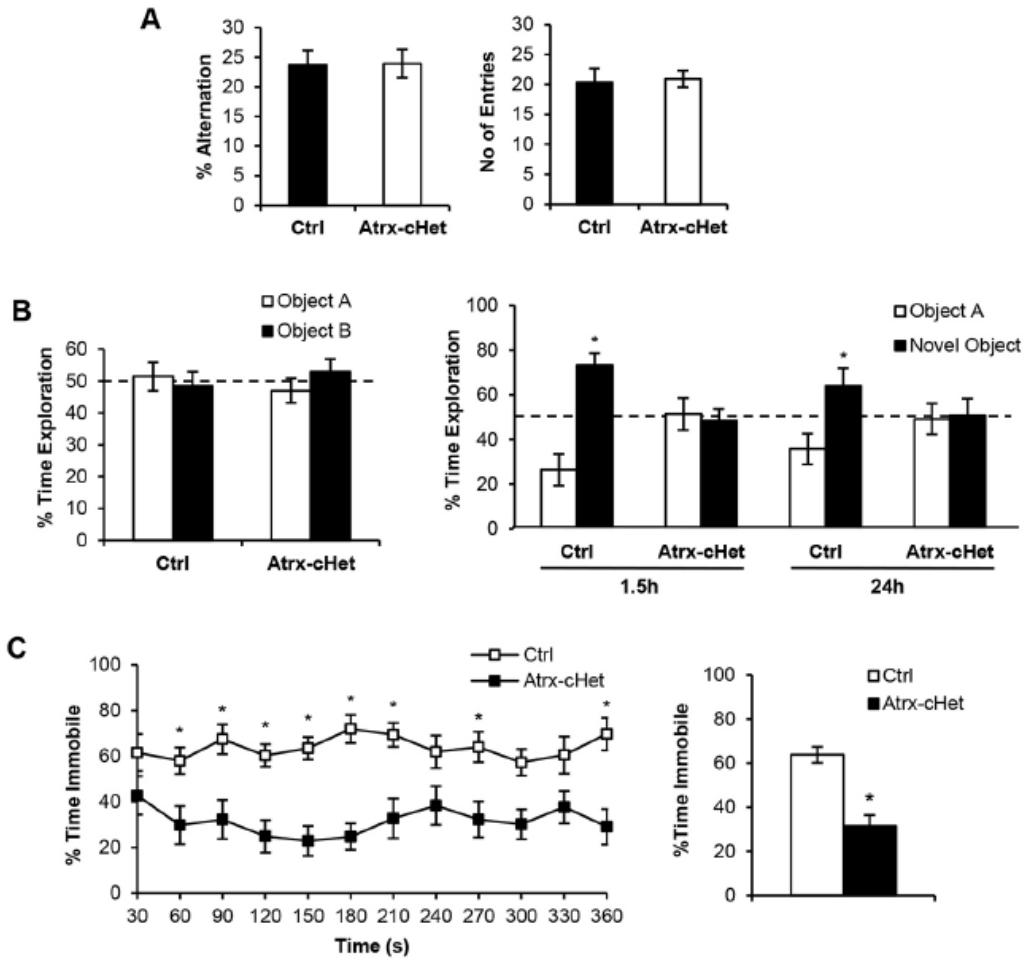

Figure 2-4 Impaired novel object recognition and contextual fear memory in *Atrx*-cHet mice.

(A) Percentage alternation and number of arm entries in the Y-maze test by control (n=14) and Atrx-cHet (n=15) female mice. (B) Control (n=14) and Atrx-cHet (n=14) mice displayed similar preference for identical objects in the training session of the novel object recognition task. The Atrx-cHet mice failed to display a preference for the novel object 1.5 and 24 h later (*P<0.05). (C) Atrx-cHet (n=14) mice spent less time immobile than control mice (n=14) in the fear-conditioning paradigm. The total percentage of time spent immobile is shown on the right (*P<0.0001). Statistical analyses made use of Student's two tailed, unpaired t-test or two-way ANOVA; data are represented as means±s.e.m. and *P<0.05.

We previously reported that mice lacking ATRX expression in the embryonic mouse forebrain have an average lifespan of 22 days (Watson et al., 2013). It is thus not surprising that inactivation of *Atrx* using the Nestin-Cre driver (which mediates deletion in the majority of CNS cells) is neonatal lethal. By contrast, the *Atrx*-cHet female mice survived to adulthood, probably because roughly half of all Nestin-expressing cells and their progeny are spared. Mosaic loss of ATRX in *Atrx*-cHet female mice still negatively affects development, as the mice are smaller compared with littermate controls, and the length of long bones is decreased. As the Nestin-Cre driver does not promote Cre expression in bone progenitors (Wiese et al., 2004), this phenotype might result from the low concentration of circulating IGF-1 in these mice. The reason for low IGF-1 is difficult to pinpoint in our mice. It has been shown that mice expressing Cre under the control of the Nestin promoter are smaller as a result of a decrease in mouse GH (Declercq et al., 2015). However, in our hands, GH concentrations are normal in the *Atrx*-cHet mice. Given the normal concentrations of both T4 and GH, there could be unanticipated expression of Cre in the liver that affects IGF-1 production. Examining the potential off-target expression of Cre will be required to elucidate the mechanism of IGF-1 downregulation in these mice.

The *Atrx*-cHet mice displayed a variety of behavioural abnormalities. We initially noticed that the mice displayed excessive hindlimb clasping, which could indicate neurological impairment (Guy, Hendrich, Holmes, Martin, & Bird, 2001). This prompted us to perform additional tests to assess neurobehaviour of the mice. We observed no change in general activity or anxiety using the open-field test and elevated plus maze, respectively, and no change in working memory in the Y-maze task. The *Atrx*-cHet mice exhibited increased latency to reach the platform in the Morris water-maze task, which might indicate a defect in spatial memory. However, the findings are difficult to interpret because *Atrx*-cHet mice swam at a lower speed, which could indicate a problem with their ability to swim rather than with memory. It was previously reported that mice lacking MeCP2 protein, an established interactor with ATRX in the brain, exhibit navigational difficulties in the Morris water maze (Stearns et al., 2007). Significant differences in swimming ability made it difficult to conclude whether the increased latency to the platform was attributable to

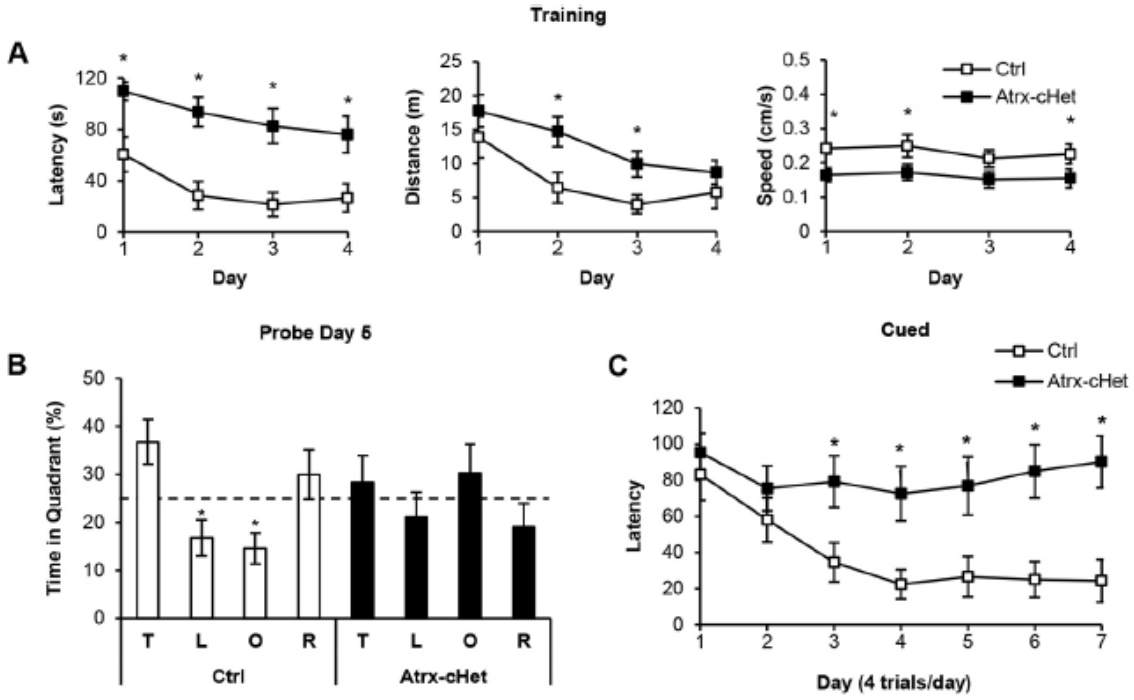

Figure 2-5 *Atrx*-cHet mice perform poorly in the Morris water-maze paradigm.

(A) Atrx-cHet mice (n=13) spent more time finding the platform compared with control mice (n=11) over the four consecutive days of training (*P<0.05). They swam longer distances but at a lower speed compared with control mice (*P<0.05). (B) Control mice spent more time swimming in the target quadrant (T) compared with the left (L) and opposite (O) quadrants (*P<0.05) on the day 5 probe test, whereas Atrx-cHet mice spent ~25% of their time in each of the quadrants. (C) In the cued version of the Morris water maze, Atrx-cHet mice (n=11) were unable to learn the location of the visible platform, whereas the control mice could effectively learn this task (n=11). Data are represented as means±s.e.m. and a two-way ANOVA test was done. *P<0.05.

motor or cognitive deficits, similar to our findings with the *Atrx*-cHet mice. Although we did not observe defective motor skills in the Rotarod or treadmill tests or decreased activity in the open-field test, we noticed that the mice failed to show normal signs of aversion to water during this task and preferred to be swimming rather than to climb on the platform during training, even jumping back into the water after being placed on the platform. We attempted to test the mice in the Barnes maze, another spatial learning and memory test, but the heterozygote mice tended to jump off the edge of the maze. This could be due to multiple factors. The mice could have decreased motivation and therefore do not care about being out of the water, or they may have a reduction in tactile sensitivity and therefore do not have an aversion to water, although pain sensitivity has been tested in mice with decreased expression of ATRX and no change was found (Nogami et al., 2011).

Despite these issues, which might require further experimentation for a full understanding, we obtained supporting evidence that memory is affected in the *Atrx*-cHet mice in the contextual fear and the novel object recognition tasks. Additional support comes from a previous study done in a mouse model of Chudley–Lowry syndrome associated with reduced expression of ATRX (Nogami et al., 2011). The authors of that study reported an impairment in contextual fear memory and suggested that ATRX might play a role in regulation of adult-born neurons. Our results show defects not only in contextual fear memory, but also in novel object recognition and, potentially, the Morris water-maze task. This might indicate a role for ATRX not only in adult-born neurons, but perhaps also in the amygdala, hippocampus and the rest of the medial temporal lobe, structures which are vital for the tasks impaired in the *Atrx*-cHet mice (Logue, Paylor, & Wehner, 1997; Phillips & LeDoux, 1992; Wan, Aggleton, & Brown, 1999).

The DAXX protein is a well-established interactor with ATRX. Although the behaviour of DAXX knockout mice has not yet been investigated, a study previously demonstrated that DAXX binds with ATRX to the promoters of several immediate-early genes upon activation of cortical neuronal cultures (Michod et al., 2012). DAXX was also shown to be crucial for the incorporation of histone H3.3 at these gene promoters, supporting a potential

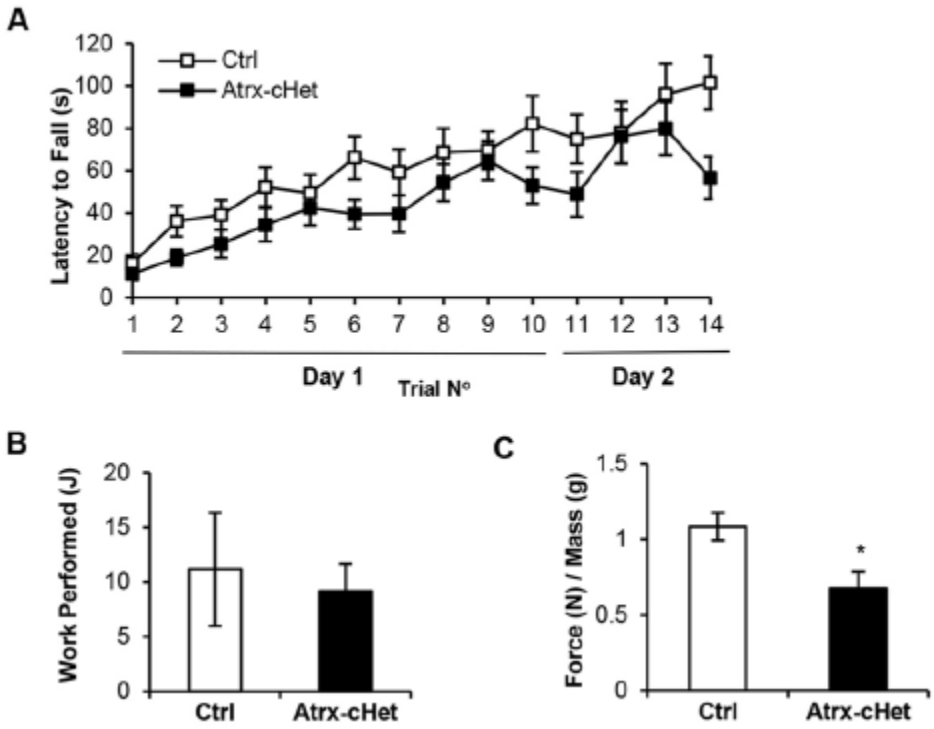

Figure 2-6 Normal motor memory and endurance but decreased grip strength in *Atrx*-cHet mice.

(A) Atrx-cHet (n=18) and control (n=16) female mice performed normally in the Rotarod test. (B) Atrx-cHet (n=15) and control (n=15) mice exhibited similar performance in the treadmill test. (C) Atrx-cHet mice (n=13) exhibited a decreased grip strength compared with control mice (n=11), normalized to body mass. Statistical analyses made use of two-way ANOVA or Student's two-tailed, unpaired t-test; data are represented as means±s.e.m. *P<0.05.

role for DAXX and ATRX the initial steps of memory consolidation. EZH2, a member of the PRC2 complex that mediates H3K27 trimethylation, is another putative binding partner of ATRX (Cardoso et al., 1998; Margueron et al., 2009). Inducible deletion of the Ezh2 gene in neural progenitor cells in the adult brain caused impaired spatial learning and memory and contextual fear memory, suggesting that EZH2 (potentially with ATRX) provides important cues in adult neural progenitor cells (Zhang et al., 2014). We emphasize that these mice do not model the ATR-X syndrome, where only males are affected and females exhibit 100% skewing of X-chromosome inactivation and are therefore largely unaffected. Rather, the *Atrx*-cHet mice are a useful tool to probe ATRX function in the CNS. Overall, our study presents compelling evidence that ATRX is required in the mouse CNS for normal cognitive processes and sets the stage for additional investigations delving into the mechanisms by which it regulates chromatin structure and gene expression in neurons in the context of learning and memory.

2.5 References

Aapola, U., Kawasaki, K., Scott, H. S., Ollila, J., Vihinen, M., Heino, M., . . . Peterson, P. (2000). Isolation and initial characterization of a novel zinc finger gene, DNMT3L, on 21q22.3, related to the cytosine-5-methyltransferase 3 gene family. *Genomics, 65*(3), 293-298. doi: 10.1006/geno.2000.6168

Bérubé, N. G., Mangelsdorf, M., Jagla, M., Vanderluit, J., Garrick, D., Gibbons, R. J., . . . Picketts, D. J. (2005). The chromatin-remodeling protein ATRX is critical for neuronal survival during corticogenesis. *J Clin Invest, 115*(2), 258-267. doi: 10.1172/JCI22329

Bérubé, N. G., Smeenk, C. A., & Picketts, D. J. (2000). Cell cycle-dependent phosphorylation of the ATRX protein correlates with changes in nuclear matrix and chromatin association. *Hum Mol Genet, 9*(4), 539-547.

Bevins, R. A., & Besheer, J. (2006). Object recognition in rats and mice: a one-trial non-matching-to-sample learning task to study 'recognition memory'. *Nat Protoc, 1*(3), 1306-1311. doi: 10.1038/nprot.2006.205

Cardoso, C., Timsit, S., Villard, L., Khrestchatisky, M., Fontes, M., & Colleaux, L. (1998). Specific interaction between the XNP/ATR-X gene product and the SET domain of the human EZH2 protein. *Hum Mol Genet, 7*(4), 679-684.

de Castro, B. M., De Jaeger, X., Martins-Silva, C., Lima, R. D., Amaral, E., Menezes, C., . . . Prado, V. F. (2009). The vesicular acetylcholine transporter is required for neuromuscular development and function. *Mol Cell Biol, 29*(19), 5238-5250. doi: 10.1128/MCB.00245-09

Declercq, J., Brouwers, B., Pruniau, V. P., Stijnen, P., de Faudeur, G., Tuand, K., . . . Creemers, J. W. (2015). Metabolic and Behavioural Phenotypes in Nestin-Cre Mice Are Caused by Hypothalamic Expression of Human Growth Hormone. *PLoS One, 10*(8), e0135502. doi: 10.1371/journal.pone.0135502

Dhayalan, A., Tamas, R., Bock, I., Tattermusch, A., Dimitrova, E., Kudithipudi, S., . . . Jeltsch, A. (2011). The ATRX-ADD domain binds to H3 tail peptides and reads the combined methylation state of K4 and K9. *Hum Mol Genet, 20*(11), 2195-2203. doi: 10.1093/hmg/ddr107

Drane, P., Ouararhni, K., Depaux, A., Shuaib, M., & Hamiche, A. (2010). The death-associated protein DAXX is a novel histone chaperone involved in the replication-independent deposition of H3.3. *Genes Dev, 24*(12), 1253-1265. doi: 10.1101/gad.566910

Ennaceur, A., & Delacour, J. (1988). A new one-trial test for neurobiological studies of memory in rats. 1: Behavioral data. *Behav Brain Res, 31*(1), 47-59.

Garrick, D., Sharpe, J. A., Arkell, R., Dobbie, L., Smith, A. J., Wood, W. G., . . . Gibbons, R. J. (2006). Loss of Atrx affects trophoblast development and the pattern of X-inactivation in extraembryonic tissues. *PLoS Genet, 2*(4), e58. doi: 10.1371/journal.pgen.0020058

Gibbons, R. J., Bachoo, S., Picketts, D. J., Aftimos, S., Asenbauer, B., Bergoffen, J., . . . Higgs, D. R. (1997). Mutations in transcriptional regulator ATRX establish the functional significance of a PHD-like domain. *Nat Genet, 17*(2), 146-148. doi: 10.1038/ng1097-146

Gibbons, R. J., Brueton, L., Buckle, V. J., Burn, J., Clayton-Smith, J., Davison, B. C., . . . et al. (1995). Clinical and hematologic aspects of the X-linked alpha-thalassemia/mental retardation syndrome (ATR-X). *Am J Med Genet, 55*(3), 288-299. doi: 10.1002/ajmg.1320550309

Grozeva, D., Carss, K., Spasic-Boskovic, O., Tejada, M. I., Gecz, J., Shaw, M., . . . Raymond, F. L. (2015). Targeted Next-Generation Sequencing Analysis of 1,000 Individuals with Intellectual Disability. *Hum Mutat, 36*(12), 1197-1204. doi: 10.1002/humu.22901

Guy, J., Hendrich, B., Holmes, M., Martin, J. E., & Bird, A. (2001). A mouse Mecp2-null mutation causes neurological symptoms that mimic Rett syndrome. *Nat Genet, 27*(3), 322-326. doi: 10.1038/85899

Law, M. J., Lower, K. M., Voon, H. P., Hughes, J. R., Garrick, D., Viprakasit, V., . . . Gibbons, R. J. (2010). ATR-X syndrome protein targets tandem repeats and influences allele-specific expression in a size-dependent manner. *Cell, 143*(3), 367-378. doi: 10.1016/j.cell.2010.09.023

Leung, J. W., Ghosal, G., Wang, W., Shen, X., Wang, J., Li, L., & Chen, J. (2013). Alpha thalassemia/mental retardation syndrome X-linked gene product ATRX is required for proper replication restart and cellular resistance to replication stress. *J Biol Chem, 288*(9), 6342-6350. doi: 10.1074/jbc.M112.411603

Levy, M. A., Kernohan, K. D., Jiang, Y., & Berube, N. G. (2015). ATRX promotes gene expression by facilitating transcriptional elongation through guanine-rich coding regions. *Hum Mol Genet, 24*(7), 1824-1835. doi: 10.1093/hmg/ddu596

Lewis, P. W., Elsaesser, S. J., Noh, K. M., Stadler, S. C., & Allis, C. D. (2010). Daxx is an H3.3-specific histone chaperone and cooperates with ATRX in replication-independent chromatin assembly at telomeres. *Proc Natl Acad Sci U S A, 107*(32), 14075-14080. doi: 10.1073/pnas.1008850107

Logue, S. F., Paylor, R., & Wehner, J. M. (1997). Hippocampal lesions cause learning deficits in inbred mice in the Morris water maze and conditioned-fear task. *Behav Neurosci, 111*(1), 104-113.

Margueron, R., Justin, N., Ohno, K., Sharpe, M. L., Son, J., Drury, W. J., 3rd, . . . Gamblin, S. J. (2009). Role of the polycomb protein EED in the propagation of repressive histone marks. *Nature, 461*(7265), 762-767. doi: 10.1038/nature08398

Martyn, A. C., De Jaeger, X., Magalhaes, A. C., Kesarwani, R., Goncalves, D. F., Raulic, S., . . . Prado, V. F. (2012). Elimination of the vesicular acetylcholine transporter in the forebrain causes hyperactivity and deficits in spatial memory and long-term potentiation. *Proc Natl Acad Sci U S A, 109*(43), 17651-17656. doi: 10.1073/pnas.1215381109

Michod, D., Bartesaghi, S., Khelifi, A., Bellodi, C., Berliocchi, L., Nicotera, P., & Salomoni, P. (2012). Calcium-dependent dephosphorylation of the histone chaperone DAXX regulates H3.3 loading and transcription upon neuronal activation. *Neuron, 74*(1), 122-135. doi: 10.1016/j.neuron.2012.02.021

Morris, R. (1984). Developments of a water-maze procedure for studying spatial learning in the rat. *J Neurosci Methods, 11*(1), 47-60.

Nan, X., Hou, J., Maclean, A., Nasir, J., Lafuente, M. J., Shu, X., . . . Bird, A. (2007). Interaction between chromatin proteins MECP2 and ATRX is disrupted by mutations that cause inherited mental retardation. *Proc Natl Acad Sci U S A, 104*(8), 2709-2714. doi: 10.1073/pnas.0608056104

Nogami, T., Beppu, H., Tokoro, T., Moriguchi, S., Shioda, N., Fukunaga, K., . . . Kitajima, I. (2011). Reduced expression of the ATRX gene, a chromatin-remodeling factor, causes hippocampal dysfunction in mice. *Hippocampus, 21*(6), 678-687. doi: 10.1002/hipo.20782

Phillips, R. G., & LeDoux, J. E. (1992). Differential contribution of amygdala and hippocampus to cued and contextual fear conditioning. *Behav Neurosci, 106*(2), 274-285.

Picketts, D. J., Higgs, D. R., Bachoo, S., Blake, D. J., Quarrell, O. W., & Gibbons, R. J. (1996). ATRX encodes a novel member of the SNF2 family of proteins: mutations point to a common mechanism underlying the ATR-X syndrome. *Hum Mol Genet, 5*(12), 1899-1907.

Ritchie, K., Watson, L. A., Davidson, B., Jiang, Y., & Berube, N. G. (2014). ATRX is required for maintenance of the neuroprogenitor cell pool in the embryonic mouse brain. *Biol Open, 3*(12), 1158-1163. doi: 10.1242/bio.20148730

Seah, C., Levy, M. A., Jiang, Y., Mokhtarzada, S., Higgs, D. R., Gibbons, R. J., & Berube, N. G. (2008). Neuronal death resulting from targeted disruption of the Snf2 protein ATRX is mediated by p53. *J Neurosci, 28*(47), 12570-12580. doi: 10.1523/JNEUROSCI.4048-08.2008

Solomon, L. A., Russell, B. A., Makar, D., Berube, N. G., & Beier, F. (2013). Loss of ATRX does not confer susceptibility to osteoarthritis. *PLoS One, 8*(12), e85526. doi: 10.1371/journal.pone.0085526

Stearns, N. A., Schaevitz, L. R., Bowling, H., Nag, N., Berger, U. V., & Berger-Sweeney, J. (2007). Behavioral and anatomical abnormalities in Mecp2 mutant mice: a model for Rett syndrome. *Neuroscience, 146*(3), 907-921. doi: 10.1016/j.neuroscience.2007.02.009

Tronche, F., Kellendonk, C., Kretz, O., Gass, P., Anlag, K., Orban, P. C., . . . Schutz, G. (1999). Disruption of the glucocorticoid receptor gene in the nervous system results in reduced anxiety. *Nat Genet, 23*(1), 99-103. doi: 10.1038/12703

Ulici, V., Hoenselaar, K. D., Agoston, H., McErlain, D. D., Umoh, J., Chakrabarti, S., . . . Beier, F. (2009). The role of Akt1 in terminal stages of endochondral bone formation: angiogenesis and ossification. *Bone, 45*(6), 1133-1145. doi: 10.1016/j.bone.2009.08.003

Vorhees, C. V., & Williams, M. T. (2006). Morris water maze: procedures for assessing spatial and related forms of learning and memory. *Nat Protoc, 1*(2), 848-858. doi: 10.1038/nprot.2006.116

Wan, H., Aggleton, J. P., & Brown, M. W. (1999). Different contributions of the hippocampus and perirhinal cortex to recognition memory. *J Neurosci, 19*(3), 1142-1148.

Watson, L. A., Solomon, L. A., Li, J. R., Jiang, Y., Edwards, M., Shin-ya, K., . . . Berube, N. G. (2013). Atrx deficiency induces telomere dysfunction, endocrine defects, and reduced life span. *J Clin Invest, 123*(5), 2049-2063. doi: 10.1172/JCI65634

Wiese, C., Rolletschek, A., Kania, G., Blyszczuk, P., Tarasov, K. V., Tarasova, Y., . . . Wobus, A. M. (2004). Nestin expression--a property of multi-lineage progenitor cells? *Cell Mol Life Sci, 61*(19-20), 2510-2522. doi: 10.1007/s00018-004-4144-6

Xing, W., Govoni, K. E., Donahue, L. R., Kesavan, C., Wergedal, J., Long, C., . . . Mohan, S. (2012). Genetic evidence that thyroid hormone is indispensable for prepubertal insulin-like growth factor-I expression and bone acquisition in mice. *J Bone Miner Res, 27*(5), 1067-1079. doi: 10.1002/jbmr.1551

Xue, Y., Gibbons, R., Yan, Z., Yang, D., McDowell, T. L., Sechi, S., . . . Wang, W. (2003). The ATRX syndrome protein forms a chromatin-remodeling complex with Daxx and localizes in promyelocytic leukemia nuclear bodies. *Proc Natl Acad Sci U S A, 100*(19), 10635-10640. doi: 10.1073/pnas.1937626100

Zhang, J., Ji, F., Liu, Y., Lei, X., Li, H., Ji, G., . . . Jiao, J. (2014). Ezh2 regulates adult hippocampal neurogenesis and memory. *J Neurosci, 34*(15), 5184-5199. doi: 10.1523/JNEUROSCI.4129-13.2014

Chapter 3

3 *Atrx* deletion in neurons leads to sexually-dimorphic dysregulation of miR-137 and spatial learning and memory deficits

Mutations in the ATRX chromatin remodeler are associated with syndromic and non-syndromic intellectual disability. Emerging evidence points to key roles for ATRX in preserving neuroprogenitor cell genomic stability, whereas ATRX function in differentiated neurons and memory processes are still unresolved. Here, I show that *Atrx* deletion in mouse forebrain glutamatergic neurons causes distinct hippocampal anatomical defects identified by magnetic resonance imaging. Ultrastructural analysis revealed fewer presynaptic vesicles and an enlarged postsynaptic area at CA1 apical dendrite-axon junctions. These synaptic defects are associated with impaired long-term contextual memory in male, but not female mice. Mechanistically, I identified ATRX-dependent and sex-specific alterations in synaptic gene expression linked to miR-137 levels, a known regulator of presynaptic processes and spatial memory. I concluded that ablation of *Atrx* in excitatory forebrain neurons leads to sexually dimorphic outcomes on miR-137 and on spatial memory, identifying a promising therapeutic target for neurological disorders caused by ATRX dysfunction.

3.1 Introduction

Alpha-thalassemia X-linked intellectual disability syndrome, or ATR-X syndrome, is a rare congenital X-linked disorder resulting in moderate to severe intellectual disability (ID), developmental delay, microcephaly, hypomyelination, and a mild form of alpha-thalassemia [OMIM: 301040] (Gibbons, Picketts, Villard, & Higgs, 1995). In a recent study of approximately 1000 individuals with ID, *ATRX* mutations were identified as one of the most frequent cause of non-syndromic ID (Grozeva et al., 2015), emphasizing a key requirement for this gene in cognitive processes. ATRX-related ID arises from hypomorphic mutations in the *ATRX* gene, most commonly in the highly conserved

ATRX/DNMT3/DNMT3L (ADD) and Switch/Sucrose non-fermenting (SWI/SNF) domains (Gibbons et al., 1997; Gibbons et al., 2008). The former targets ATRX to chromatin by means of a histone reader domain that recognizes specific histone tail modifications (Eustermann et al., 2011), and the latter confers ATPase activity and is critical for its chromatin remodeling activity (Lewis, Elsaesser, Noh, Stadler, & Allis, 2010; Picketts et al., 1996).

ATRX, in a complex with the histone chaperone DAXX, promotes the deposition of the histone variant H3.3 at heterochromatic domains including telomeres and pericentromeres (Goldberg et al., 2010; Law et al., 2010). However, ATRX is also required for H3.3 deposition within the gene body of a subset of G-rich genes, presumably to reduce G-quadruplex formation and promote transcriptional elongation (Levy, Kernohan, Jiang, & Berube, 2015). ATRX is also required for the postnatal suppression of a network of imprinted genes in the neonatal brain by promoting long range chromatin interactions via CTCF and cohesin (Kernohan et al., 2010).

In mice, germline deletion of *Atrx* results in embryonic lethality (Garrick et al., 2006) while conditional deletion of *Atrx* in neuroprogenitors leads to excessive DNA damage caused by DNA replication stress and subsequent Tp53-dependent apoptosis (Seah et al., 2008; Watson et al., 2013). Mice with deletion of exon 2 of *Atrx* ($Atrx^{\Delta E2}$) were generated that result in global reduction of *Atrx* expression. These mice are viable and exhibit impaired novel object recognition memory, spatial memory in the Barnes maze, and contextual fear memory (Shioda et al., 2011). Some of the molecular defects identified in these mice included decreased activation of CaMKII and the AMPA receptor in the hippocampus as well as decreased spine density in the medial prefrontal cortex, and altered DNA methylation and increased expression of *Xlr3b* in neurons (Shioda et al., 2018). Our group also reported similar behavioural impairments in female mice exhibiting mosaic expression of ATRX in the central nervous system (Tamming et al., 2017). However, the contribution of different cell types and sex difference to behavioural abnormalities have not yet been resolved.

To start addressing these questions, we deleted *Atrx* specifically in glutamatergic forebrain neurons in male and female mice. This approach bypasses deleterious effects of ATRX loss of function that we previously observed during brain development caused by replication stress in proliferating neuroprogenitors (Garrick et al., 2006; Watson et al., 2013). A comprehensive analysis of these mice reveals that ATRX promotes long-term spatial learning and memory associated with morphological and synaptic ultrastructural changes in the hippocampus. We show that female mice lacking ATRX in neurons are protected from spatial learning and memory defects and identify sex-specific effects of ATRX loss on the expression of synaptic genes and miR-137. Overall, we identify a novel sex-specific function for ATRX in neurons in the regulation of long-term spatial memory associated with abnormal synapse ultrastructure.

3.2 Methods

3.2.1 Animal care and husbandry

Mice were exposed to a 12-hour-light/12-hour-dark cycle and with water and chow *ad libitum*. The *Atrx*^{loxP} mice have been described previously (Bérubé et al., 2005). *Atrx*^{loxP} mice were mated with C57BL/6 mice expressing Cre recombinase under the control of the *αCaMKII* gene promoter (Tsien et al., 1996). The progeny includes hemizygous male mice that produce no ATRX protein in forebrain excitatory neurons (*Atrx*-cKO). The *Atrx*-cKO males were mated to *Atrx*^{loxP} females to yield homozygous deletion of *Atrx* in female mice (*Atrx*-cKO^{Fem}). Male and female littermate floxed mice lacking the Cre allele were used as controls (Ctrl; Ctrl^{Fem}). For embryo cultures, *Atrx*^{loxP} were mated to mice expressing Cre recombinase under the control of the *Nestin* promoter (*Atrx*^{Nestin}-cKO) (Tronche et al., 1999). The progeny includes hemizygous male mice that produce no ATRX protein in all neural and glial precursors of the central and peripheral nervous system. Male littermate floxed mice lacking the Cre allele were use as controls (Ctrl^{Nestin}). Genotyping of tail biopsies for the presence of the floxed and Cre alleles was performed as described previously (Bérubé et al., 2005). All procedures involving animals were conducted in accordance with the regulations of the Animals for Research Act of the province of Ontario

and approved by the University of Western Ontario Animal Care and Use Committee (2017-048). Behavioural assessments started with less demanding tasks (open field tests, elevated plus maze) to more demanding ones (Morris water maze). ARRIVE guidelines were followed: mouse groups were randomized, experimenters were blind to the genotypes, and software-based analysis was used to score mouse performance in all the tasks. All behavioural experiments were performed between 9:00 AM and 4:00 PM.

3.2.2 Cortical cultures

Cortices were removed from E16.5 control and *Atrx*^{Nestin}-cKO embryos and placed in Hanks balanced salt solution (ThermoFisher). Tissue was dissociated gently using a P1000 pipette by pipetting up and down 10-15 times. Cells were plated in 2 wells of a 6-well plate at a density of $8x10^5$ cells/mL in neurobasal media (Invitrogen) supplemented with B27 serum, GlutaMAX, and penicillin/streptomycin (all Invitrogen). At 9 DIV cells were treated with 1 µm tetrodotoxin (Tocris). At 10 DIV one well per sample was activated with potassium chloride while the other well was left at basal conditions. 1 hour post-stimulation cells were collected, pelleted, and froze until later use.

3.2.3 Immunofluorescence staining

Mice were perfused with 25mL phosphate buffered saline (PBS) followed by 25mL 4% paraformaldehyde (PFA) in PBS and the brain fixed for 24 hours in 4% PFA in PBS and cryopreserved in 30% sucrose/PBS. Brains were flash frozen in Cryomatrix (Thermo Scientific) and sectioned at 8µm thickness as described previously (Watson et al., 2013). For immunostaining, antigen retrieval was performed by incubating slides in 10 mM sodium citrate at 95°C for 10 min. Cooled sections were washed and blocked with 10% normal goat serum Sigma). The slides were incubated overnight in primary antibody (ATRX: 1:200, H-300 Santa Cruz Biotechnology Inc; GFAP: 1:200, Agilent Technologies, Inc; IBA1: 1:500, Wako Pure Chemical Corporation) diluted in 0.3% Triton-X/PBS. Sections were washed in 0.3% Triton-X/PBS 3x 5 min and incubated with secondary antibody (goat anti-rabbit-Alexa Fluor 594: 1:800, Life Technologies) for one hour. Sections were washed again three times for 5 min, counterstained with DAPI and mounted

with SlowFade Gold (Invitrogen). All images were captured using an inverted microscope (Leica DMI 6000b) with a digital camera (Hamamatsu ORCA-ER). Openlab image software was used for manual image capture, and images were processed using the Volocity software (Demo Version 6.0.1; PerkinElmer) and Adobe Photoshop CS6 (Version 13.0). Cell counts of DAPI, GFAP, and IBA1 were performed in Adobe Photoshop. DAPI was counted per mm^2 and GFAP and IBA1 were counted as percentages of $DAPI^+$ cells. One section from five pairs of Ctrl/*Atrx*-cKO was counted. Statistical significance was determined using an unpaired Student's T-test.

3.2.4 Reverse transcriptase real-time PCR (qRT-PCR)

Total RNA was isolated from control and *Atrx*-cKO frontal cortex and hippocampus using the miRVANA total RNA isolation kit (ThermoFisher) and reverse transcribed to cDNA using 1 μg RNA and SuperScript II Reverse Transcriptase (Invitrogen). RNA was isolated from cortical cultures using the RNeasy Mini Kit (Qiagen) and reverse transcribed to cDNA as above.

Real-time PCR was performed in duplicate using gene-specific primers under the following conditions: 95°C for 10 s, 58°C for 20 s, 72°C for 30 s for 35 cycles. All data were normalized against β-actin expression levels. Primers used were as follows:

Gene	Forward Primer	Reverse Primer
β-actin	CTGTCGAGTCGCGTCCACCC	ACATGCCGGAGCCGTTGTCG
Atrx	AGAAATTGAGGATGCTTCACC	TGAACCTGGGGACTTCTTTG
c-Fos	ATGGGCTCTCCTGTCAACAC	GACACGGTCTTCACCATTCC
Junb	CGGAGATCATCGCTTTTAGC	TCATTTTTCAACACGCCGTA
Egr1	GAGCGAACAACCCTATGAGC	GAGTCGTTTGGCTGGGATAA
Arc	GAAGTGGTGGGAGTTCAAGC	CTCCTCAGCGTCCACATAGA
Npas4	GTGGCAGCACTACCTGGATT	AGATGGTCAGCAGGGTCAAT
Gadd45g	TCTACGAGTCCGCCAAAGTC	AATGAGGATGCAATGCAGGT

Total RNA was also used for reverse transcription of miRNA using the TaqMan Advanced MicroRNA reverse transcription kit (ThermoFisher). qRT-PCR was performed using the TaqMan Universal PCR Master Mix, no AmpErase (ThermoFisher) using advanced probes for miR-137-3p (mmu480924_mir), miR-34a-5p (mmu481304_mir), miR-27b-3p

(mmu478270_mir), miR-485-5p (mmu482774_mir), and normalized to miR-191-5p (mmu481584_mir) under the following protocol: 95 °C for 10 min, 45 cycles of 95 °C for 15 s and 60 °C for 1 min.

3.2.5 Western blot analysis

Whole cell lysates were collected in standard RIPA buffer and quantified using a Bradford assay (BioRad). Protein lysates (50µg) were loaded on a 6% SDS-PAGE gel and transferred to nitrocellulose membrane (BioRad) using a wet electroblotting system (BioRad). The membrane was blocked in 5% milk in Tris-buffered saline with 0.1% Tween-20 (SigmaAldrich) for 1 hour and incubated overnight at 4°C with primary antibody (ATRX: 1:500, H-300 Santa Cruz Biotechnology Inc.; INCENP: 1:3000, Sigma). The following day the membrane was washed and incubated in the appropriate horseradish peroxidase-conjugated secondary antibody (1:4000, Jackson ImmunoResearch Laboratories, Inc.). The membrane was rinsed briefly in enhanced chemiluminescence substrate (BioRad) before exposure on a ChemiDoc Gel Imaging System (BioRad).

3.2.6 Magnetic resonance imaging

Mice were perfused with 30mL of PBS supplemented with 1µL/mL heparin (Sandoz) and 2mM ProHance (Bracco Imaging Canada) followed by 30mL 4% paraformaldehyde supplemented with 2mM ProHance. After perfusion, mice were decapitated, and the skin, cartilaginous nose tip, and lower jaw were removed. The remaining brain and skull structures were incubated in PBS supplemented with 2mM ProHance and 0.02% sodium azide for at least one month before MRI scanning (de Guzman, Wong, Gleave, & Nieman, 2016). A multi-channel 7.0 Tesla MRI scanner (Agilent Inc., Palo Alto, CA) was used to image the brains within their skulls. Sixteen custom-built solenoid coils were used to image the brains in parallel (Nieman et al., 2018). In order to detect volumetric changes, we used the following parameters for the MRI scan: T2- weighted, 3-D fast spin-echo sequence, with a cylindrical acquisition of k-space, a TR of 350 ms, and TEs of 12 ms per echo for 6 echoes, field-of-view equaled to 20 x 20 x 25 mm3 and matrix size equaled to 504 x 504 x

630. Our parameters output an image with 0.040 mm isotropic voxels. The total imaging time was 14 hours (Spencer Noakes, Henkelman, & Nieman, 2017).

3.2.7 MRI Registration and Analysis

To visualize and compare any changes in the mouse brains, the images are linearly (6 followed by 12 parameter) and non-linearly registered together. Registrations were performed with a combination of mni_autoreg tools (Collins, Neelin, Peters, & Evans, 1994) and ANTS (advanced normalization tools) (Avants, Tustison, Wu, Cook, & Gee, 2011). All scans are then resampled with the appropriate transform and averaged to create a population atlas representing the average anatomy of the study sample. The result of the registration is to have all images deformed into alignment with each other in an unbiased fashion. For the volume measurements, this allows for the analysis of the deformations needed to take each individual mouse's anatomy into this final atlas space, the goal being to model how the deformation fields relate to genotype (Lerch et al., 2008; Nieman, Flenniken, Adamson, Henkelman, & Sled, 2006). The jacobian determinants of the deformation fields are then calculated as measures of volume at each voxel. Significant volume differences can then be calculated by warping a pre-existing classified MRI atlas onto the population atlas, which allows for the volume of 182 different segmented structures encompassing cortical lobes, large white matter structures (i.e. corpus callosum), ventricles, cerebellum, brain stem, and olfactory bulbs (Dorr, Lerch, Spring, Kabani, & Henkelman, 2008; Qiu et al., 2018; Richards et al., 2011; Steadman et al., 2014; Ullmann et al., 2014) to be assessed in all brains. Further, these measurements can be examined on a voxel-wise basis to localize the differences found within regions or across the brain. Multiple comparisons in this study were controlled for using the False Discovery Rate (Genovese, Lazar, & Nichols, 2002).

3.2.8 Golgi staining and analysis

Brains from 3-month-old mice were stained using the FD Rapid GolgiStain Kit (FD Neurotechnologies, Inc). They were then flash frozen and sectioned on a cryostat at 100µm thickness and further processed as per kit instructions. Hippocampal CA1 pyramidal

neurons were imaged on a laser scanning confocal microscope (Leica SP5). *z*-Stacks were obtained of whole neurons (10-15 *z*-intervals per neuron). 65 Ctrl and 51 *Atrx*-cKO neurons were traced from 3 Ctrl/*Atrx*-cKO pairs. Dendrites were analyzed in ImageJ (FIJI) using the Simple Neurite Tracer plugin; the traces were analyzed using the Sholl plugin in ImageJ (FIJI) at a radius step size of 4µm (Ferreira et al., 2014; Longair, Baker, & Armstrong, 2011). Statistics were calculated by two-way repeated measures ANOVA with Sidak's multiple comparison test or unpaired Student's T-tests where applicable.

3.2.9 Open field test

In the open field test, locomotor activity was automatically recorded (AccuScan Instrument). The mice were placed in an arena with an area of 20 cm x 20 cm with 30 cm high walls. Mice were acclimated to the room for ten minutes prior to testing. Locomotor activity was measured in 5 min intervals over 2 hours as previously described (Tamming et al., 2017). Distance travelled and time spent in the center were recorded. Statistics were calculated by two-way repeated measures ANOVA with Sidak's multiple comparison test or unpaired Student's T-tests where applicable.

3.2.10 Elevated plus maze

Animals were placed in the center of the elevated plus maze (Med Associate Inc) and their activity was recorded over 5 min. Total time spent in the open and closed arms was recorded using computer software (AnyMaze). The center of the mouse body was used as an indicator of which zone they were in. Statistics were calculated by unpaired Student's T-tests.

3.2.11 Y maze

Animals were placed in the center of a symmetrical three-armed Y maze as described (de Castro et al., 2009; Tamming et al., 2017). Each mouse underwent one trial of 5 minutes. Order of arm entry was recorded using computer software (AnyMaze) and spontaneous alternation was counted when a mouse entered all three arms in a row without visiting a previous arm.

3.2.12 Novel object recognition

Mice were habituated in an open arena with no objects for 5 minutes on Day 1 and Day 2, as described (Tamming et al., 2017). On Day 3, mice were exposed to two identical objects for ten minutes (A; a red plastic ball attached on top of a yellow cube base). Video tracking (AnyMaze) was used to record time spent with each object. To test short-term memory, mice were exposed to the original object (A) and a novel object (B; a blue plastic pyramid attached on top of a green prism base) 1.5 hours after training. To test long-term memory, mice were exposed to (A) and (B) 24 hours after training. Novel object recognition was expressed as the percentage of time spent with the novel object as a fraction of the total time spent interacting. Interaction was defined as sniffing or touching the object, but not leaning against or climbing on the object.

3.2.13 Morris water maze

The Morris water maze was conducted as described previously (Vorhees & Williams, 2006). The task was performed in a 1.5 m diameter pool with 25°C water and the platform was submerged 1 cm beneath the water surface. Spatial cues (shapes printed in black & white) were distributed around the pool. Mice were given four trials (90 s) a day for 4 consecutive days with a 15 min intertrial period. The latency, distance, and swim speed to find the platform was recorded using video tracking software (AnyMaze). If the mice did not find the platform within 90 s, they were gently guided onto the platform. On the fifth and the twelfth days the platform was removed and time spent in each quadrant of the maze was recorded using the video software. Statistics were calculated by one- or two-way repeated measures ANOVA with Sidak's multiple comparison test, where applicable.

3.2.14 Contextual fear conditioning

To measure contextual fear memory, mice were placed in a 20 cm x 10 cm clear acrylic enclosure with a metal grid floor and one wall distinct from the others (stripes were drawn on one of the walls). The chamber was equipped with an electric shock generator. Videos were recorded using the AnyMaze video tracking software. On Day 1, mice could explore

the enclosure freely and at 150 s the mice were given a shock (2 mA, 180 V, 2 s). After 30 s, the mice were returned to their home cage. The next day (24 h), the mice were placed back into the enclosure for 6 min and freezing time was measured in 30 s intervals. Freezing was defined as immobility lasting more than 0.5 s. Statistics were calculated by two-way repeated measures ANOVA with Sidak's multiple comparison test or unpaired Student's T-tests where applicable.

3.2.15 Touchscreen assays

The paired associate learning (dPAL) and visual paired discrimination (VPD) and reversal tasks were performed as previously described (Bussey et al., 2008; Delotterie et al., 2015; Talpos, Winters, Dias, Saksida, & Bussey, 2009). Animals were food-restricted to 85% starting body weight. Animals were separated into two counter-balanced subgroups to control for time of day of testing, and equipment variation. Mice were tested in Bussey-Saksida mouse touch screen chambers (Lafayette Neuroscience) with strawberry milkshake given as a reward.

For the dPAL acquisition phase, animals were tested for their ability to associate objects with locations. Mice were presented with two images in two of three windows; one image was in its correct location (S+) and one was in one of its two incorrect locations (S-). The third window was blank. A correct response triggered reward presentation and start of an inter-trial period. The pre-training was repeated until mice reached criterion (completion of 36 trials within 60 minutes). The dPAL evaluation phase was performed for 45 sessions over 9 weeks. A correct response triggered reward presentation, whereas an incorrect response caused a 5 s time out and the house lights to turn on. An incorrect response also resulted in a correction trial, where the same S+/S- images were presented in the same two locations until the mouse responded correctly. The mouse was given 36 trials over 60 minutes per day. Percent correct, number of correction trials, latency to a correct or incorrect response, and latency to retrieve reward were recorded for each week.

VPD acquisition required the animal to touch the same image (S+) no matter which window it appeared in. The other screen had an incorrect image (S-). A correct response triggered reward presentation, whereas an incorrect response triggered the house lights to turn on, a time out of 5 s, and a correction trial to begin (previous trial repeated until a correct choice is made). This was repeated until mice reached criterion of 24/30 trials correct within 60 minutes over 2 consecutive days, after which baseline measurements were done for two sessions. Parameters for baseline were identical to the acquisition steps.

Immediately following baseline measurements, the VPD task reversal began, where most parameters were the same as the acquisition, but the correct image associated with the reward was S-, and the incorrect response that triggers house lights was S+. The mouse was given 30 trials per day over 10 days. Percent correct, number of correction trials needed, latency to a correct or incorrect response, and latency to retrieve reward on each day were recorded. Statistics were calculated by two-way repeated measures ANOVA with Sidak's multiple comparison test or unpaired Student's T-tests where applicable.

3.2.16 RNA sequencing and analysis

Hippocampal total RNA was isolated using the miRVANA RNA isolation kit (ThermoFisher) from three pairs of 3-month-old control and *Atrx*-cKO male and female mice (12 samples total). RNA was quantified using the Qubit 2.0 Fluorometer (Thermo Fisher Scientific, Waltham, MA) and quality was assessed using the Agilent 2100 Bioanalyzer (Agilent Technologies Inc., Palo Alto, CA) with the RNA 6000 Nano kit (Caliper Life Sciences, Mountain View, CA). Libraries were prepared, including rRNA reduction, using the ScriptSeq Complete Gold Kit (H/M/R) (Illumina Inc., San Diego, CA). Samples were fragmented, cDNA was synthesized, tagged, cleaned-up and subjected to PCR with barcoded reverse primers (ScriptSeq Index PCR Primers) to permit equimolar pooling of samples into one library. The pooled library size distribution was assessed on an Agilent High Sensitivity DNA Bioanalyzer chip and quantitated using the Qubit 2.0 Fluorometer. All samples were sequenced at the London Regional Genomics Centre (Robarts Research Institute, London, Ontario, Canada; http://www.lrgc.ca) using the

Illumina NextSeq 500 (Illumina Inc., San Diego, CA). The libraries were sequenced as a paired end run, 2 x76 bp, using a High Output v2 kit (150 cycles). Fastq data files were downloaded from BaseSpace. At least 60 million fragments were obtained for each sample. Raw reads were pre-processed with the sequence-grooming tool cutadapt (Zerbino et al., 2018) version 0.4.1 with the following quality trimming and filtering parameters (`--phred33 --length36 -q 5 --stringency 1 -e 0.1`). Each set of paired-end reads was mapped against the Mus Musculus GRCm38.p6 primary assembly downloaded from Ensembl (Pertea et al., 2015) release 94 (https://useast.ensembl.org/Mus_musculus/Info/Annotation) using HISAT2 version 2.0.4. SAMtools was then used to sort and convert SAM files. The read alignments and Mus Musculus GRCm38 genome annotation were provided as input into StringTie v1.3.3 (Soneson, Love, & Robinson, 2015) which returned gene and transcript abundances for each sample. We imported coverage and abundances for transcripts into R using the tximport (Love, Huber, & Anders, 2014) R package and conducted differential analysis of transcript count data stratified or not on sex using the DESeq2 R package. For the unstratified analysis, an interaction term was added to the model in order to test if the effect of ATRX deletion differs across sex. We used the independent hypothesis weighting (IHW) Bioconductor package (Ignatiadis, Klaus, Zaugg, & Huber, 2016) to weight p-values and adjust for multiple testing using the procedure of Benjamini Hochberg (BH) (Benjamini & Hochberg, 1995). Functional enrichment of significant genes with aggregated p-value <0.05 was evaluated by the ‘weight01’ algorithm implemented in the R topGO package (Alexa, Rahnenfuhrer, & Lengauer, 2006) that assesses, prunes and weighs for local dependencies of gene ontology (GO) terms, and Fisher exact test.

3.2.17 Transmission electron microscopy

Mice were perfused with 4% paraformaldehyde (VWR) dissolved in phosphate buffer and sectioned at 500µm on a Vibratome Series 1000 Sectioning System. Sections were post-fixed overnight in 4% paraformaldehyde for 24h and in 1% glutaraldehyde for 1 hour, then washed and left in phosphate buffer until preparation of ultra-thin sections. Slices were transferred to the Biotron facility at Western University for the remaining steps. Coronal

slices from the hippocampal layer were rinsed in distilled water, post-fixed for one hour at room temperature in 1% osmium tetroxide (Electron Microscopy Sciences Warrington, PA) and 1.5% potassium ferrocyanide and post-fixed for a second hour in 1% osmium tetroxide (Harris, Jensen, & Tsao, 1992). The slices were quickly dehydrated through a graded series of ethanol, rinsed in 100% acetone and then infiltrated with inversion for one hour in 50% epon-araldite resin and placed overnight in 100% resin on a rotator. The slices were polymerized overnight at 60°C in a vented oven, sandwiched between two sheets of Aclar film covered with a light weight (Bisht, El Hajj, Savage, Sanchez, & Tremblay, 2016). The hippocampal region was cut from the resin-embedded slice using a razor blade and mounted on a blank epoxy block using cyanoacrylate glue. Semi-thin sections were made with a Reichert Ultracut ultramicrotome and stained with toluidine blue and used to select the CA1 neuropil region for ultrathin sectioning. Thin sections (100nm) were collected on 200 mesh nickel grids (EMS), post-stained with lead citrate and images were collected with a Philips 420 transmission electron microscope equipped with an AMT 4K megapixel XR41S-B camera (Woburn, MA). Images were captured within the stratum radiatum / stratum lacunosum moleculare at 9200X in a semi-random manner to obtain at least 50 synapses containing a distinct synaptic cleft without regard to the length of the cleft. Image analysis was performed in ImageJ. A total of 104 Ctrl and 84 *Atrx*-cKO synapses were quantified from 3 Ctrl/*Atrx*-cKO pairs. Synapses were binned in 50nm increments from the active zone and the number of docked vesicles and vesicles in each bin were counted; this also determined total number of vesicles per synapse. Vesicle cluster size was measured to calculate vesicle density. The area of the post-synaptic density was also quantified. Statistics were calculated by two-way repeated measures ANOVA with Sidak's multiple comparison test or unpaired Student's T-tests where applicable.

3.2.18 Statistical analyses

All data were analyzed using GraphPad Prism software with Student's T test (unpaired, two-tailed) or one or two-way repeated measures ANOVA with Sidak's post-test where applicable. All results are depicted as mean +/- SEM unless indicated otherwise. P values

of less than 0.05 were considered to indicate significance. For neuron branching and transmission electron microscopy analyses, individual neurons or synapses were counted as a single *n* value, based on previous literature (de Vivo et al., 2017; Molnar et al., 2016).

3.1 Results

3.1.1 Generation and validation of mice with neuron-specific Atrx deletion

We generated mice lacking ATRX in postnatal forebrain excitatory neurons by Cre/loxP mediated recombination of the mouse *Atrx* gene with the *CaMKII*-Cre driver line of mice (Tronche et al., 1999). To confirm loss of ATRX, we performed immunofluorescence staining of control and conditional knockout (*Atrx*-cKO) brain cryosections obtained from 3-month-old mice (Figure 3-1A,B). ATRX is highly expressed in excitatory neurons of the hippocampus of control mice, including the cortex and hippocampal CA1, CA2/3, and dentate gyrus neurons, but is absent in these cells in the *Atrx*-cKO mice. Additional validation of *Atrx* inactivation in *Atrx*-cKO mice was achieved by qRT-PCR (Figure 3-1C), showing that *Atrx* expression is decreased by 78% (+/- 9.4%) and 81% (+/- 1.7%) in the cortex and the hippocampus, respectively, which is expected from a neuron-specific deletion. The brain sub-region specificity of ATRX loss was demonstrated by western blot analysis, showing reduced protein levels in the rostral and caudal cortices and hippocampus, but not in the cerebellum (Figure 3-1D). The mice survived to adulthood and had normal general appearance and behaviour. However, body weight measurements revealed a small but significant reduction in *Atrx*-cKO compared to control mice (Figure 3-1E). These findings demonstrate that we achieved specific deletion of *Atrx* in excitatory neurons and while the mice were slightly smaller, they survived to adulthood, allowing further analyses in the adult brain.

3.1.2 MRI analysis reveals anatomical abnormalities in the hippocampus of Atrx-cKO mice

We first examined control and *Atrx*-cKO mouse brains for neuroanatomical anomalies by magnetic resonance imaging (MRI). Using a T2-weighted MRI sequence, we

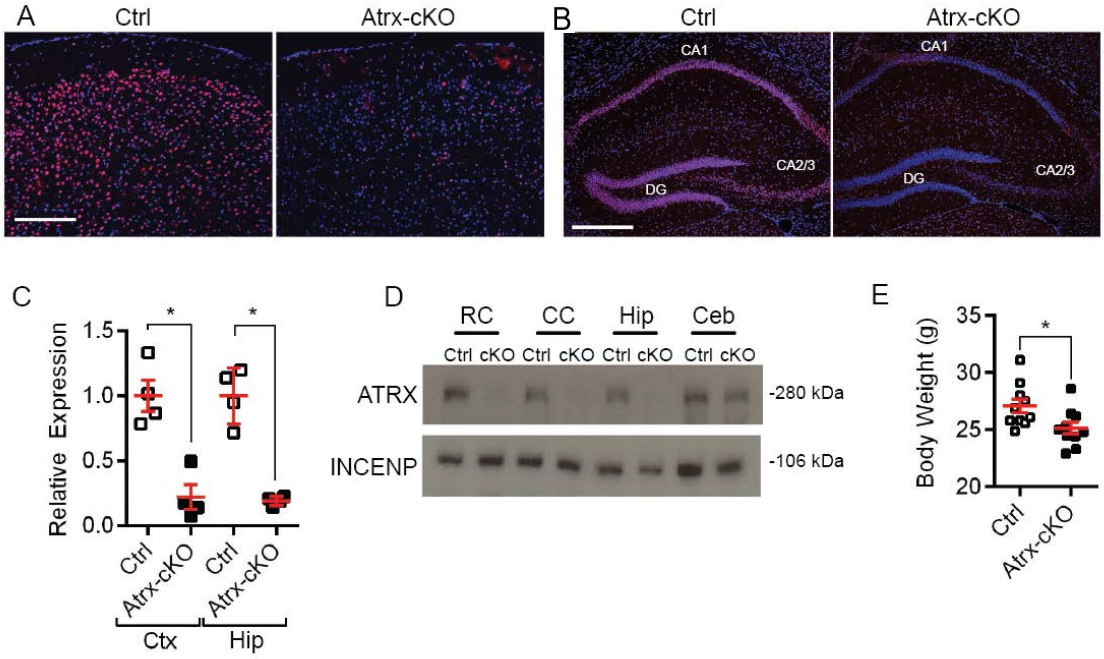

Figure 3-1 Validation of Atrx inactivation in pyramidal neurons of the forebrain.

Immunofluorescence in cortex of control (Ctrl) and knockout (*Atrx*-cKO) male mice. ATRX: red; DAPI: blue. Scale bar: 100 µm. (B) Immunofluorescence in hippocampus of control (Ctrl) and knockout (*Atrx*-cKO) male mice. ATRX: red; DAPI: blue. Scale bar: 200 µm. (C) *Atrx* RNA transcripts measured by qRT-PCR in the rostral cortex (Ctx) ($p<0.005$) and hippocampus (HI) ($p<0.001$) ($n=4$). (D) Western blot of ATRX and INCENP using protein extracts from rostral cortex (RC), caudal cortex (CC), hippocampus (Hip) and cerebellum (Ceb). (E) Body weight of control and *Atrx*-cKO male mice at 3 months of age ($n=10$) ($p<0.05$). Statistics by unpaired Student's T-test.

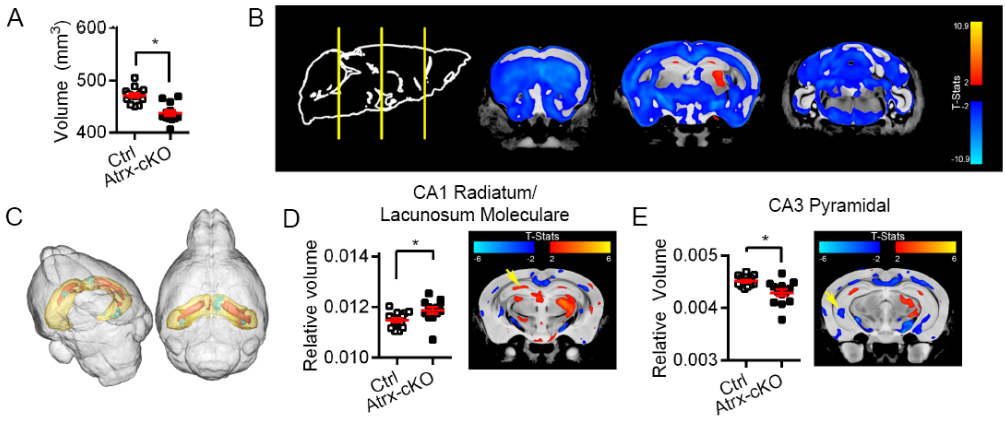

F

Relative Volumes Structures	Ctrl Mean	*Atrx*-cKO Mean	%Diff	Effect	P-Value	FDR
CA1 Oriens	0.005283	0.005295	0.24	0.07	0.88	0.01
CA1 Pyramidal	0.002731	0.002768	1.35	0.45	0.38	0.02
CA1 Radiatum	0.006050	0.006248	3.28	1.22	0.01*	0.04
CA2 Pyramidal	0.000470	0.000466	-0.89	-0.27	0.55	0.00
CA2 Radiatum	0.001059	0.001067	0.80	0.29	0.52	0.00
CA3 Oriens	0.006386	0.006197	-2.95	-0.90	0.02*	0.00
CA3 Pyramidal (Inner)	0.000341	0.000335	-1.68	-0.33	0.47	0.00
CA3 Pyramidal (Outer)	0.002372	0.002271	-4.25	-1.01	0.02*	0.00
CA3 Radiatum	0.004511	0.004287	-4.98	-2.52	0.00*	0.00
Stratum Lucidum	0.001801	0.001714	-4.83	-1.22	0.01*	0.00
Stratum Lacunosum Moleculare	0.005425	0.005618	3.55	1.27	0.01*	0.03
Dentate Gyrus (Molecular)	0.009067	0.009439	4.10	1.45	0.02*	0.14
Dentate Gyrus (Polymoprhic)	0.001423	0.001408	-1.03	-0.19	0.73	0.02

Figure 3-2 MRI reveals altered morphology of Atrx-cKO hippocampi.

(A) Absolute volumes of Ctrl and *Atrx*-cKO mouse brains in mm3 ($p<0.0001$). (B) Cumulative images of Ctrl and *Atrx*-cKO brains displaying changes in density of absolute volume. (C) Cumulative 3D image from Ctrl and *Atrx*-cKO mouse brains displaying changes in density of hippocampus volume relative to brain size. Hippocampus is colored yellow, areas of increased volume in *Atrx*-KO are colored orange and areas of decreased volume in green. (D) Relative size of CA1 stratum radiatum and lacunosum moleculare in Ctrl and *Atrx*-cKO mouse brains ($p<0.05$), with MRI image showing cumulative changes in *Atrx*-cKO compared to control. (E) Relative size of CA3 pyramidal layer in Ctrl and *Atrx*-cKO mouse brains ($p<0.005$), with MRI image showing cumulative changes in *Atrx*-cKO compared to control. (F) Relative volumes of all hippocampal structures, including mean and standard deviation (SD) of Ctrl and *Atrx*-cKO, percent difference (%Diff), effect size, P-value, and false discovery rate (FDR). Asterisks indicate $p<0.05$. All data is derived from 16 Ctrl and 13 *Atrx*-cKO mouse brains.

were able to analyze and compare the entire brain as well as independent brain regions from 16 control and 13 Atrx-cKO male animals. The data obtained showed that the overall volume of the *Atrx*-cKO brain is significantly smaller compared to controls (92.8% of control volume, $P<0.0001$), as indicated by whole volume in mm^3 and cumulative serial slices of control and *Atrx*-cKO brains (Figure 3-2A,B), which correlates with the smaller body size of the mice. Due to the reduction in body size and absolute total brain and hippocampal volumes of the *Atrx*-cKO mice, we next examined hippocampal neuroanatomy relative to total brain volume (Figure 3-2C). The relative volume of the CA1 stratum radiatum (SR) and stratum lacunosum moleculare (SLM) was significantly increased in the *Atrx*-cKO mice compared to controls (Figure 3-2D) whereas the CA3 pyramidal layer was significantly decreased in size (Figure 3-2E). Relative volumes of all hippocampal regions are tabulated in Figure 3-2F.

We postulated that the increase in relative volume of the CA1 SR/SLM may be due to increased length or branching of CA1 apical dendrites. To investigate this possibility, Golgi staining was used to sporadically label neurons (Figure 3-3A) and Sholl analysis was performed on confocal microscopy images to evaluate apical dendrite branching of CA1 hippocampal neurons. However, no significant difference in dendritic branching or length was observed between control and *Atrx*-cKO mice, whether analyzed separately for apical or basal dendrites (Figure 3-3B-G). Increased relative volume might also be caused by an increased number of cells, but immunofluorescence staining and quantification of astrocytes (GFAP+) and microglia (IBA1+) and total number of cells (inferred from DAPI+ staining) revealed no differences in *Atrx*-cKO hippocampi (Figure 3-3H-J). Overall, the increased relative volume of the CA1 SR/SLM cannot be explained by increased length or complexity of dendritic trees or by an increased number of glial cells.

3.1.3 Pre- and post-synaptic structural defects in Atrx-cKO male mice

Based on the hippocampal structural alterations we detected by MRI, we looked more closely at potential ultrastructural changes in the CA1 SR/SLM area using transmission

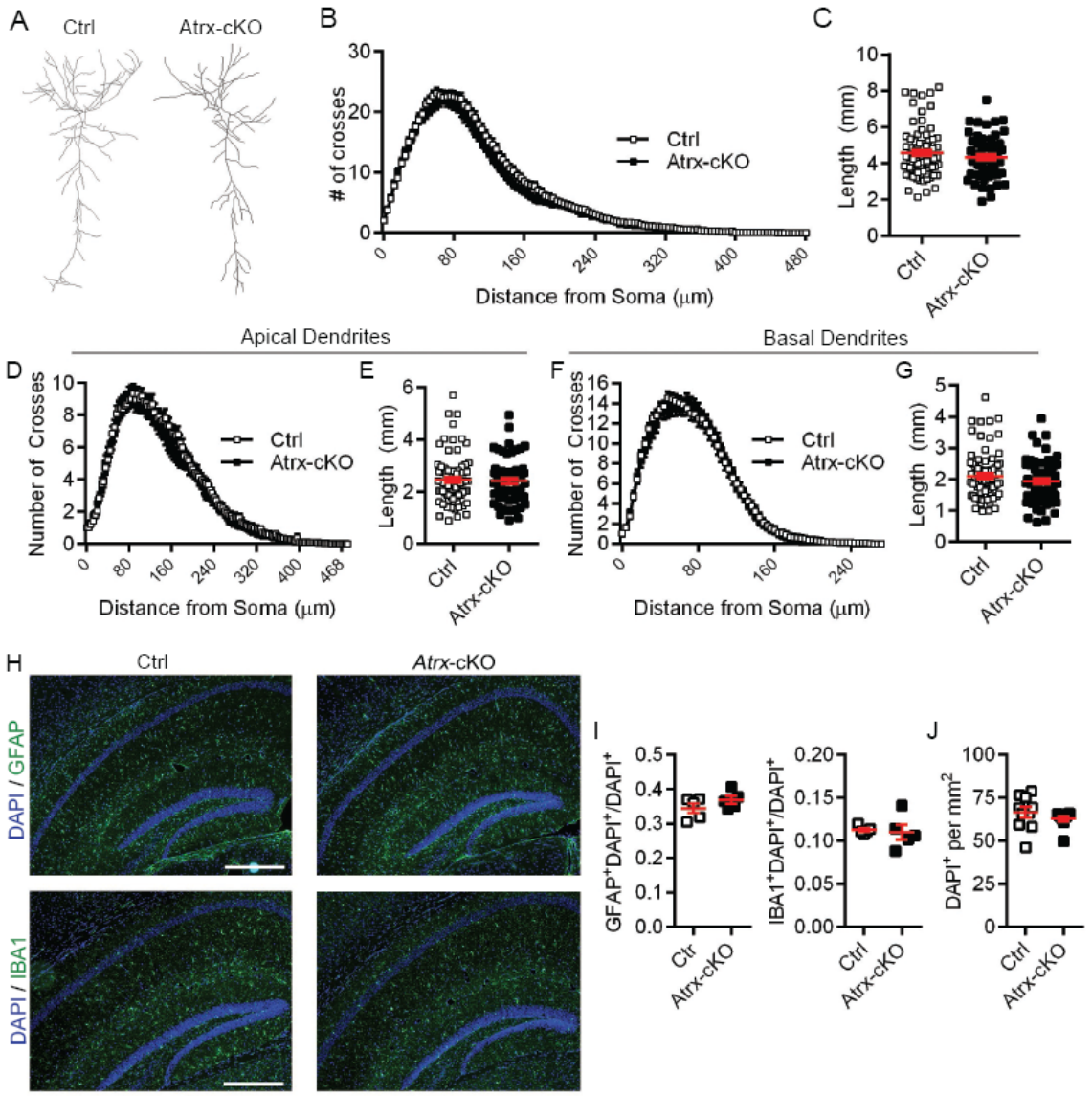

Figure 3-3 CA1 dendritic length and branching and the number of non-neuronal cells are not affected in Atrx-cKO mouse hippocampi.

(A) Representative Golgi traces from Ctrl and Atrx-cKO hippocampal CA1 pyramidal neurons. (B) Sholl analysis of Ctrl (n=73) and Atrx-cKO (n=53) CA1 pyramidal neurons (p=0.0842). (C) Total length of Ctrl and Atrx-cKO CA1 dendrites (p=0.2994). (D) Sholl analysis of Ctrl and Atrx-cKO CA1 apical dendrites (p=0.3858). (E) Total length of Ctrl and Atrx-cKO CA1 apical dendrites (p=0.7832). (F) Sholl analysis of Ctrl and Atrx-cKO

CA1 basal dendrites (p=0.7339). (G) Total length of Ctrl and Atrx-cKO CA1 basal dendrites (p=0.2237). (H) Immunofluorescence staining of GFAP or IBA1 in Ctrl and Atrx-cKO hippocampi. DAPI was used as a counterstain. Scale bar indicates 400 µm. (I) Quantification of the proportion of GFAP+ (p=0.2151) and IBA1+ (p=0.7903) cells in stratum radiatum/stratum lucidem moleculare of Ctrl and Atrx-cKO hippocampi (n=5). (J) Quantification of DAPI+ cells per mm2 in n stratum radiatum/stratum lucidem moleculare of Ctrl and Atrx-cKO hippocampi (n=10, p=0.2904). Data was analyzed by unpaired Student's T-Test or two-way repeated measures ANOVA with Sidak's multiple comparisons test where applicable, and asterisks indicate p<0.05. Data is displayed as mean +/-SEM.

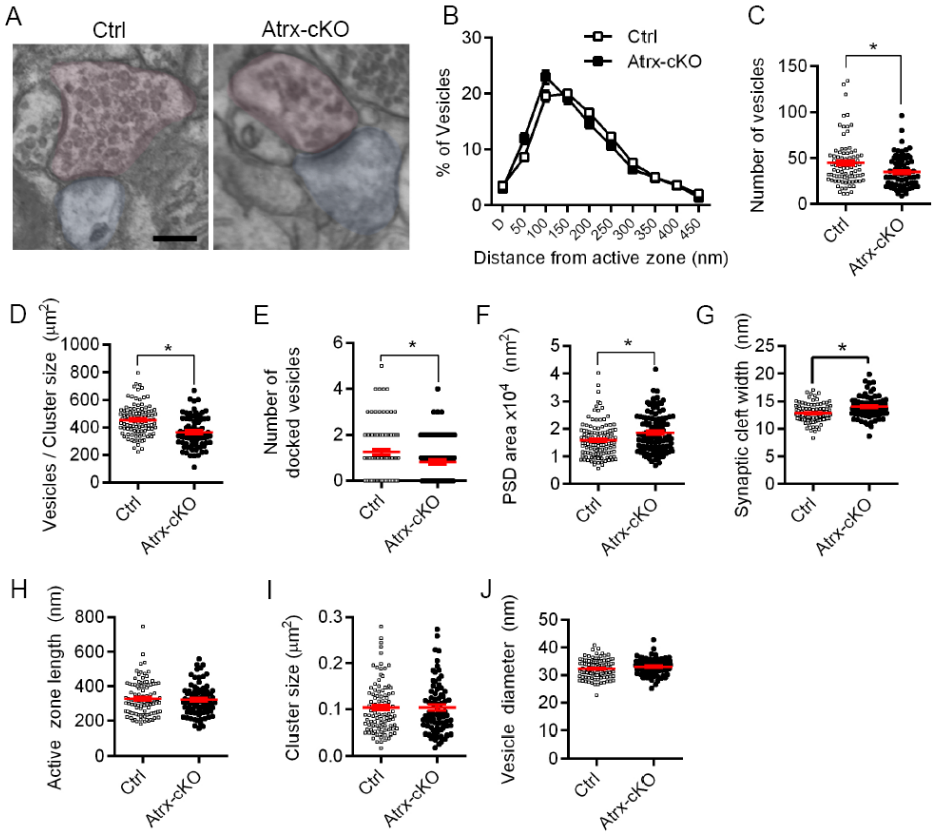

Figure 3-4 Ultrastructural analysis of Atrx-cKO CA1 apical synapses reveals a reduced number of total or docked presynaptic vesicles, wider synaptic cleft and larger post-synaptic density.

(A) Representative images of Ctrl and *Atrx*-cKO CA1 synapses imaged by transmission electron microscopy. Red shading indicates presynaptic neuron, blue shading indicates postsynaptic neuron. Scale bar = 200 nm. (B) Number of vesicles in 50nm bins from the active zone (p=0.9504) (Ctrl n=60, *Atrx*-cKO n=63). (C) Number of total vesicles (p<0.01). (D) Density of vesicles per cluster (p<0001). (E) Number of docked vesicles (p<0.05). (F) Post-synaptic density (PSD) area (p<0.005). (G) Synaptic cleft width (p< 0.0001). (H) Length of the pre-synaptic active zone (p=0.7039). (I) Synaptic vesicle cluster size (p=0.9917). (J) Vesicle diameter (p=0.1895). Data was analyzed by unpaired Student's T-test or two-way repeated measures ANOVA with Sidak's multiple comparisons test where applicable, and asterisks indicate p<0.05. Data is displayed as mean +/- SEM.

electron microscopy (TEM) (Figure 3-4A). The presynaptic boutons were divided in 50nm bins from the active zone, and the number of vesicles in each bin was counted. The spatial distribution of vesicles in relation to the cleft was unchanged between the *Atrx*-cKO mice and controls (Figure 3-4B). However, we found that the total number of vesicles, the density of the vesicles, and the number of docked vesicles was significantly decreased at *Atrx*-cKO compared to control synapses (Figure 3-4C-E). We also analysed other structural aspects of synapses and found that the size of the post-synaptic density and the width of the synaptic cleft were both increased in *Atrx*-cKO compared to controls (Figure 3-4F,G). The length of the active zone, cluster size, or diameter of the vesicles did not vary significantly between control and *Atrx*-cKO samples (Figure 3-4H-J). These results suggest that ATRX is required for structural integrity of the pre- and post-synapse, including maintenance of the synaptic vesicle pool at pre-synaptic termini and potential defects in postsynaptic protein clustering.

3.1.4 Loss of ATRX in neurons leads to long-term spatial learning and memory deficits

We next performed a battery of behaviour tests on male *Atrx*-cKO mice. Locomotor activity in the open field test was not significantly different between *Atrx*-cKO mice compared to controls, either over time (F=0.1722, P=0.6803) or if considering total distance travelled (T=0.6691, P=0.5072; Figure3-5A,B). The *Atrx*-cKO mice did not spend significantly more time in the centre of the chamber over time (F=2.960, P=0.0927; Figure 3-5C). However, they spent significantly more total time in the centre of the chamber when compared to controls (T=2.262, P=0.0291; Figure 3-5D), suggesting that loss of ATRX in neurons has an anxiolytic effect. This was confirmed by the behaviour of the *Atrx*-cKO mice in the elevated plus maze, as they spent significantly more time in the open arm of the maze compared to controls (T=2.158, P=0.0403; Figure 3-5E,F). We observed no difference in percent alternation in the Y-maze (T=0.9431, P=0.3543 Figure 3-5G), nor in the training phase of the novel object recognition task (Ctrl T=1.128, P=0.2697; cKO T=1.657, P=0.1096; Figure 3-5H) or memory tests at 1.5 hours (Ctrl T=4.277, P<0.001;

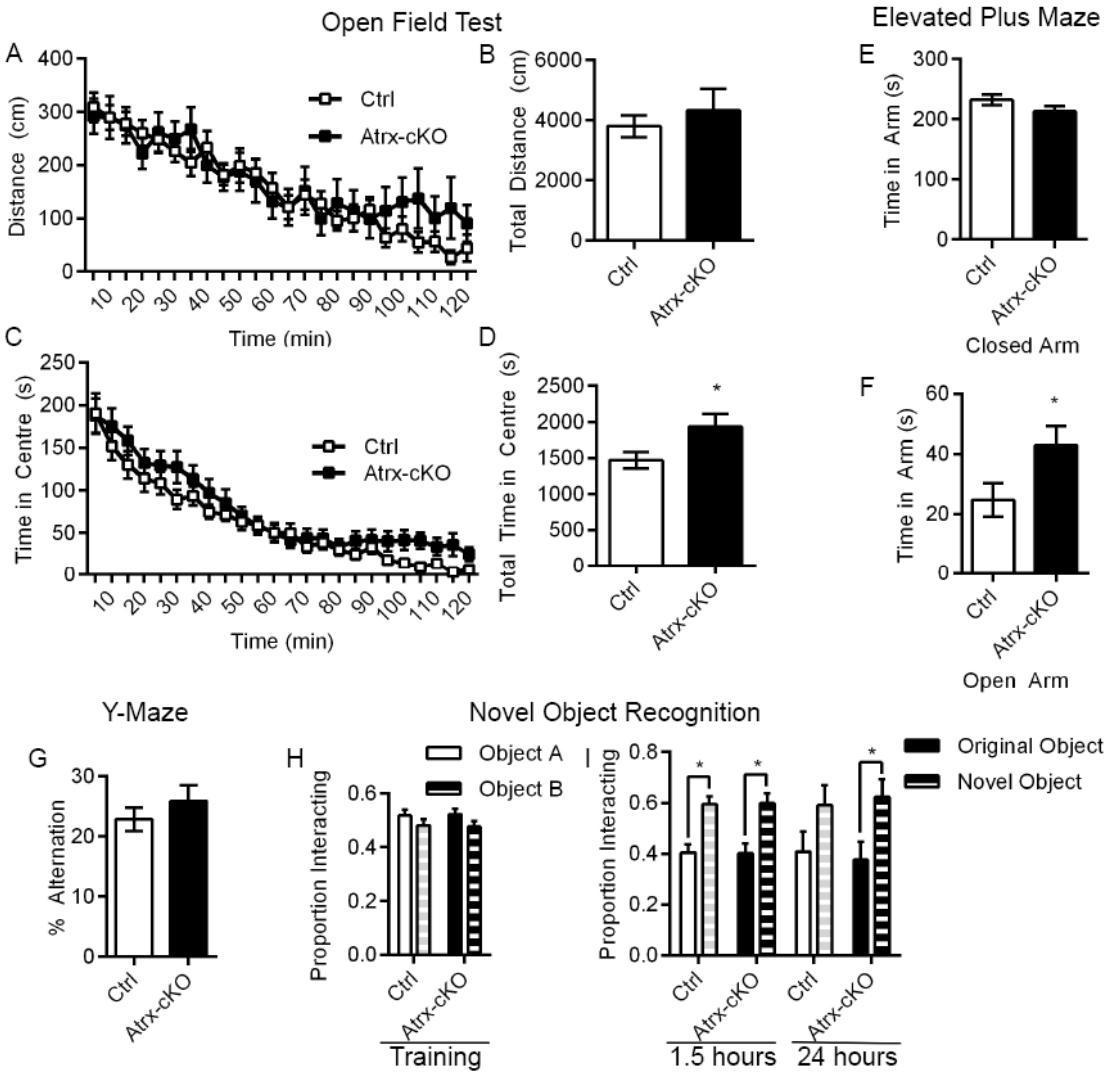

Figure 3-5 The Atrx-cKO males displayed decreased anxiety in the open field test and elevated plus maze.

(A) Distance travelled over 120 minutes in the open field test (p=0.6803) (n=22). (B) Total distance travelled (p=0.5072). (C) Time spent in the centre over 120 minutes in the open field test (p=0.0927) (n=22). (D) Total time spent in the centre (p<0.05). (E) Time spent in the closed (p=0.1308) and open (p<0.05) arm of the elevated plus maze (n=14). Statistics by two-way repeated measures ANOVA with Sidak's multiple comparisons test or Student's T-test where applicable, asterisks indicate p<0.05.

cKO T=3.545, P<0.005) or 24 hours (Ctrl T=1.645, P=0.112; cKO T=2.459, P<0.05; Figure 3-5I).

To investigate the effects of neuronal-specific ATRX ablation on spatial learning and memory, we tested the mice in the Morris water maze task. The *Atrx*-cKO mice showed a significant delay in latency to find the platform on day 3 of the learning portion of the task; however, by day 4 they were able to find the platform as quickly as the control mice (F=4.622, P=0.0404; Figure 3-6A). This finding was reflected in the distance traveled to find the platform (F=4.829, P=0.0364; Figure 3-6B). Swim speed was comparable to controls over the four days of learning the task (F=0.04238, P=0.8384; Figure 3-6C), confirming the findings of the open field test which showed similar activity levels between control and *Atrx*-cKO mice. Memory was tested on day 5 (24h after last training day) and day 12 (7 days after last training day). Both controls (F=29.36, P<0.0001) and the *Atrx*-cKO male mice (F=18.97, P<0.0001) spent significantly more time in the target quadrant than the left, opposite, or right quadrants (Figure 3-6D). However, on day 12, *Atrx*-cKO male mice failed to spend significantly more time in the target quadrant (F=1.420, P=0.2594) whereas controls were still able to remember (F=6.785, P<0.01), suggesting a long-term spatial memory deficit (Figure 3-6E). Moreover, *Atrx*-cKO male mice froze significantly less in the contextual fear memory task in comparison to their control counterparts 24h after a foot shock (over time F=5.392, P=0.0251; total time T=2.322; P=0.0251; Figure 3-6F,G). These behavioural analyses suggest that ATRX in required in excitatory neurons for long-term hippocampal-dependent spatial learning and memory.

3.1.5 Neuron-specific deletion of *Atrx* in female mice does not cause memory deficits

To determine whether loss of ATRX in female mice would exhibit similar behavioural defects as seen in male mice, we generated *Atrx*-cKO female mice (*Atrx*-cKO^{Fem}) and validated loss of ATRX in forebrain excitatory neurons by immunofluorescence staining and qRT-PCR (Figure 3-7A-C). *Atrx*-cKO^{Fem} mice displayed normal locomotion over time (F=1.239, P=0.2796) or in total distance travelled in the open field test (T=1.113,

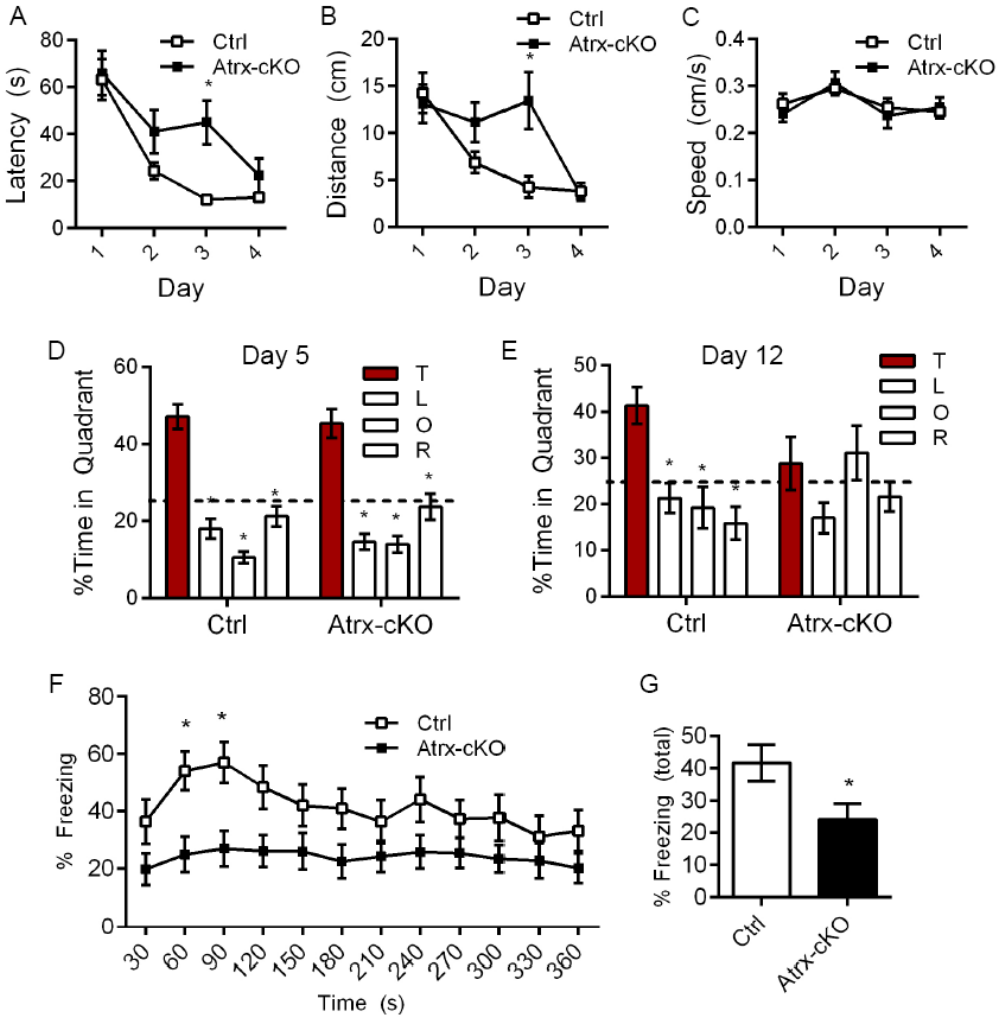

Figure 3-6 The *Atrx*-cKO mice exhibit impaired long-term spatial memory in the Morris water maze paradigm and in the contextual fear conditioning task.

(A,B,C) Latency to reach the platform ($p<0.05$), distance travelled ($p<0.05$), and swimming speed ($p=0.8384$) over four days (four trials per day) in the Morris water maze ($n=15$). (D) Percent time spent in each quadrant after removal of the platform on day 5. Dotted line indicates chance at 25%. (E) Percent time spent in each quadrant after removal of the platform on day 12. Dotted line indicates chance at 25%. (F) Percent of time freezing over 360s during the contextual fear conditioning task ($p<0.05$) ($n=22$). (G) Total time freezing ($p<0.05$). Statistics by two-way repeated measures ANOVA with Sidak's multiple comparisons test or Student's T-test where applicable, asterisks indicate $p<0.05$.

P=0.2796). Furthermore, we observed no changes in anxiety in the open field test over time (F=0.009, P=0.9254), total time spent in centre (T=0.095, P=0.9254; Figure 3-8A-D) nor in the time spent in the open arm (T=0.4947, P=0.6250) and closed arm (T=0.4907, P=0.6277; Figure 3-8E) in the elevated plus maze in the *Atrx*-cKO^{Fem} mice compared to control, indicating that the decreased anxiety levels are sex-specific.

Conversely to what was observed in the *Atrx*-cKO male mice we failed to observe differences between *Atrx*-cKO^{Fem} and control mice in latency in the Morris water maze training sessions (latency F=3.631, P=0.0683; distance F=1.385, P=0.2503; speed F=1.243, P=0.2754; Figure 3-9A-C). Memory of the platform location remained equivalent to that of controls when tested on day 5 or day 12 (Ctrl day 5 F=12.80, P<0.0001; cKO day 5 F=11.63, P=0.0006; Ctrl day 12 F=16.47, P<0.0001; *Atrx*-cKO^{Fem} day 12 F=12.97, P<0.0001; Figure 3-9D,E). Finally, there was no difference in freezing between control and *Atrx*-cKO^{Fem} 24h after foot shock in the contextual fear conditioning task (over time F=0.02257, P=0.8818; total time T=0.1502, P=0.8818; Figure 3-9F,G). We conclude that learning and memory is not impaired by ATRX loss in forebrain excitatory neurons of the *Atrx*-cKO^{Fem} mice.

3.1.6 Impaired object location associative memory in the rodent version of the paired associate learning (dPAL) task.

Given the observed male-specific defects in spatial memory, we performed additional translational cognitive tasks on the *Atrx*-cKO male mice. The dPAL touchscreen task in mice is analogous to cognitive testing done in humans by the Cambridge Neuropsychological Test Automated Battery (CANTAB) (Nithianantharajah et al., 2015; Sahakian et al., 1988) and normal performance in this task is thought to partly depend on the hippocampus (Delotterie et al., 2015; C. H. Kim, Heath, Kent, Bussey, & Saksida, 2015).

Control and *Atrx*-cKO mice were trained to identify the position of three images as depicted in Figure 3-10A, undergoing 36 trials per day for 10 weeks. The results demonstrate that

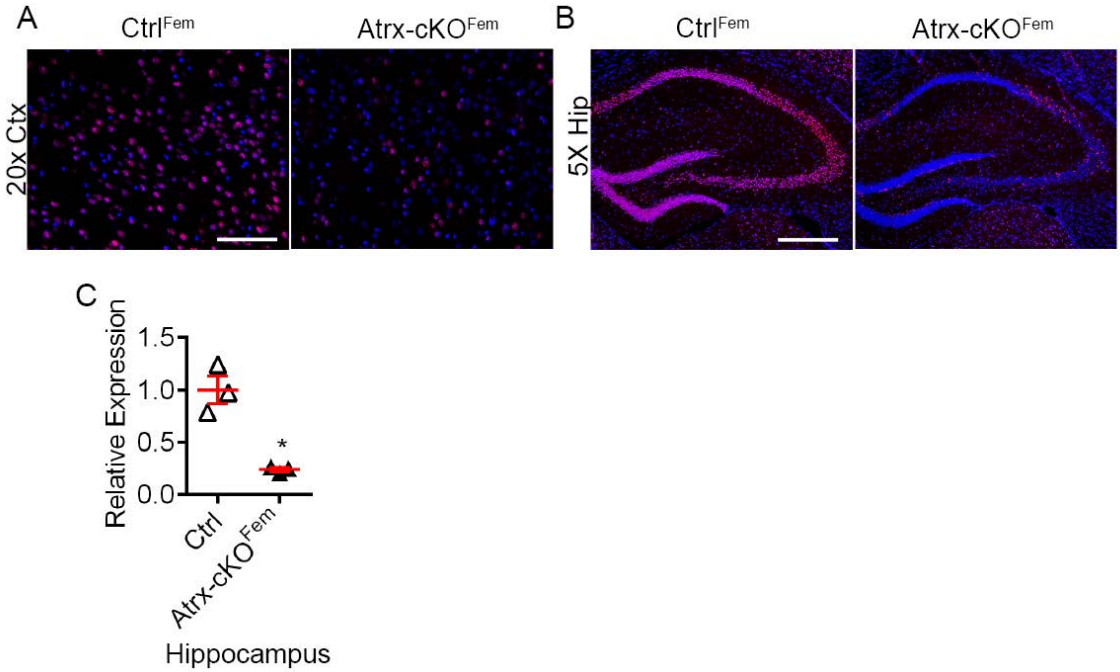

Figure 3-7 Expression of Atrx in Atrx-cKO females.

Immunofluorescence in cortex of control (Ctrl^{Fem}) and knockout (*Atrx*-cKO^{Fem}) female mice. ATRX: red; DAPI: blue. Scale bar: 50 µm. (B) Immunofluorescence in hippocampus of control (Ctrl^{Fem}) and knockout (*Atrx*-cKO^{Fem}) female mice. ATRX: red; DAPI: blue. Scale bar: 200 µm. (C) Expression of *Atrx* in the hippocampus by qRT-PCR (n=4) ($p<0.005$). Statistics by unpaired Student's T-test.

the *Atrx*-cKO mice exhibit a profound deficit in this task, indicated by both the percent correct (F=10.53, P=0.0031; Figure 3-10B) and the number of correction trials required (F=30.64, P<0.0001; Figure 3-10C). These defects were not due to an inability to perform within the chamber or to attentional deficits, as latency to a correct answer (F=0.4802, P=0.4943), to an incorrect answer (F=0.1259, P=0.7255), and to retrieve the reward (F=0.9840, P=0.3300) was not significantly different between control and *Atrx*-cKO mice (Figure 3-10D-F). To determine if the impairment in the dPAL task is caused by a vision problem rather than a learning defect, the mice were also tested in the visual paired discrimination (VPD) touchscreen task which requires the mice to discriminate between two images regardless of position on the screen. While the *Atrx*-cKO mice took significantly longer to reach the criterion pre-testing (T=2.945, P=0.0067; Figure 3-10G), there was no difference in the percent correct during baseline tests or after reversal compared to controls, suggesting that vision is intact in the *Atrx*-cKO mice (F=1.388, P=0.2490; Figure 3-10H). They did however require an increased number of correction trials, indicating that their cognitive flexibility may be marginally impaired compared to controls (F=11.84, P=0.0019; Figure 3-10I). The results of these touchscreen tests reinforce the findings that the *Atrx*-cKO male mice have impaired learning and memory.

3.1.7 RNA sequencing of the hippocampus reveals sex-specific transcriptional changes

Immediate early genes (IEGs) are activated rapidly and transiently upon neuronal stimulation (Cole, Saffen, Baraban, & Worley, 1989; Minatohara, Akiyoshi, & Okuno, 2015). In cultured neurons, ATRX is localized to a subset of IEG regulatory elements, and its protein binding partner DAXX is required for transcriptional activation of IEGs upon neuronal activation. Therefore, we investigated whether this was true for ATRX. In cultured E16.5 cortical neurons upon neuronal activation we found no significant changes in expression of a variety of immediate early genes (Appendix A), indicating that ATRX is not required in cortical neurons for activity-dependent regulation of IEG expression.

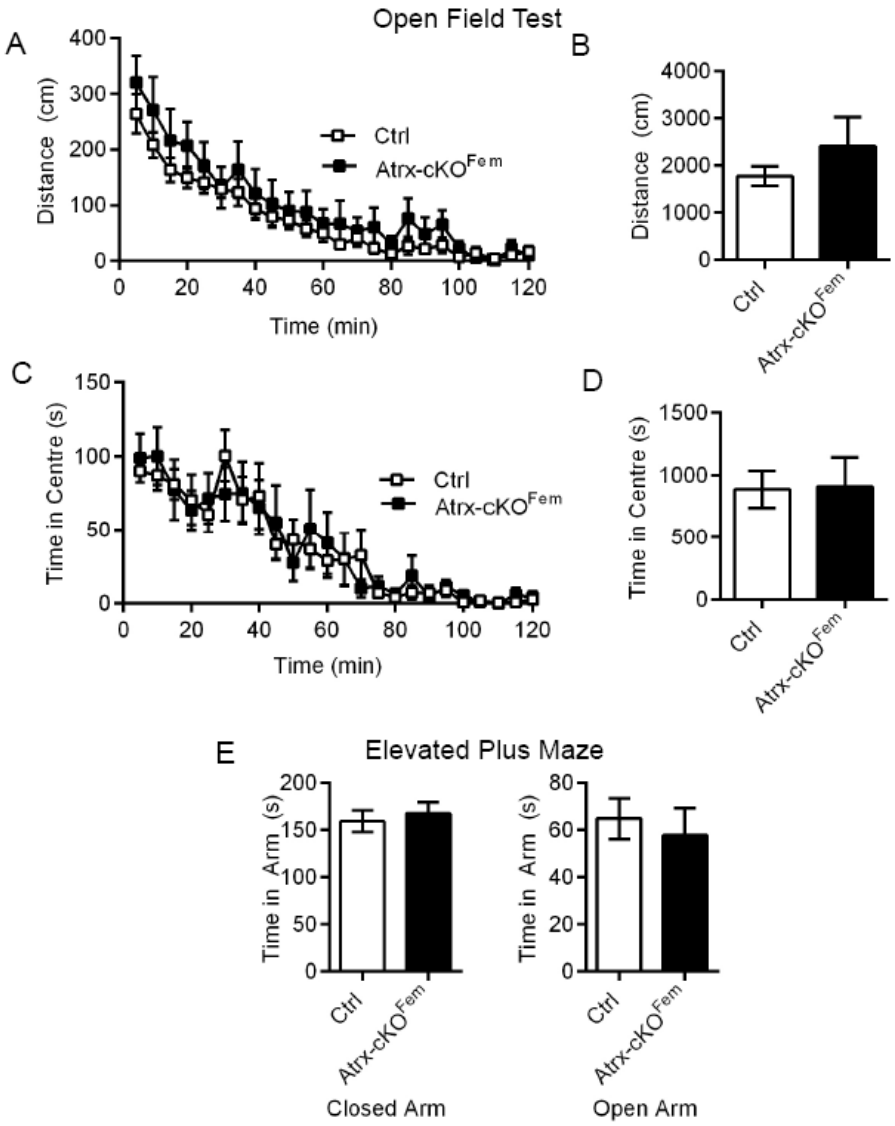

Figure 3-8 Atrx-cKO females have no change in anxiety.

(A) Distance travelled over 120 minutes in the open field test (p=0.2796) ($Ctrl^{Fem}$ n=12, *Atrx*-cKO^{Fem} n=9). (B) Total distance travelled (p=0.2796). (C) Time spent in the centre over 120 minutes in the open field test (p=0.9254) ($Ctrl^{Fem}$ n=12, *Atrx*-cKO^{Fem} n=9). (D) Total time spent in the centre (p=0.9254). (E) Time spent in the closed (p=0.6277) and open (p=0.6250) arm of the elevated plus maze ($Ctrl^{Fem}$ n=15, *Atrx*-cKO^{Fem} n=12). Statistics by two-way repeated measures ANOVA with Sidak's multiple comparisons test or Student's T-test where applicable.

To identify the molecular mechanism(s) leading to spatial memory impairment, we performed RNA-sequencing in both male and female hippocampi obtained from three pairs of littermate-matched Ctrl/*Atrx*-cKO and Ctrl^{Fem}/*Atrx*-cKO^{Fem} mice. There were 1520 transcripts differentially expressed in the *Atrx*-cKO males compared to control counterparts and 9068 transcripts in *Atrx*-cKO^{Fem} compared to the female controls (FDR < 0.20). To isolate transcripts that were likely to be causative to the impaired learning and memory phenotype in the male mice which was not found in the female mice, we focused on transcripts whose changes in expression with the *Atrx*-cKO were differential between male and female mice (n = 1054 transcripts, interaction term FDR < 0.05, Supplementary Table 1). The expression heat map of these transcripts illustrates that their expression levels are similar in control males and females but are differentially expressed when ATRX is lost depending on sex (Figure 3-11A). We then utilized PANTHER (Mi et al., 2017), a tool for gene enrichment analysis based on functional annotations to examine Gene Ontology biological processes for which our list of transcripts was enriched (Figure 3-11B). The top five pathways included neurotransmitter receptor transport to postsynaptic membrane, protein localization to postsynaptic membrane, non-motile cilium assembly, and vesicle-mediated transport to the membrane. Therefore, the RNA sequencing revealed many transcripts related to synapses, supporting the TEM data.

Certain miRNA are enriched within presynaptic terminals and have been implicated in neurotransmitter release by controlling expression of SNARE and other synaptic vesicle proteins (Ryan, Joilin, & Williams, 2015). These miRNA include miR-485, miR-34a, miR-137, and miR-27b. miR-485 targets a vesicular glycoprotein SV2A and overexpression results in decreased neurotransmitter release (Cohen, Lee, Chen, Li, & Fields, 2011), while miR-34a also targets vesicular proteins SYT1 and SYN1, affecting miniature excitatory postsynaptic currents (Agostini et al., 2011). miR-27b regulates two-thirds of the presynaptic transcriptome by silencing expression of the negative transcriptional regulator *Bmi1* (Poon, Gu, Ji, VanDongen, & Fivaz, 2016), and miR-137 overexpression affects synaptic vesicle localization and LTP (Siegert et al., 2015). To determine whether any of these miRNAs might be regulated by ATRX, with differential effects in male and female

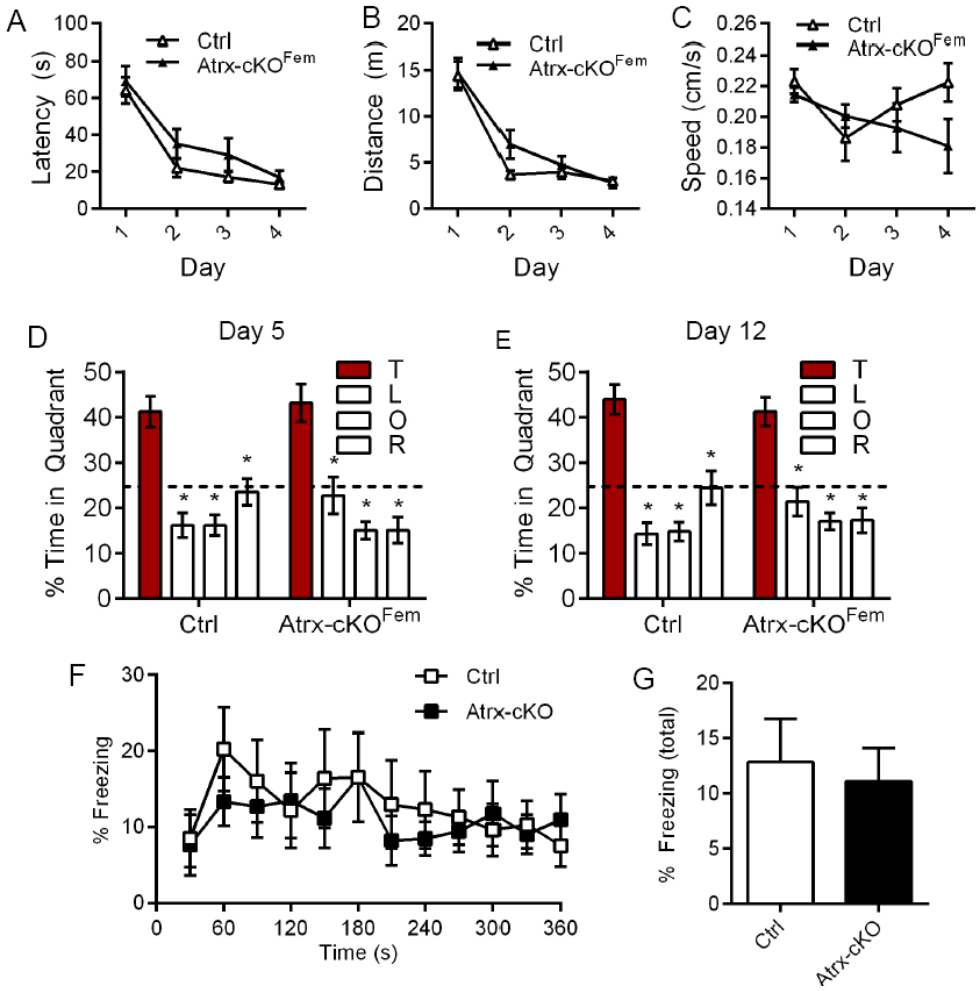

Figure 3-9 No change in spatial learning or memory in Atrx-cKO females in the Morris water maze or contextual fear conditioning tasks.

(A,B,C) Latency (p=0.0683), distance (p=0.2503), and speed (p=0.2754) over four days (four trials per day) in the Morris water maze (Ctrl^{Fem} n=15, *Atrx*-cKO^{Fem} n=12). (D) Percent time spent in each quadrant after removal of the platform on day 5. Dotted line indicates chance at 25%. (E) Percent time spent in each quadrant after removal of the platform on day 12. Dotted line indicates chance at 25%. (F) Percent of time freezing over 360s during the contextual fear conditioning task (p=0.8818) (Ctrl^{Fem} n=15, *Atrx*-cKO^{Fem} n=12. (G) Total time freezing (p=0.8818). Statistics by two-way repeated measures ANOVA with Sidak's multiple comparisons test or Student's T-test where applicable, asterisks indicate p<0.05.

cKO hippocampi, we assessed their expression by qRT-PCR. This analysis revealed no significant changes in the expression the miR-485, miR-34a, and miR-27b (Figure 3-11C-E). Conversely, we observed a striking and significant sex-specific effect of ATRX loss on the expression of miR-137 in *Atrx*-cKO hippocampi, with an upregulation of expression in the male hippocampi and a downregulation in the female hippocampi (Figure 3-11f). To further confirm this finding, we mined previous microarray data of neonatal forebrain tissue of mice lacking ATRX in the forebrain (*Atrx*$^{fl/fl}$ x *FoxG1*-Cre cross) (Levy, Fernandes, Tremblay, Seah, & Berube, 2008). Analysis of this data through the gene enrichment analysis tool TOPPGENE (Chen, Bardes, Aronow, & Jegga, 2009) revealed enrichment of downregulated genes in Gene Ontology categories including synaptic signalling and regulation of excitatory potential (Figure 3-12A) as well as an enrichment for targets of miR-137 (Figure 3-12B). We compared the list of genes downregulated in the *Atrx*-cKO male hippocampi to those predicted to be regulated by miR-137 through miRNA.org. We found *Shank2, Cadps2, Glrb,* and *Sgip1* expression to be inversely related to miR-137, with expression decreased in *Atrx*-cKO and increased in *Atrx*-cKO^{Fem}. Shank2 and Glrb are both postsynaptic proteins, with Shank2 (SH3 and multiple ankyrin repeat domains 2) acting as a scaffolding protein within the PSD (Sheng & Kim, 2000) and GlrB (Glycine receptor beta), is the beta subunit of the glycine receptor (Rajendra, Lynch, & Schofield, 1997). Cadps2 and Sgip1 are found at the presynaptic terminal, where Cadps2 (Ca2+-dependent activator protein for secretion 2) regulates exocytosis of vesicles (Cisternas, Vincent, Scherer, & Ray, 2003) and Sgip1 (Src homology 3-domain growth factor receptor-bound 2-like interacting protein 1) is involved in clathrin-mediated endocytosis (Dergai et al., 2010). This data provides additional evidence that loss of ATRX in the cortex and hippocampus of male mice leads to increased miR-137 expression and consequent downregulation of its target genes, starting at early stages of forebrain development.

3.2 Discussion

This study presents evidence that ATRX is required in a sex-specific manner in excitatory forebrain neurons for normal spatial learning and memory. We found that loss

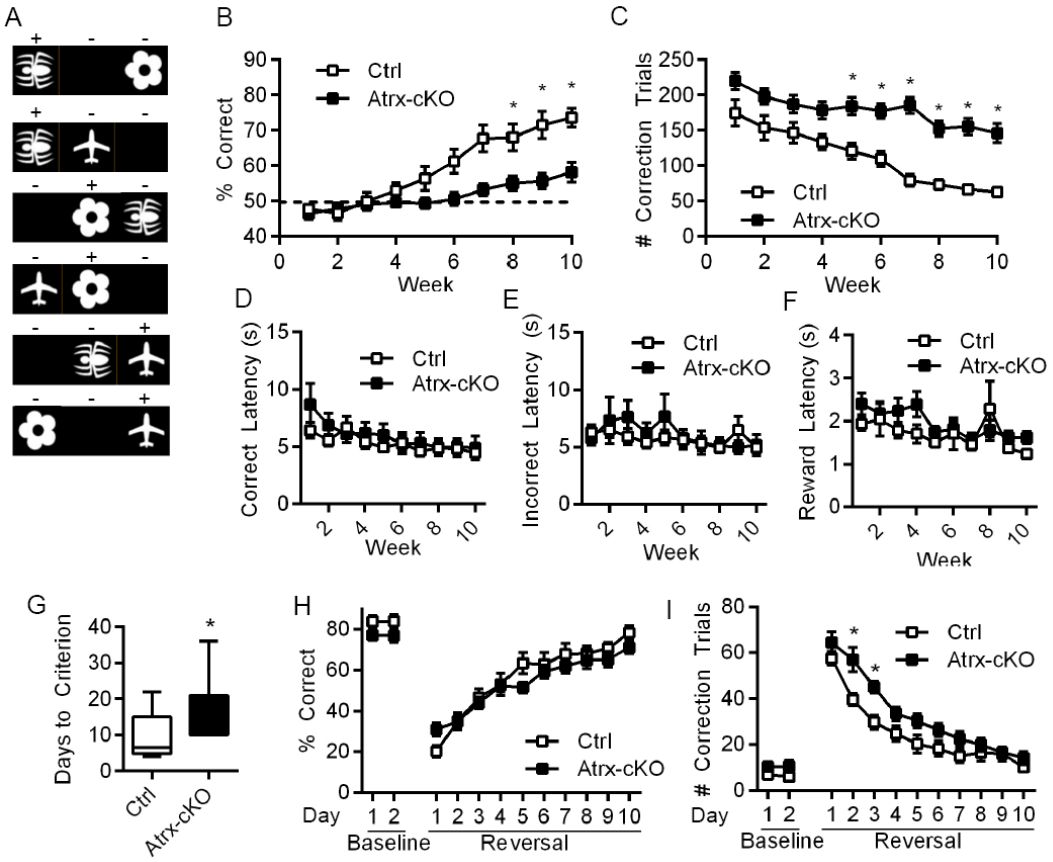

Figure 3-10 Atrx-cKO mice display deficits in spatial learning in the Paired-Associate Learning operant task.

(A) Representative images used in the paired-associate learning task, where touching the (+) stimuli on the screen results in reward and the (-) stimuli results in negative reinforcement (Talpos et al., 2009). (B) Percent correct over 10 weeks ($p<0.005$). Dotted line indicates % correct by chance. (C) Number of correction trials required over ten weeks ($p<0.0001$). (D) Latency to choose a correct answer ($p=0.49$). (E) Latency to choose an incorrect answer ($p=0.72$). (F) Latency to retrieve the reward ($p=0.33$). (G) Number of days to reach criterion in the Visual Paired Discrimination task ($p<0.01$). (H) Percent correct during baseline (two days) and reversal (10 days) ($p=0.25$). (I) Number of correction trials required during baseline and reversal trials ($p<0.005$). Statistics by two-way repeated measures ANOVA with Sidak's multiple comparisons test or Student's T-test where applicable, asterisks indicate $p<0.05$.

of ATRX in these neurons resulted in impaired long-term memory in the Morris water maze, contextual fear conditioning task, and impaired learning in the dPAL touchscreen assay. Magnetic resonance imaging revealed a higher relative volume of hippocampal CA1 SR/SLM and decreased relative volume of the CA3 pyramidal cell layer. There are two hippocampal pathways implicated in spatial learning and memory, the Schaffer collateral pathway and the temporoammonic pathway. The Schaffer collateral pathway involves the CA3 axons projecting to the CA1 medial apical dendrites (Vago & Kesner, 2008), whereas the temporoammonic pathway initiates in layer III of the entorhinal cortex and projects to the CA1 middle apical dendritic layer (Nguyen & Kandel, 1996). We originally hypothesized that the increased volume of the CA1 SR/SLM may be due to increased branching of pyramidal neurons, particularly the apical dendrites that project to this region. However, analysis of Golgi stained CA1 neurons failed to show abnormalities in dendritic branching that would explain the MRI data. Astrocyte and microglia infiltration have been linked with defects in learning and memory in various mouse models (Bian et al., 2012; McGill et al., 2018; Tanaka et al., 2006). Yet after examination of these cell types by immunofluorescence staining, we saw no change in either astrocyte or microglia cell number. The reason for volume increase thus remains undetermined, but might be caused by other cell types infiltrating the hippocampus such as T cells or to increased volume of the perineuronal net (changes to the extracellular matrix), which has been shown in mouse models to help regulate learning and memory (Bukalo, Schachner, & Dityatev, 2001; Hylin, Orsi, Moore, & Dash, 2013). An alternative explanation is that volumetric measurements are normal in these areas but decreased elsewhere in the hippocampus.

Loss of ATRX in the *Atrx*-cKO male mice resulted in various hippocampal-dependent memory impairments including contextual fear memory, and spatial learning and memory in the Morris water maze and paired-associate touchscreen task. The results from the touchscreen task were especially interesting considering the translational aspect of these tests (Bussey et al., 2012), and comparable results to humans are achieved using mouse models of cognitive impairments (Nithianantharajah et al., 2013; Nithianantharajah et al., 2015). Unexpectedly, *Atrx*-cKO^{Fem} mice displayed normal memory in several

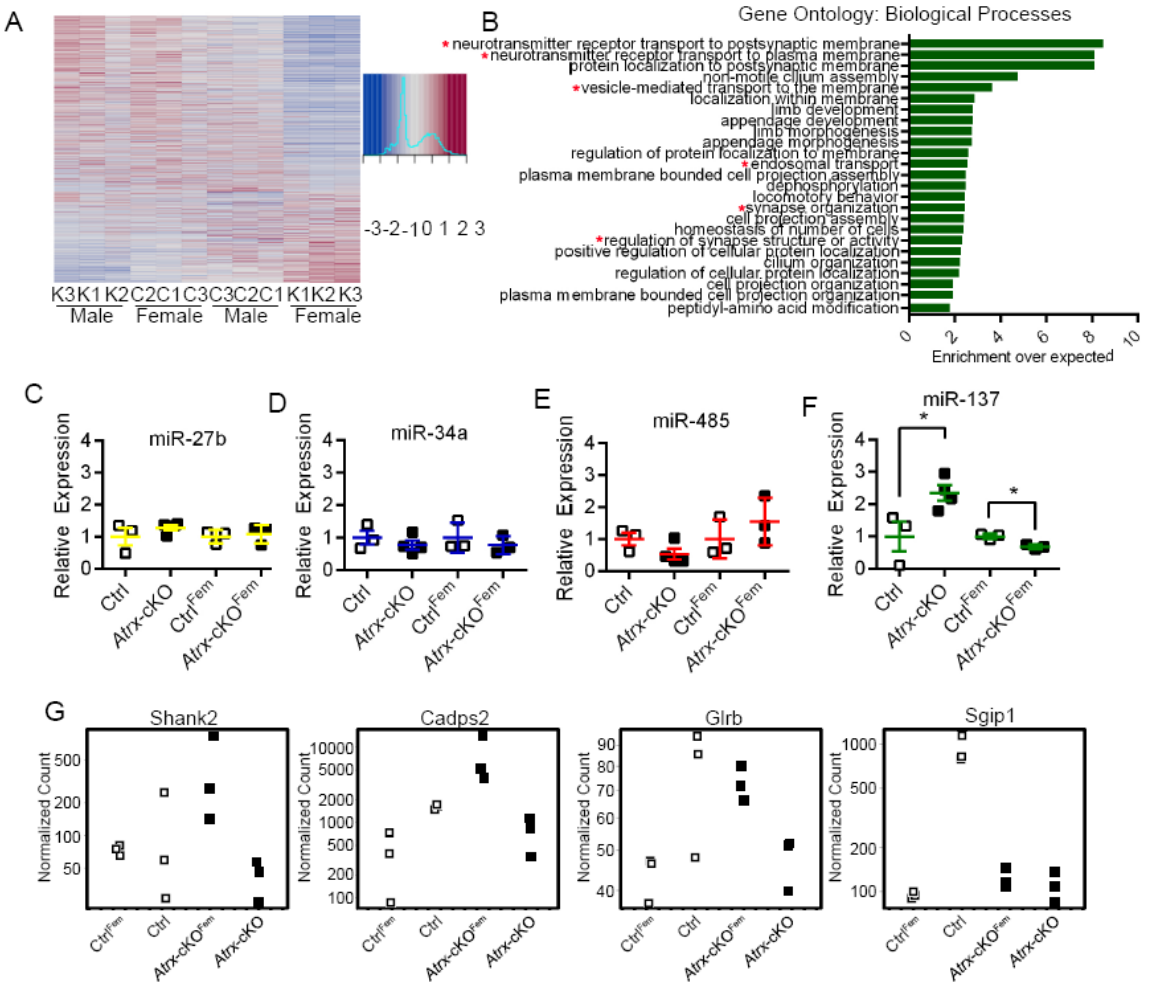

Figure 3-11 Transcriptional profiling reveals dysregulation of presynaptic vesicular genes possibly resulting from miR-137 overexpression.

(A) Heat map analysis of differentially expressed transcripts according to sex (FDR < 0.05) by RNA sequencing from Ctrl, *Atrx*-cKO, Ctrl^{Fem}, and *Atrx*-cKO^{Fem} hippocampi. (B) Unique transcripts that were regulated in a sex-specific manner upon loss of ATRX were used for Gene Ontology analysis and top 25 Biological Processes were listed by Enrichment value (p<0.001, FDR<0.05). Those related to synapses were noted with a red asterisk. (C) Expression of miR-485 in Ctrl and *Atrx*-cKO (p=0.1284), Ctrl^{Fem} and *Atrx*-cKO^{Fem} (p=0.3787) hippocampi normalized to miR-191. (D) Expression of miR-34a in Ctrl and *Atrx*-cKO (p=0.3072), Ctr^{lFem} and *Atrx*-cKO^{Fem} (p=0.7193) hippocampi normalized to

miR-191. (E) Expression of miR-27b in Ctrl and *Atrx*-cKO (p=0.3953), Ctrl^{Fem} and *Atrx*-cKO^{Fem} (p=0.4968) hippocampi normalized to miR-191. (F) Expression of miR-137 in Ctrl and *Atrx*-cKO ($p<0.05$), Ctrl^{Fem} and *Atrx*-cKO^{Fem} ($p<0.01$) hippocampi normalized to miR-191. (G) Transcript expression of *Shank2*, *Cadsp2*, *Glrb*, and *Sgip1* in Ctrl, *Atrx*-cKO, Ctrl^{Fem} and *Atrx*-cKO^{Fem} hippocampi. Data was analyzed by unpaired Student's T-test where applicable, and asterisks indicate $p<0.05$. Data is displayed as mean +/- SEM.

paradigms, indicating a sex-specific phenomenon upon ATRX inactivation. In humans, females harbouring *ATRX* mutations are protected from the disease by complete skewing of X-inactivation (Gibbons, Suthers, Wilkie, Buckle, & Higgs, 1992); however this cannot be the case here since the mice were homozygous for the "floxed" allele and we confirmed by immunofluorescence staining that ATRX is indeed absent from hippocampal excitatory neurons. We did not sync estrous cycles of the *Atrx*-cKO^{Fem} mice (except those housed together), which has been shown to influence some behaviours (Meziane, Ouagazzal, Aubert, Wietrzych, & Krezel, 2007), however we did not see a difference in variability compared to the male mice. Sexual dimorphism has been reported in other mouse models with mutations in chromatin remodeling proteins, including CHD8 and MeCP2, where females are unaffected by loss of the protein of interest or are affected differently (Jung et al., 2018; K. C. Kim et al., 2016; Kurian, Bychowski, Forbes-Lorman, Auger, & Auger, 2008). In humans, neurological disorders such as autism-spectrum disorders tend to preferentially affect males rather than females, possibly due to combinatorial contributions of hormonal and genetic factors in a phenomenon known as the female protective effect (Fombonne, 2009; Jacquemont et al., 2014; Voineagu et al., 2011), and this is regularly supported with mouse models (Hu, Sarachana, Sherrard, & Kocher, 2015; Sato et al., 2012; Tsutiya et al., 2017). The presence of estrogen and estrogen receptor in the female brain has been shown to be neuroprotective and leads to enhanced Schaffer-collateral LTP (Wang et al., 2018). In addition, certain X-linked genes involved in chromatin regulation (e.g. *Utx*, a histone demethylase) are able to escape X-inactivation and so are expressed two-fold in females compared to males (Xu, Deng, Watkins, & Disteche, 2008). These mechanisms could lead to protective gene regulation in the *Atrx*-cKO^{Fem}, causing the sexually dimorphic defects in learning and memory. We previously reported impairment of spatial learning and memory in a female mouse model with mosaic expression of ATRX in all cells of the central nervous system (Tamming et al., 2017). This suggests the intriguing possibility that female-specific protective factors originate from cell types other than the excitatory neurons targeted in the present study. Female-specific glial factors, for example might provide important protection against the loss of ATRX in neurons.

MicroRNAs (miRNAs) are critical for the regulation of transcriptional programs in the brain. Excitation of whole neuronal networks results in drastic changes to miRNA levels, such as in seizures or traumatic brain injury (Jimenez-Mateos et al., 2011; Lei, Li, Chen, Yang, & Zhang, 2009). miRNA levels can also change after exposure to certain behavioural tasks including contextual fear conditioning or novel object recognition (Lin et al., 2011; Woldemichael et al., 2016). At the molecular level, miRNAs can target 100s to 1000s of genes thereby altering expression of proteins at the presynaptic terminal, postsynaptic membrane, or both. The TEM and RNA-sequencing data obtained in the current study identified impaired presynaptic vesicular function, with decreased number of docked and total vesicles, prompting us to focus on miRNAs previously implicated in these functions: miR-485, miR-34a, miR-27b, and miR-137. Of the four miRNA tested, only miR-137 was significantly increased in *Atrx*-cKO male hippocampi while decreased in expression in the *Atrx*-cKO^{Fem} hippocampi, identifying another mechanism by which the females may be protected by ATRX loss. miR-137 overexpression has previously been linked to impaired hippocampal-dependent learning and memory in mice through the Morris water maze and contextual fear conditioning task, similar to the *Atrx*-cKO mice (Siegert et al., 2015). Additionally, miR-137 overexpression results in altered vesicular trafficking and reduced LTP *in vivo* and a reduction in the number of docked and total vesicles *in vitro* (He et al., 2018; Siegert et al., 2015), again paralleling our findings in the *Atrx*-cKO mice. miR-137 is also known to regulate expression of genes involved in postsynaptic function, including NMDA and AMPA receptor synthesis (Olde Loohuis et al., 2015; Zhao et al., 2013) and multiple targets in the PI3K-Akt-mTOR pathway (Thomas et al., 2017). Therefore, increased expression of miR-137 could explain the presynaptic defects seen in the *Atrx*-cKO male mice and may have other effects within the post-synaptic density and downstream signalling that should be examined in more detail in the future.

The previously reported ATRX$^{\Delta E2}$ mice had impaired contextual fear memory, working memory, novel object recognition memory, and spatial memory in the Barnes maze (Nogami et al., 2011; Shioda et al., 2011). Molecular analyses revealed decreased levels of CaMKII protein at synapses and increased expression of the *Xlr3b* gene, which is proposed

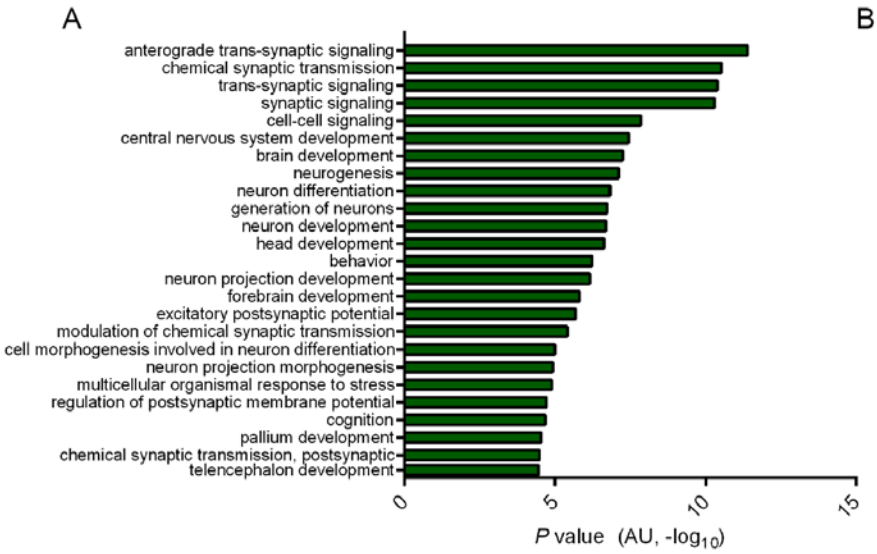

B

miRNA	Source	P-value	Bonferroni
hsa-miR-30e	microRNA.org	6.149E-29	2.866E-25
hsa-miR-30a	microRNA.org	1.404E-26	6.543E-23
hsa-miR-30b	microRNA.org	3.405E-26	1.587E-22
hsa-miR-92a-1	microRNA.org	1.494E-25	6.962E-22
hsa-miR-383	microRNA.org	8.114E-24	3.782E-20
hsa-miR-30d	microRNA.org	9.719E-24	4.530E-20
hsa-let-7f-2	microRNA.org	3.396E-23	1.583E-19
hsa-miR-30c	microRNA.org	5.349E-23	2.493E-19
hsa-miR-410	microRNA.org	1.070E-22	4.988E-19
hsa-miR-93	microRNA.org	1.348E-22	6.281E-19
hsa-miR-376c	microRNA.org	1.171E-21	5.458E-18
hsa-miR-137	microRNA.org	1.520E-21	7.086E-18
hsa-miR-466	microRNA.org	1.771E-21	8.255E-18
hsa-miR-425	microRNA.org	1.965E-21	9.160E-18
hsa-miR-562	microRNA.org	5.606E-21	2.613E-17
hsa-miR-4276	microRNA.org	6.086E-21	2.837E-17
hsa-miR-579	microRNA.org	6.719E-21	3.132E-17
hsa-miR-106b	microRNA.org	9.214E-21	4.295E-17
hsa-miR-493	microRNA.org	9.572E-21	4.462E-17
hsa-miR-137	Target Scan	9.987E-21	4.655E-17
hsa-miR-106b	PITA	1.077E-20	5.019E-17
hsa-miR-93	PITA	1.077E-20	5.019E-17
hsa-miR-106a	PITA	1.077E-20	5.019E-17
hsa-miR-20b	PITA	1.077E-20	5.019E-17
hsa-miR-20a	PITA	1.077E-20	5.019E-17

Figure 3-12 Transcriptional profiling reveals dysregulation of presynaptic genes in Atrx-FoxG1 mice.

(A) Differentially expressed genes between Control and *Atrx*-FoxG1 P0.5 forebrain were used for Gene Ontology analysis and top 25 Biological Processes were listed by P-value. (B) Top miRNA predicted to regulate differentially expressed genes from Control and *Atrx*-FoxG1 mice.

to bind synaptic mRNAs and inhibit transport to dendritic spines (Shioda et al., 2018). In comparison, the *Atrx*-cKO male mice had no defects in working memory (Y-maze) or in novel object recognition. These differences point to potential cell-type specific effects, where ATRX downregulation or loss contributes to spatial memory, while loss in other cell types affects working and recognition memory. The timing of inactivation might also explain differences in behavioural outcomes. The ATRX$^{\Delta E2}$ mice may display a greater number of defects because ATRX depletion is present from the beginning of brain development, while *Atrx* inactivation occurs postnatally in the *CamKII*-Cre conditional approach taken here. Future investigations should discern the effects of inactivating ATRX in various cell types on cognitive output.

In conclusion, our study presents strong evidence that ATRX is required in forebrain excitatory neurons for spatial learning and long-term memory and regulation of genes required for efficient synaptic transmission.

3.3 References

Agostini, M., Tucci, P., Steinert, J. R., Shalom-Feuerstein, R., Rouleau, M., Aberdam, D., . . . Melino, G. (2011). microRNA-34a regulates neurite outgrowth, spinal morphology, and function. *Proc Natl Acad Sci U S A, 108*(52), 21099-21104. doi: 10.1073/pnas.1112063108

Alexa, A., Rahnenfuhrer, J., & Lengauer, T. (2006). Improved scoring of functional groups from gene expression data by decorrelating GO graph structure. *Bioinformatics, 22*(13), 1600-1607. doi: 10.1093/bioinformatics/btl140

Avants, B. B., Tustison, N. J., Wu, J., Cook, P. A., & Gee, J. C. (2011). An open source multivariate framework for n-tissue segmentation with evaluation on public data. *Neuroinformatics, 9*(4), 381-400. doi: 10.1007/s12021-011-9109-y

Benjamini, Yoav, & Hochberg, Yosef. (1995). Controlling the false discovery rate: a practical and powerful approach to multiple testing. *Journal of the Royal statistical society: series B (Methodological), 57*(1), 289-300.

Bérubé, N. G., Mangelsdorf, M., Jagla, M., Vanderluit, J., Garrick, D., Gibbons, R. J., . . . Picketts, D. J. (2005). The chromatin-remodeling protein ATRX is critical for neuronal survival during corticogenesis. *J Clin Invest, 115*(2), 258-267. doi: 10.1172/JCI22329

Bian, Y., Pan, Z., Hou, Z., Huang, C., Li, W., & Zhao, B. (2012). Learning, memory, and glial cell changes following recovery from chronic unpredictable stress. *Brain Res Bull, 88*(5), 471-476. doi: 10.1016/j.brainresbull.2012.04.008

Bisht, K., El Hajj, H., Savage, J. C., Sanchez, M. G., & Tremblay, M. E. (2016). Correlative Light and Electron Microscopy to Study Microglial Interactions with beta-Amyloid Plaques. *J Vis Exp*(112). doi: 10.3791/54060

Bukalo, O., Schachner, M., & Dityatev, A. (2001). Modification of extracellular matrix by enzymatic removal of chondroitin sulfate and by lack of tenascin-R differentially affects several forms of synaptic plasticity in the hippocampus. *Neuroscience, 104*(2), 359-369.

Bussey, T. J., Holmes, A., Lyon, L., Mar, A. C., McAllister, K. A., Nithianantharajah, J., . . . Saksida, L. M. (2012). New translational assays for preclinical modelling of cognition in schizophrenia: the touchscreen testing method for mice and rats. *Neuropharmacology, 62*(3), 1191-1203. doi: 10.1016/j.neuropharm.2011.04.011

Bussey, T. J., Padain, T. L., Skillings, E. A., Winters, B. D., Morton, A. J., & Saksida, L. M. (2008). The touchscreen cognitive testing method for rodents: how to get the best out of your rat. *Learn Mem, 15*(7), 516-523. doi: 10.1101/lm.987808

Chen, J., Bardes, E. E., Aronow, B. J., & Jegga, A. G. (2009). ToppGene Suite for gene list enrichment analysis and candidate gene prioritization. *Nucleic Acids Res, 37*(Web Server issue), W305-311. doi: 10.1093/nar/gkp427

Cisternas, F. A., Vincent, J. B., Scherer, S. W., & Ray, P. N. (2003). Cloning and characterization of human CADPS and CADPS2, new members of the Ca2+-dependent activator for secretion protein family. *Genomics, 81*(3), 279-291.

Cohen, J. E., Lee, P. R., Chen, S., Li, W., & Fields, R. D. (2011). MicroRNA regulation of homeostatic synaptic plasticity. *Proc Natl Acad Sci U S A, 108*(28), 11650-11655. doi: 10.1073/pnas.1017576108

Cole, A. J., Saffen, D. W., Baraban, J. M., & Worley, P. F. (1989). Rapid increase of an immediate early gene messenger RNA in hippocampal neurons by synaptic NMDA receptor activation. *Nature, 340*(6233), 474-476. doi: 10.1038/340474a0

Collins, D. L., Neelin, P., Peters, T. M., & Evans, A. C. (1994). Automatic 3D intersubject registration of MR volumetric data in standardized Talairach space. *J Comput Assist Tomogr, 18*(2), 192-205.

de Castro, B. M., Pereira, G. S., Magalhaes, V., Rossato, J. I., De Jaeger, X., Martins-Silva, C., . . . Prado, M. A. (2009). Reduced expression of the vesicular acetylcholine

transporter causes learning deficits in mice. *Genes Brain Behav, 8*(1), 23-35. doi: 10.1111/j.1601-183X.2008.00439.x

de Guzman, A. E., Wong, M. D., Gleave, J. A., & Nieman, B. J. (2016). Variations in post-perfusion immersion fixation and storage alter MRI measurements of mouse brain morphometry. *Neuroimage, 142*, 687-695. doi: 10.1016/j.neuroimage.2016.06.028

de Vivo, L., Bellesi, M., Marshall, W., Bushong, E. A., Ellisman, M. H., Tononi, G., & Cirelli, C. (2017). Ultrastructural evidence for synaptic scaling across the wake/sleep cycle. *Science, 355*(6324), 507-510. doi: 10.1126/science.aah5982

Delotterie, D. F., Mathis, C., Cassel, J. C., Rosenbrock, H., Dorner-Ciossek, C., & Marti, A. (2015). Touchscreen tasks in mice to demonstrate differences between hippocampal and striatal functions. *Neurobiol Learn Mem, 120*, 16-27. doi: 10.1016/j.nlm.2015.02.007

Dergai, O., Novokhatska, O., Dergai, M., Skrypkina, I., Tsyba, L., Moreau, J., & Rynditch, A. (2010). Intersectin 1 forms complexes with SGIP1 and Reps1 in clathrin-coated pits. *Biochem Biophys Res Commun, 402*(2), 408-413. doi: 10.1016/j.bbrc.2010.10.045

Dorr, A. E., Lerch, J. P., Spring, S., Kabani, N., & Henkelman, R. M. (2008). High resolution three-dimensional brain atlas using an average magnetic resonance image of 40 adult C57Bl/6J mice. *Neuroimage, 42*(1), 60-69. doi: 10.1016/j.neuroimage.2008.03.037

Eustermann, S., Yang, J. C., Law, M. J., Amos, R., Chapman, L. M., Jelinska, C., . . . Neuhaus, D. (2011). Combinatorial readout of histone H3 modifications specifies localization of ATRX to heterochromatin. *Nat Struct Mol Biol, 18*(7), 777-782. doi: 10.1038/nsmb.2070

Ferreira, T. A., Blackman, A. V., Oyrer, J., Jayabal, S., Chung, A. J., Watt, A. J., . . . van Meyel, D. J. (2014). Neuronal morphometry directly from bitmap images. *Nat Methods, 11*(10), 982-984. doi: 10.1038/nmeth.3125

Fombonne, E. (2009). Epidemiology of pervasive developmental disorders. *Pediatr Res, 65*(6), 591-598. doi: 10.1203/PDR.0b013e31819e7203

Garrick, D., Sharpe, J. A., Arkell, R., Dobbie, L., Smith, A. J., Wood, W. G., . . . Gibbons, R. J. (2006). Loss of Atrx affects trophoblast development and the pattern of X-inactivation in extraembryonic tissues. *PLoS Genet, 2*(4), e58. doi: 10.1371/journal.pgen.0020058

Genovese, C. R., Lazar, N. A., & Nichols, T. (2002). Thresholding of statistical maps in functional neuroimaging using the false discovery rate. *Neuroimage, 15*(4), 870-878. doi: 10.1006/nimg.2001.1037

Gibbons, R. J., Bachoo, S., Picketts, D. J., Aftimos, S., Asenbauer, B., Bergoffen, J., . . . Higgs, D. R. (1997). Mutations in transcriptional regulator ATRX establish the functional significance of a PHD-like domain. *Nat Genet, 17*(2), 146-148. doi: 10.1038/ng1097-146

Gibbons, R. J., Picketts, D. J., Villard, L., & Higgs, D. R. (1995). Mutations in a putative global transcriptional regulator cause X-linked mental retardation with alpha-thalassemia (ATR-X syndrome). *Cell, 80*(6), 837-845.

Gibbons, R. J., Suthers, G. K., Wilkie, A. O., Buckle, V. J., & Higgs, D. R. (1992). X-linked alpha-thalassemia/mental retardation (ATR-X) syndrome: localization to Xq12-q21.31 by X inactivation and linkage analysis. *Am J Hum Genet, 51*(5), 1136-1149.

Gibbons, R. J., Wada, T., Fisher, C. A., Malik, N., Mitson, M. J., Steensma, D. P., . . . Traeger-Synodinos, J. (2008). Mutations in the chromatin-associated protein ATRX. *Hum Mutat, 29*(6), 796-802. doi: 10.1002/humu.20734

Goldberg, A. D., Banaszynski, L. A., Noh, K. M., Lewis, P. W., Elsaesser, S. J., Stadler, S., . . . Allis, C. D. (2010). Distinct factors control histone variant H3.3 localization at specific genomic regions. *Cell, 140*(5), 678-691. doi: 10.1016/j.cell.2010.01.003

Grozeva, D., Carss, K., Spasic-Boskovic, O., Tejada, M. I., Gecz, J., Shaw, M., . . . Raymond, F. L. (2015). Targeted Next-Generation Sequencing Analysis of 1,000 Individuals with Intellectual Disability. *Hum Mutat, 36*(12), 1197-1204. doi: 10.1002/humu.22901

Harris, K. M., Jensen, F. E., & Tsao, B. (1992). Three-dimensional structure of dendritic spines and synapses in rat hippocampus (CA1) at postnatal day 15 and adult ages: implications for the maturation of synaptic physiology and long-term potentiation. *J Neurosci, 12*(7), 2685-2705.

He, E., Lozano, M. A. G., Stringer, S., Watanabe, K., Sakamoto, K., den Oudsten, F., . . . Verhage, M. (2018). MIR137 schizophrenia-associated locus controls synaptic function by regulating synaptogenesis, synapse maturation and synaptic transmission. *Hum Mol Genet, 27*(11), 1879-1891. doi: 10.1093/hmg/ddy089

Hu, V. W., Sarachana, T., Sherrard, R. M., & Kocher, K. M. (2015). Investigation of sex differences in the expression of RORA and its transcriptional targets in the brain as a potential contributor to the sex bias in autism. *Mol Autism, 6*, 7. doi: 10.1186/2040-2392-6-7

Hylin, M. J., Orsi, S. A., Moore, A. N., & Dash, P. K. (2013). Disruption of the perineuronal net in the hippocampus or medial prefrontal cortex impairs fear conditioning. *Learn Mem, 20*(5), 267-273. doi: 10.1101/lm.030197.112

Ignatiadis, N., Klaus, B., Zaugg, J. B., & Huber, W. (2016). Data-driven hypothesis weighting increases detection power in genome-scale multiple testing. *Nat Methods, 13*(7), 577-580. doi: 10.1038/nmeth.3885

Jacquemont, S., Coe, B. P., Hersch, M., Duyzend, M. H., Krumm, N., Bergmann, S., . . . Eichler, E. E. (2014). A higher mutational burden in females supports a "female protective model" in neurodevelopmental disorders. *Am J Hum Genet, 94*(3), 415-425. doi: 10.1016/j.ajhg.2014.02.001

Jimenez-Mateos, E. M., Bray, I., Sanz-Rodriguez, A., Engel, T., McKiernan, R. C., Mouri, G., . . . Henshall, D. C. (2011). miRNA Expression profile after status epilepticus and hippocampal neuroprotection by targeting miR-132. *Am J Pathol, 179*(5), 2519-2532. doi: 10.1016/j.ajpath.2011.07.036

Jung, H., Park, H., Choi, Y., Kang, H., Lee, E., Kweon, H., . . . Kim, E. (2018). Sexually dimorphic behavior, neuronal activity, and gene expression in Chd8-mutant mice. *Nat Neurosci, 21*(9), 1218-1228. doi: 10.1038/s41593-018-0208-z

Kernohan, K. D., Jiang, Y., Tremblay, D. C., Bonvissuto, A. C., Eubanks, J. H., Mann, M. R., & Berube, N. G. (2010). ATRX partners with cohesin and MeCP2 and contributes to developmental silencing of imprinted genes in the brain. *Dev Cell, 18*(2), 191-202. doi: 10.1016/j.devcel.2009.12.017

Kim, C. H., Heath, C. J., Kent, B. A., Bussey, T. J., & Saksida, L. M. (2015). The role of the dorsal hippocampus in two versions of the touchscreen automated paired associates learning (PAL) task for mice. *Psychopharmacology (Berl), 232*(21-22), 3899-3910. doi: 10.1007/s00213-015-3949-3

Kim, K. C., Choi, C. S., Kim, J. W., Han, S. H., Cheong, J. H., Ryu, J. H., & Shin, C. Y. (2016). MeCP2 Modulates Sex Differences in the Postsynaptic Development of the Valproate Animal Model of Autism. *Mol Neurobiol, 53*(1), 40-56. doi: 10.1007/s12035-014-8987-z

Kurian, J. R., Bychowski, M. E., Forbes-Lorman, R. M., Auger, C. J., & Auger, A. P. (2008). Mecp2 organizes juvenile social behavior in a sex-specific manner. *J Neurosci, 28*(28), 7137-7142. doi: 10.1523/JNEUROSCI.1345-08.2008

Law, M. J., Lower, K. M., Voon, H. P., Hughes, J. R., Garrick, D., Viprakasit, V., . . . Gibbons, R. J. (2010). ATR-X syndrome protein targets tandem repeats and influences allele-specific expression in a size-dependent manner. *Cell, 143*(3), 367-378. doi: 10.1016/j.cell.2010.09.023

Lei, P., Li, Y., Chen, X., Yang, S., & Zhang, J. (2009). Microarray based analysis of microRNA expression in rat cerebral cortex after traumatic brain injury. *Brain Res, 1284*, 191-201. doi: 10.1016/j.brainres.2009.05.074

Lerch, J. P., Carroll, J. B., Dorr, A., Spring, S., Evans, A. C., Hayden, M. R., . . . Henkelman, R. M. (2008). Cortical thickness measured from MRI in the YAC128 mouse model of Huntington's disease. *Neuroimage, 41*(2), 243-251. doi: 10.1016/j.neuroimage.2008.02.019

Levy, M. A., Fernandes, A. D., Tremblay, D. C., Seah, C., & Berube, N. G. (2008). The SWI/SNF protein ATRX co-regulates pseudoautosomal genes that have translocated to autosomes in the mouse genome. *BMC Genomics, 9*, 468. doi: 10.1186/1471-2164-9-468

Levy, M. A., Kernohan, K. D., Jiang, Y., & Berube, N. G. (2015). ATRX promotes gene expression by facilitating transcriptional elongation through guanine-rich coding regions. *Hum Mol Genet, 24*(7), 1824-1835. doi: 10.1093/hmg/ddu596

Lewis, P. W., Elsaesser, S. J., Noh, K. M., Stadler, S. C., & Allis, C. D. (2010). Daxx is an H3.3-specific histone chaperone and cooperates with ATRX in replication-independent chromatin assembly at telomeres. *Proc Natl Acad Sci U S A, 107*(32), 14075-14080. doi: 10.1073/pnas.1008850107

Lin, Q., Wei, W., Coelho, C. M., Li, X., Baker-Andresen, D., Dudley, K., . . . Bredy, T. W. (2011). The brain-specific microRNA miR-128b regulates the formation of fear-extinction memory. *Nat Neurosci, 14*(9), 1115-1117. doi: 10.1038/nn.2891

Longair, M. H., Baker, D. A., & Armstrong, J. D. (2011). Simple Neurite Tracer: open source software for reconstruction, visualization and analysis of neuronal processes. *Bioinformatics, 27*(17), 2453-2454. doi: 10.1093/bioinformatics/btr390

Love, M. I., Huber, W., & Anders, S. (2014). Moderated estimation of fold change and dispersion for RNA-seq data with DESeq2. *Genome Biol, 15*(12), 550. doi: 10.1186/s13059-014-0550-8

McGill, B. E., Barve, R. A., Maloney, S. E., Strickland, A., Rensing, N., Wang, P. L., . . . Milbrandt, J. (2018). Abnormal Microglia and Enhanced Inflammation-Related Gene Transcription in Mice with Conditional Deletion of Ctcf in Camk2a-Cre-Expressing Neurons. *J Neurosci, 38*(1), 200-219. doi: 10.1523/JNEUROSCI.0936-17.2017

Meziane, H., Ouagazzal, A. M., Aubert, L., Wietrzych, M., & Krezel, W. (2007). Estrous cycle effects on behavior of C57BL/6J and BALB/cByJ female mice: implications for phenotyping strategies. *Genes Brain Behav, 6*(2), 192-200. doi: 10.1111/j.1601-183X.2006.00249.x

Mi, H., Huang, X., Muruganujan, A., Tang, H., Mills, C., Kang, D., & Thomas, P. D. (2017). PANTHER version 11: expanded annotation data from Gene Ontology and Reactome pathways, and data analysis tool enhancements. *Nucleic Acids Res, 45*(D1), D183-D189. doi: 10.1093/nar/gkw1138

Minatohara, K., Akiyoshi, M., & Okuno, H. (2015). Role of Immediate-Early Genes in Synaptic Plasticity and Neuronal Ensembles Underlying the Memory Trace. *Front Mol Neurosci, 8*, 78. doi: 10.3389/fnmol.2015.00078

Molnar, G., Rozsa, M., Baka, J., Holderith, N., Barzo, P., Nusser, Z., & Tamas, G. (2016). Human pyramidal to interneuron synapses are mediated by multi-vesicular release and multiple docked vesicles. *Elife, 5*. doi: 10.7554/eLife.18167

Nguyen, P. V., & Kandel, E. R. (1996). A macromolecular synthesis-dependent late phase of long-term potentiation requiring cAMP in the medial perforant pathway of rat hippocampal slices. *J Neurosci, 16*(10), 3189-3198.

Nieman, B. J., Flenniken, A. M., Adamson, S. L., Henkelman, R. M., & Sled, J. G. (2006). Anatomical phenotyping in the brain and skull of a mutant mouse by magnetic resonance imaging and computed tomography. *Physiol Genomics, 24*(2), 154-162. doi: 10.1152/physiolgenomics.00217.2005

Nieman, B. J., van Eede, M. C., Spring, S., Dazai, J., Henkelman, R. M., & Lerch, J. P. (2018). MRI to Assess Neurological Function. *Curr Protoc Mouse Biol, 8*(2), e44. doi: 10.1002/cpmo.44

Nithianantharajah, J., Komiyama, N. H., McKechanie, A., Johnstone, M., Blackwood, D. H., St Clair, D., . . . Grant, S. G. (2013). Synaptic scaffold evolution generated components of vertebrate cognitive complexity. *Nat Neurosci, 16*(1), 16-24. doi: 10.1038/nn.3276

Nithianantharajah, J., McKechanie, A. G., Stewart, T. J., Johnstone, M., Blackwood, D. H., St Clair, D., . . . Saksida, L. M. (2015). Bridging the translational divide: identical cognitive touchscreen testing in mice and humans carrying mutations in a disease-relevant homologous gene. *Sci Rep, 5*, 14613. doi: 10.1038/srep14613

Nogami, T., Beppu, H., Tokoro, T., Moriguchi, S., Shioda, N., Fukunaga, K., . . . Kitajima, I. (2011). Reduced expression of the ATRX gene, a chromatin-remodeling factor, causes hippocampal dysfunction in mice. *Hippocampus, 21*(6), 678-687. doi: 10.1002/hipo.20782

Olde Loohuis, N. F., Ba, W., Stoerchel, P. H., Kos, A., Jager, A., Schratt, G., . . . Aschrafi, A. (2015). MicroRNA-137 Controls AMPA-Receptor-Mediated Transmission and mGluR-Dependent LTD. *Cell Rep, 11*(12), 1876-1884. doi: 10.1016/j.celrep.2015.05.040

Pertea, M., Pertea, G. M., Antonescu, C. M., Chang, T. C., Mendell, J. T., & Salzberg, S. L. (2015). StringTie enables improved reconstruction of a transcriptome from RNA-seq reads. *Nat Biotechnol, 33*(3), 290-295. doi: 10.1038/nbt.3122

Picketts, D. J., Higgs, D. R., Bachoo, S., Blake, D. J., Quarrell, O. W., & Gibbons, R. J. (1996). ATRX encodes a novel member of the SNF2 family of proteins: mutations point to a common mechanism underlying the ATR-X syndrome. *Hum Mol Genet, 5*(12), 1899-1907.

Poon, V. Y., Gu, M., Ji, F., VanDongen, A. M., & Fivaz, M. (2016). miR-27b shapes the presynaptic transcriptome and influences neurotransmission by silencing the polycomb group protein Bmi1. *BMC Genomics, 17*(1), 777. doi: 10.1186/s12864-016-3139-7

Qiu, L. R., Fernandes, D. J., Szulc-Lerch, K. U., Dazai, J., Nieman, B. J., Turnbull, D. H., . . . Lerch, J. P. (2018). Mouse MRI shows brain areas relatively larger in males emerge before those larger in females. *Nat Commun, 9*(1), 2615. doi: 10.1038/s41467-018-04921-2

Rajendra, S., Lynch, J. W., & Schofield, P. R. (1997). The glycine receptor. *Pharmacol Ther, 73*(2), 121-146.

Richards, K., Watson, C., Buckley, R. F., Kurniawan, N. D., Yang, Z., Keller, M. D., . . . Reutens, D. C. (2011). Segmentation of the mouse hippocampal formation in magnetic resonance images. *Neuroimage, 58*(3), 732-740. doi: 10.1016/j.neuroimage.2011.06.025

Ryan, B., Joilin, G., & Williams, J. M. (2015). Plasticity-related microRNA and their potential contribution to the maintenance of long-term potentiation. *Front Mol Neurosci, 8*, 4. doi: 10.3389/fnmol.2015.00004

Sahakian, B. J., Morris, R. G., Evenden, J. L., Heald, A., Levy, R., Philpot, M., & Robbins, T. W. (1988). A comparative study of visuospatial memory and learning in Alzheimer-type dementia and Parkinson's disease. *Brain, 111 (Pt 3)*, 695-718.

Sato, D., Lionel, A. C., Leblond, C. S., Prasad, A., Pinto, D., Walker, S., . . . Scherer, S. W. (2012). SHANK1 Deletions in Males with Autism Spectrum Disorder. *Am J Hum Genet, 90*(5), 879-887. doi: 10.1016/j.ajhg.2012.03.017

Seah, C., Levy, M. A., Jiang, Y., Mokhtarzada, S., Higgs, D. R., Gibbons, R. J., & Berube, N. G. (2008). Neuronal death resulting from targeted disruption of the Snf2 protein ATRX is mediated by p53. *J Neurosci, 28*(47), 12570-12580. doi: 10.1523/JNEUROSCI.4048-08.2008

Sheng, M., & Kim, E. (2000). The Shank family of scaffold proteins. *J Cell Sci, 113 (Pt 11)*, 1851-1856.

Shioda, N., Beppu, H., Fukuda, T., Li, E., Kitajima, I., & Fukunaga, K. (2011). Aberrant calcium/calmodulin-dependent protein kinase II (CaMKII) activity is associated with abnormal dendritic spine morphology in the ATRX mutant mouse brain. *J Neurosci, 31*(1), 346-358. doi: 10.1523/JNEUROSCI.4816-10.2011

Shioda, N., Yabuki, Y., Yamaguchi, K., Onozato, M., Li, Y., Kurosawa, K., . . . Fukunaga, K. (2018). Targeting G-quadruplex DNA as cognitive function therapy for ATR-X syndrome. *Nat Med, 24*(6), 802-813. doi: 10.1038/s41591-018-0018-6

Siegert, S., Seo, J., Kwon, E. J., Rudenko, A., Cho, S., Wang, W., . . . Tsai, L. H. (2015). The schizophrenia risk gene product miR-137 alters presynaptic plasticity. *Nat Neurosci, 18*(7), 1008-1016. doi: 10.1038/nn.4023

Soneson, C., Love, M. I., & Robinson, M. D. (2015). Differential analyses for RNA-seq: transcript-level estimates improve gene-level inferences. *F1000Res, 4*, 1521. doi: 10.12688/f1000research.7563.2

Spencer Noakes, T. L., Henkelman, R. M., & Nieman, B. J. (2017). Partitioning k-space for cylindrical three-dimensional rapid acquisition with relaxation enhancement imaging in the mouse brain. *NMR Biomed, 30*(11). doi: 10.1002/nbm.3802

Steadman, P. E., Ellegood, J., Szulc, K. U., Turnbull, D. H., Joyner, A. L., Henkelman, R. M., & Lerch, J. P. (2014). Genetic effects on cerebellar structure across mouse models of autism using a magnetic resonance imaging atlas. *Autism Res, 7*(1), 124-137. doi: 10.1002/aur.1344

Talpos, J. C., Winters, B. D., Dias, R., Saksida, L. M., & Bussey, T. J. (2009). A novel touchscreen-automated paired-associate learning (PAL) task sensitive to pharmacological manipulation of the hippocampus: a translational rodent model of cognitive impairments in neurodegenerative disease. *Psychopharmacology (Berl), 205*(1), 157-168. doi: 10.1007/s00213-009-1526-3

Tamming, R. J., Siu, J. R., Jiang, Y., Prado, M. A., Beier, F., & Berube, N. G. (2017). Mosaic expression of Atrx in the mouse central nervous system causes memory deficits. *Dis Model Mech, 10*(2), 119-126. doi: 10.1242/dmm.027482

Tanaka, S., Ide, M., Shibutani, T., Ohtaki, H., Numazawa, S., Shioda, S., & Yoshida, T. (2006). Lipopolysaccharide-induced microglial activation induces learning and memory deficits without neuronal cell death in rats. *J Neurosci Res, 83*(4), 557-566. doi: 10.1002/jnr.20752

Thomas, K. T., Anderson, B. R., Shah, N., Zimmer, S. E., Hawkins, D., Valdez, A. N., . . . Bassell, G. J. (2017). Inhibition of the Schizophrenia-Associated MicroRNA miR-137 Disrupts Nrg1alpha Neurodevelopmental Signal Transduction. *Cell Rep, 20*(1), 1-12. doi: 10.1016/j.celrep.2017.06.038

Tronche, F., Kellendonk, C., Kretz, O., Gass, P., Anlag, K., Orban, P. C., . . . Schutz, G. (1999). Disruption of the glucocorticoid receptor gene in the nervous system results in reduced anxiety. *Nat Genet, 23*(1), 99-103. doi: 10.1038/12703

Tsien, J. Z., Chen, D. F., Gerber, D., Tom, C., Mercer, E. H., Anderson, D. J., . . . Tonegawa, S. (1996). Subregion- and cell type-restricted gene knockout in mouse brain. *Cell, 87*(7), 1317-1326.

Tsutiya, A., Nakano, Y., Hansen-Kiss, E., Kelly, B., Nishihara, M., Goshima, Y., . . . Ohtani-Kaneko, R. (2017). Human CRMP4 mutation and disrupted Crmp4 expression in mice are associated with ASD characteristics and sexual dimorphism. *Sci Rep, 7*(1), 16812. doi: 10.1038/s41598-017-16782-8

Ullmann, J. F., Watson, C., Janke, A. L., Kurniawan, N. D., Paxinos, G., & Reutens, D. C. (2014). An MRI atlas of the mouse basal ganglia. *Brain Struct Funct, 219*(4), 1343-1353. doi: 10.1007/s00429-013-0572-0

Vago, D. R., & Kesner, R. P. (2008). Disruption of the direct perforant path input to the CA1 subregion of the dorsal hippocampus interferes with spatial working memory and novelty detection. *Behav Brain Res, 189*(2), 273-283. doi: 10.1016/j.bbr.2008.01.002

Voineagu, I., Wang, X., Johnston, P., Lowe, J. K., Tian, Y., Horvath, S., . . . Geschwind, D. H. (2011). Transcriptomic analysis of autistic brain reveals convergent molecular pathology. *Nature, 474*(7351), 380-384. doi: 10.1038/nature10110

Vorhees, C. V., & Williams, M. T. (2006). Morris water maze: procedures for assessing spatial and related forms of learning and memory. *Nat Protoc, 1*(2), 848-858. doi: 10.1038/nprot.2006.116

Wang, W., Le, A. A., Hou, B., Lauterborn, J. C., Cox, C. D., Levin, E. R., . . . Gall, C. M. (2018). Memory-Related Synaptic Plasticity Is Sexually Dimorphic in Rodent Hippocampus. *J Neurosci, 38*(37), 7935-7951. doi: 10.1523/JNEUROSCI.0801-18.2018

Watson, L. A., Solomon, L. A., Li, J. R., Jiang, Y., Edwards, M., Shin-ya, K., . . . Berube, N. G. (2013). Atrx deficiency induces telomere dysfunction, endocrine defects, and reduced life span. *J Clin Invest, 123*(5), 2049-2063. doi: 10.1172/JCI65634

Woldemichael, B. T., Jawaid, A., Kremer, E. A., Gaur, N., Krol, J., Marchais, A., & Mansuy, I. M. (2016). The microRNA cluster miR-183/96/182 contributes to long-term memory in a protein phosphatase 1-dependent manner. *Nat Commun, 7*, 12594. doi: 10.1038/ncomms12594

Xu, J., Deng, X., Watkins, R., & Disteche, C. M. (2008). Sex-specific differences in expression of histone demethylases Utx and Uty in mouse brain and neurons. *J Neurosci, 28*(17), 4521-4527. doi: 10.1523/JNEUROSCI.5382-07.2008

Zerbino, D. R., Achuthan, P., Akanni, W., Amode, M. R., Barrell, D., Bhai, J., . . . Flicek, P. (2018). Ensembl 2018. *Nucleic Acids Res, 46*(D1), D754-D761. doi: 10.1093/nar/gkx1098

Zhao, L., Li, H., Guo, R., Ma, T., Hou, R., Ma, X., & Du, Y. (2013). miR-137, a new target for post-stroke depression? *Neural Regen Res, 8*(26), 2441-2448. doi: 10.3969/j.issn.1673-5374.2013.26.005

Chapter 4

4 General Discussion and Future Directions

4.1 Thesis Summary

The overall goal of my thesis was to explore how ATRX regulates cognition in the adult brain. To achieve this, I used two mouse models of ATRX loss: one resulting in mosaic expression of ATRX in different cell types of the mouse brain (*Atrx*-cHet), and another with ATRX loss specifically in adult glutamatergic neurons (*Atrx*-cKO and *Atrx*-cKO^{Fem}) and used these animals to examine the effect of ATRX loss on learning, memory, and the molecular mechanisms of cognition.

The first part of my thesis, presented in chapter two, attempted to uncover the role of ATRX in the brain in relation to learning and memory. I created a novel mouse model, deleting ATRX in neuronal and glial cell precursors of the mouse central nervous system starting at embryonic day 11.5. The males with complete loss of ATRX died perinatally, but the females which were mosaic for ATRX expression survived to adulthood.

The female mosaics (*Atrx*-cHet) were smaller than the control counterparts, correlating with low circulating IGF-1. We found many behavioural impairments in this model, including recognition memory, contextual fear, and impaired spatial learning in the Morris water maze. Unfortunately, we were unable to test the Barnes maze due to a tendency of the mice to run off the platform edge. Additionally, the *Atrx*-cHet results in the Morris water maze had confounding factors: the mice had a slower swim speed, though not due to motor abnormalities as tested in the treadmill task, and many of the *Atrx*-cHet mice showed no aversion to the water. These factors made it difficult to conclusively state that impairments in the water maze were due to spatial learning.

To reduce confounding behaviours, I developed a model where ATRX is only inactivated after birth, at postnatal day 20, in glutamatergic neurons of the forebrain (*Atrx*-cKO).

Besides an increased CA1 stratum radiatum / lacunosum moleculare there were no obvious gross morphological differences in the brain, nor neuronal morphology differences in the CA1 layer of the hippocampus of these mice. Similar to the *Atrx*-cHet mice, the *Atrx*-cKO males displayed impaired spatial learning and memory in the contextual fear task and Morris water maze, in addition to the touchscreen paired-associate learning task. There were no behaviour differences between control and *Atrx*-cKO^{Fem} mice. The changes in the male knockouts correlated to altered ultrastructural changes in the proximal-apical CA1 dendritic synapses: decreased number of total and docked vesicles and increased cleft and post-synaptic density width. Transcriptional profiling revealed decreased expression of many genes related to synaptic vesicle release corresponding to an increase in the presynaptic plasticity microRNA miR-137. Therefore, I believe we have identified a potential mechanism by which loss of ATRX causes an increase in miR-137 and deregulation of target genes resulting in presynaptic impairment.

4.2 The role of ATRX in cognition

Previously, only one other group had investigated ATRX in the context of learning and memory using mice lacking exon 2 of ATRX (ATRX$^{\Delta E2}$), resulting in decreased ATRX protein expression throughout the body (Nogami et al., 2011). They found no impairments in the Morris water maze, however, decreased memory in the contextual fear task, which correlated to impaired hippocampal long-term potentiation within the Schaffer-collateral pathway. Additionally, the ATRX$^{\Delta E2}$ mice displayed impaired working memory, recognition memory, and spatial learning in the Barnes maze test (Shioda et al., 2011).

Neither the *Atrx*-cHet or *Atrx*-cKO mice behaviour completely match with the ATRX$^{\Delta E2}$ results. The *Atrx*-cHet mice had similar behaviour impairments, the only exceptions being normal working memory, and impaired Morris water maze. As stated above, the Barnes maze gave unreliable results due to the tendency of the mice to run off the edge, possibly due to decreased fear as identified in the contextual fear task. However, the Barnes maze and Morris water maze both test spatial learning and memory, with the only difference being the Morris water maze is more stressful to the animals resulting in increased stress-hormone corticosterone (Harrison, Hosseini, & McDonald, 2009). The *Atrx*-cHet mice

performed poorly in the Morris water maze but the test is inconclusive because they tended to jump off the platform to continue swimming. Even when tasked with the cued Morris water maze, which removes spatial dependency, the *Atrx*-cHet mice were unable to find the platform, and the swim speed of the animals was considerably lower than control mice. Undoubtedly, the mice did have impaired spatial memory in the contextual fear task. The *Atrx*-cHet mice also had normal working memory, compared to the impaired $ATRX^{\Delta E2}$. It is possible that retained expression of ATRX in half of all cells in the brain has a protective effect.

Since the *Atrx*-cKO model results in loss of ATRX in only adult forebrain glutamatergic neurons, I expected to see fewer behavioural impairments compared to the *Atrx*-cHet mice. Differences in learning and memory between the *Atrx*-cHet and *Atrx*-cKO mice are outlined in Table 4-1. Spatial memory in the contextual fear task was impaired in this model, similar to the *Atrx*-cHet mice. The *Atrx*-cHet mice could not be trained in the Morris water maze, indicating severe learning and memory problems, while the *Atrx*-cKO merely had a delay in learning. The *Atrx*-cKO mice also displayed impaired long-term memory in this task, tested at 12 days (7 days after training). The *Atrx*-cKO mice did not display impaired novel object recognition, unlike the *Atrx*-cHet. This may be due to expression of ATRX in other cell types in the *Atrx*-cKO model, such as astrocytes and oligodendrocytes. Indeed, it has been shown that impairment of astrocyte function reduces gamma oscillations and novel object recognition behaviour, while having no effect on contextual fear conditioning (Lee et al., 2014). Therefore, the impairments in object recognition memory might be due to the mosaic expression of ATRX in the *Atrx*-cHet model, instead of in glutamatergic neurons.

Another impairment observed in the *Atrx*-cKO males but not the *Atrx*-cHet mice was a decrease in anxiety. Again, this may be due to the complete loss of ATRX in forebrain glutamatergic neurons of the *Atrx*-cKO mice while the *Atrx*-cHet have mosaic expression of ATRX. Indeed, anxiolytic behaviour results mainly from impairments in the mPFC, in

Behavioural test	***Atrx*-cHet**	***Atrx*-cKO**
Open field test (general activity)	✓ Normal	✓ Normal
Open field test (anxiety)	✓ Normal	× Impaired
Elevated plus maze (anxiety)	✓ Normal	× Impaired
Novel object recognition (recognition memory)	× Impaired	✓ Normal
Y-maze (working memory)	✓ Normal	✓ Normal
Morris water maze (spatial learning)	× Impaired	× Impaired
Morris water maze (spatial memory)	Not tested	× Impaired
Contextual fear conditioning (spatial fear memory)	× Impaired	× Impaired
Paired-associate learning task (spatial learning)	Not tested	× Impaired

Table 4-1 Behaviour impairments in *Atrx*-cHet and *Atrx*-cKO mice

addition to the hippocampus and amygdala (Adhikari, Topiwala, & Gordon, 2010; Davidson, 2002). The main neurotransmitter responsible for anxiety-related behaviours is serotonin, derived from tryptophan and produced in the Raphe nuclei of the brainstem (Moore, Halaris, & Jones, 1978). In the *Atrx*-cKO model, production of serotonin should be normal as ATRX is still expressed in the brainstem. However, defects in serotonin receptors in glutamatergic neurons in the cortex and hippocampus could be causing decreased anxiety in this mouse model.

One of the more advanced behavioural techniques performed on the *Atrx*-cKO mice was the touchscreen methods for assessing cognitive ability in mice. Tests performed using these chambers are superior to conventional behaviour paradigms for multiple reasons. First, they are automated, which not only allows multiple animals to be tested at once, but also reduces variability related to handling of the animals (Wahlsten et al., 2003). Second, they are low-stress, unlike other paradigms such as the Morris water maze which relies on aversive stimuli (in this case water) to learn (Harrison et al., 2009). Stress responses in the animal can interfere with normal behaviour (Joels & Baram, 2009), and so the touchscreen assays are reward-based to avoid confounding effects. Third, the touchscreen chambers can be used to test multiple types of cognition, in our case the paired-associate learning and visual-paired discrimination tests. This allows for uniformity over the tests – same apparatus, same reward, and same types of stimuli – and allows for better comparison between tasks. Finally, the touchscreen tests are translational from mouse to clinic. When mice lacking the Discs large homolog 2 (*Dlg2*) gene and humans with a copy number variation (CNV) deletion in the *DLG2* gene are tested in the exact same paired-association task, by the end of training both mouse knockouts and human patients still performed at chance levels (Nithianantharajah et al., 2015). The dPAL test in the *Atrx*-cKO mouse revealed profound impairments in learning, but we could not test memory as the mice were never able to learn to the same extent as control. The Morris water maze did reveal a slight impairment to learning, as there was a delay in latency and distance travelled to the platform on day 3 of the learning trials, but by day 4 were performing similar to control. This could be due to the less stressful nature of the test, or that the touchscreen tests give a

more precise result so that slight deficits in another paradigm may be exacerbated in the dPAL task. It would be interesting to test the mildly-intellectually disabled patients of ATRX syndrome in the human dPAL task to see if similar results are achieved.

Many other chromatin modifying proteins have been implicated in spatial learning and memory, much like ATRX, and spine density is a common defect across several mouse models. They include the insulator protein CTCF, MeCP2 which binds methylated DNA, the chromatin organizer SATB1, and the histone deacetylase HDAC2 (Balamotis et al., 2012; Chapleau et al., 2009; Guan et al., 2009; McGill et al., 2018; Zhou et al., 2006). Overexpression of miR-137, which is increased in expression in the *Atrx*-cKO hippocampus, led to decreased dendritic spine density but no changes to neuronal morphology (Smrt et al., 2010) while sequestration of miR-137 increases dendritic spine density (Olde Loohuis et al., 2015). Therefore, it may be informative to examine dendritic spine density and maturation in the *Atrx*-cHet and *Atrx*-cKO mouse models to determine whether synapse number is changed as spine density is directly correlated to synaptic contacts (Woolley & McEwen, 1992).

4.3 Synaptic plasticity and ATRX

In chapter three, I found that loss of ATRX in forebrain glutamatergic neurons resulted in ultrastructural changes at the synapse through transmission electron microscopy. This included a presynaptic decrease in the number of total and docked vesicles, as well as a decrease in vesicle density. It’s been known for almost 30 years that vesicle number is directly related to presynaptic excitatory potential (Koenig, Kosaka, & Ikeda, 1989). There are two main electrophysiological tests that directly relate to presynaptic function: paired-pulse facilitation (PPF), and post-tetanus plasticity (PTP). Paired-pulse facilitation is the observation that when a second impulse follows immediately after a first impulse, it results in a greater potentiation, which is correlated to the size of the readily releasable pool of vesicles (Dobrunz & Stevens, 1997). There are many rodent models in which vesicle number, localization, or density are decreased which results in a reduction in PPF (Klemmer et al., 2011; Walters et al., 2014). Conversely, an increase in the number of

docked vesicles causes enhanced PPF (Kushner et al., 2005). MiRNAs have also been shown to regulate PPF, with loss of miR-132 enhancing PPF, although the molecular mechanism is still unknown (Lambert, Storm, & Sullivan, 2010). Of relevance to the present study, it has been shown that miR-137 gain-of-function causes impaired vesicle release and changes in vesicle pool distribution (Siegert et al., 2015).

The other electrophysiological test related to presynaptic function, PTP, records the transient increase in neurotransmitter release due to calcium ion accumulation in the axon terminal post-tetanus (Kamiya & Zucker, 1994; Wang, Ferguson, Pineda, Cundiff, & Storm, 2004). PTP has also been shown to correlate to a decreased number of docked and reserve pool vesicles (Xiao et al., 2007). Considering the reduction in both docked and total vesicle number in the *Atrx*-cKO CA1 stratum radiatum / stratum lacunosum layers of the hippocampus, we would expect to see impairments in both paired-pulse facilitation and post-tetanus potentiation in this area.

A reduction in total and docked vesicles have been previously linked to impaired hippocampal-dependent learning and memory. Gain-of-function mutations of the mouse *HDAC4* histone deacetylase in cultured hippocampal neurons resulted in a reduction in the docked vesicle pool, and mice with the same mutation displayed impaired spatial learning and memory in the Barnes maze (Sando et al., 2012). Similarly, deficiency of lipoprotein lipase, involved in triglyceride hydrolysis, decreases docked and total vesicle numbers as well as vesicle density in CA1 hippocampal neurons and mice displayed altered learning in both the Morris water maze and the passive avoidance tasks (Mead, Irvine, & Ramji, 2002; Xian et al., 2009), indicating that proper regulation of the vesicle cycle is critical for learning and memory.

A reduction in long-term potentiation (LTP) is another type of electrophysiological impairment commonly found in mouse models of intellectual disability disorders. Specifically, attenuation in both the Schaffer collateral pathway, which involves signal from the CA3 to the stratum radiatum region of the CA1, and in the temporoammonic pathway, which signals from the entorhinal cortex to the stratum lacunosum moleculare of

the CA1, have been identified in mouse models of impaired spatial memory (Andersen, Bliss, Lomo, Olsen, & Skrede, 1969; Aou et al., 2003; Hjorth-Simonsen & Jeune, 1972; Kallarackal et al., 2013). Similar to short-term plasticity, the inverse is also true: enhanced LTP often correlates to improved spatial memory over controls (Li, Zhong, Chau, Williams, & Chang, 2011), although there are examples where enhanced LTP is found in mouse models with impaired hippocampal-dependent memory (Kaksonen et al., 2002; Meng et al., 2002). In the *Atrx*-cKO male mice, we not only see impaired spatial memory through the Morris water maze, contextual fear task, and paired-associate learning, but we also observed an increase in the size of the CA1 stratum radiatum / stratum lacunosum regions, which receive input from the Schaffer collateral and temporammonic pathways, respectively (Andersen et al., 1969; Hjorth-Simonsen & Jeune, 1972). Additionally, the TEM images were taken in this area, revealing ultrastructural changes at both the pre- and post-synapse. Taking these observations into account, I would expect that either the Schaffer collateral pathway or temporoammonic pathway to be impaired in this mouse model, and current electrophysiological experiments are being conducted to address the effects of ATRX loss on LTP in several hippocampal synaptic pathways (Gugustea et al, unpublished).

4.4 ATRX in gene regulation

Ever since the sequence discovery of ATRX revealed its similarity to the SWI/SNF family of proteins, it has been hypothesized that ATRX regulates transcription in some manner (Stayton et al., 1994; Winston & Carlson, 1992). Due to the importance of ATRX in cognition, it was not surprising that this chromatin remodeler regulates transcription in the brain. Previous research has shown that ATRX localizes to G-rich sequences to regulate the expression of pseudoautosomal genes, including *Neuroligin 4*, an autism-associated gene (Levy, Kernohan, Jiang, & Berube, 2015). ATRX can also regulate the expression of imprinted genes in the brain, by altering nucleosome density allowing for CTCF and cohesin binding, resulting in chromatin looping (Kernohan et al., 2010; Kernohan, Vernimmen, Gloor, & Berube, 2014). Additionally, ATRX can regulate DNA methylation in neurons, resulting in overexpression of *X-linked lymphocyte-regulated 3B* (*Xlr3b*) which

binds dendritic mRNA an inhibits its translocation to the spines (Shioda et al., 2018). Therefore, I was interested in the effect that ATRX loss has on transcription in the *Atrx*-cKO mice.

Immediate early genes (IEGs) are a group of genes that are activated quickly and transiently upon neuronal stimulation (Cole, Saffen, Baraban, & Worley, 1989; Minatohara, Akiyoshi, & Okuno, 2015). It has been shown that ATRX is localized to a subset of these genes in basal conditions, and that DAXX, the binding partner of ATRX, is required for expression of some of these genes upon neuronal stimulation (Michod et al., 2012). We hypothesized then, that ATRX may also be required to regulate the expression of these same genes. However, we did not find this to be the case, with IEG expression increasing upon stimulation to the same extent in ATRX-null cortical neuron cultures as control. However, while DAXX was shown to be required for IEG in cortical cultures, the impairments in spatial learning and memory are largely hippocampal-dependent, and so perhaps repeating the experiments in hippocampal cultures would have a different outcome.

RNA sequencing of the male and female hippocampi identified transcripts decreased in the males and increased in the females that are predicted targets of Mir-137. These included *SH3 And Multiple Ankyrin Repeat Domains 2* (*Shank2*), *Calcium Dependent Secretion Activator 2* (*Cadps2*), *Glycine Receptor Beta* (*Glrb*), and *SH3-containing GRB2-like protein 3-interacting protein 1* (*Sgip1*). SHANK2 functions as a molecular scaffold in the PSD, where it mediates receptor localization in the post-synaptic membrane (Brandstatter, Dick, & Boeckers, 2004; Sheng & Kim, 2000). GLRB is also found in the PSD, as the beta subunit for the glycine receptor, an inhibitory neurotransmitter (Langosch, Becker, & Betz, 1990; Xu & Gong, 2010). CADSP2 and SGIP1 are both found in the presynaptic terminal, with CADPS2 mediating vesicle exocytosis and SGIP1 involved in the formation of clathrin-coated pits, including vesicles (Dergai et al., 2010; Grishanin et al., 2004; Schmid, 1997). The decreased expression of these pre- and post-synaptic genes in the *Atrx*-cKO model might cause the reduction in number of docked and total vesicles observed, and in turn, the behaviour changes in these animals.

There are many miRNA that are enriched in the presynaptic terminal and postsynaptic spine and have been implicated in proper synaptic plasticity (Lagos-Quintana et al., 2002; Ryan, Joilin, & Williams, 2015; Schratt, 2009). Due to the obvious vesicle-related phenotype in the *Atrx*-cKO male hippocampi, we decided to focus on miRNA that have been identified in the regulation of presynaptic plasticity: miR-27b, miR-34a, miR-485, and miR-137 (Agostini et al., 2011; Cohen, Lee, Chen, Li, & Fields, 2011; Poon, Gu, Ji, VanDongen, & Fivaz, 2016; Siegert et al., 2015). Of these, we were interested in miRNA that were increased in expression in the *Atrx*-cKO males (resulting in a decrease of target genes) and decreased in the *Atrx*-cKO^{Fem} (resulting in increase of target genes). From the four miRNA tested, only miR-137 fit this pattern. Additionally, miR-137 was identified to target many genes decreased in the *Atrx*-cKO RNA sequencing, including *Shank2*, *Sgip1*, *Cadsp2*, and *Glrb*. Previously, ATRX has been shown to regulate expression of the non-coding RNA *Xist*, by promoting binding of the Polycomb repressive complex 2 (Sarma et al., 2014), but this is the first evidence for the involvement of ATRX in regulating miRNA expression, but whether this regulation is direct or indirect is still unknown.

For analysis of the RNA-sequencing, we decided to focus on transcript instead of gene counts. The use of gene counts for statistical analysis can mask what is occurring at the transcript level. For instance, if a gene has 10 transcripts and only one is changed, this would not present as statistically significant. However, changes to single or few transcripts could have drastic effects on biological function due to the presence of splice variants and non-coding sequences. When examining gene expression compared to transcript expression in the *Atrx*-cKO hippocampi, there are 146 genes that are differentially expressed, compared to 1520 transcripts. Therefore, we decided to use transcript analysis for further tests such as Gene Ontology.

4.5 ATRX and miR-137

The discovery that ATRX regulates miR-137 was particularly interesting as it is the first ever evidence of miRNA regulation by ATRX. Genome-wide association studies had previously linked single nucleotide polymorphisms in miR-137 to schizophrenia and

autism-related disorders (Cross-Disorder Group of the Psychiatric Genomics, 2013; Ripke et al., 2013). Enriched within the synaptosome of mature neurons in the hippocampal formation, miR-137 has numerous targets – over 4,000 identified by the microRNA.org database (Betel, Wilson, Gabow, Marks, & Sander, 2008; Siegel et al., 2009; Smrt et al., 2010). Additionally, miR-137 gain-of-function results in downregulation of presynaptic target genes and impaired vesicle release, vesicle pool distribution, impaired LTP, and defective contextual fear memory (Siegert et al., 2015). Therefore, it may be the increase in miR-137 expression that is causing the presynaptic phenotype in the *Atrx*-cKO hippocampi and resultant impaired spatial learning and memory. miR-137 overexpression is also implicated in autistic-like features in mice, including repetitive behaviours and social learning (Cheng et al., 2018). Taken together with the finding that ATRX regulates *Nlgn4* expression from Levy et al. (2015), this may indicate that the *Atrx*-cKO mice might also display autistic-like features and this is currently being tested.

It is still unknown how ATRX regulates the expression of miR-137. In adult neural stem cells, chromatin immunoprecipitation of MeCP2 revealed binding of this epigenetic regulator upstream of miR-137, and deletion of MeCP2 resulted in an increase in miR-137 expression (Szulwach et al., 2010). Additionally, MeCP2 silences miR-137 expression in human colorectal adenoma and carcinoma (Chen et al., 2017). Previously, it has been demonstrated that ATRX and MeCP2 form a complex with cohesin to regulate gene expression at imprinted genes in the brain by controlling nucleosome density and CTCF binding (Kernohan et al., 2010; Kernohan et al., 2014; Nan et al., 2007). Therefore, it is possible that MeCP2 and ATRX are working as a complex to regulate miR-137, and loss of this complex, whether through MeCP2 deletion or ATRX loss, causes derepression of miR-137. However, the experiments demonstrating regulation of miR-137 expression by MeCP2 were performed in adult neural stem cells and colorectal cancer, not differentiated neurons. In a different cell type, such as CA1 pyramidal neurons, ATRX may be regulating miR-137 expression in a different manner, such as through other identified mechanisms of transcriptional control including G-quadruplex resolution or controlling promoter methylation (Levy et al., 2015; Shioda et al., 2018).

The *Atrx*-cKO males displayed significant behavioural impairments whereas the *Atrx*-cKO^{Fem} exhibited normal learning and memory. This sex-specific phenomenon is similar to ATR-X syndrome where females are protected from severe ID, however in humans this is due to preferential inactivation of the X-chromosome (Gibbons, Suthers, Wilkie, Buckle, & Higgs, 1992). However, it is known that many developmental disorders including autism spectrum disorders and intellectual disability can affect males more frequently than females, likely due to a combination of genetic and hormonal factors (Fombonne, 2009; Jacquemont et al., 2014). I sought to uncover a mechanism by which the *Atrx*-cKO^{Fem} is protected by ATRX loss, and differential expression of miR-137 might be partially causing this phenomenon. miR-137 was significantly increased in expression in the *Atrx*-cKO mice, which has been demonstrated to cause behavioural and ultrastructural impairments in the mouse hippocampus (Siegert et al., 2015), yet miR-137 expression was significantly decreased in the *Atrx*-cKO^{Fem}, causing increased expression of target genes and possibly enhancing synaptic transmission and protecting against ATRX loss. Several sex hormones including estrogen and progesterone regulate miRNA biogenesis and in the embryonic mouse brain there is a distinct, sex-specific pattern of miRNA expression, indicating that miRNA can be regulated in a sexually-dimorphic manner (Bhat-Nakshatri et al., 2009; Kuokkanen et al., 2010; Morgan & Bale, 2011). It is possible that the *Atrx*-cKO^{Fem} are protected from the behavioural impairments in the *Atrx*-cKO males due to sex hormone regulation of miRNA expression. Therefore, we are the first to describe the sexually dimorphic regulation of miRNA to protect females from intellectual disability.

4.6 Proposed model of ATRX function in the hippocampus

By integrating the results of my work with previously published research on ATRX, miR-137, gene regulation, and cognition, I propose a model where ATRX regulates learning and memory (**Figure 4-1**). Upon deletion of *Atrx* in forebrain glutamatergic neurons, hippocampal miR-137 expression is altered in a sex-specific manner, leading to the inverse expression of its target synaptic genes, such as *Shank2* and *Glrb*. In the male hippocampi, increased miR-137 levels cause presynaptic defects including decrease in vesicle number,

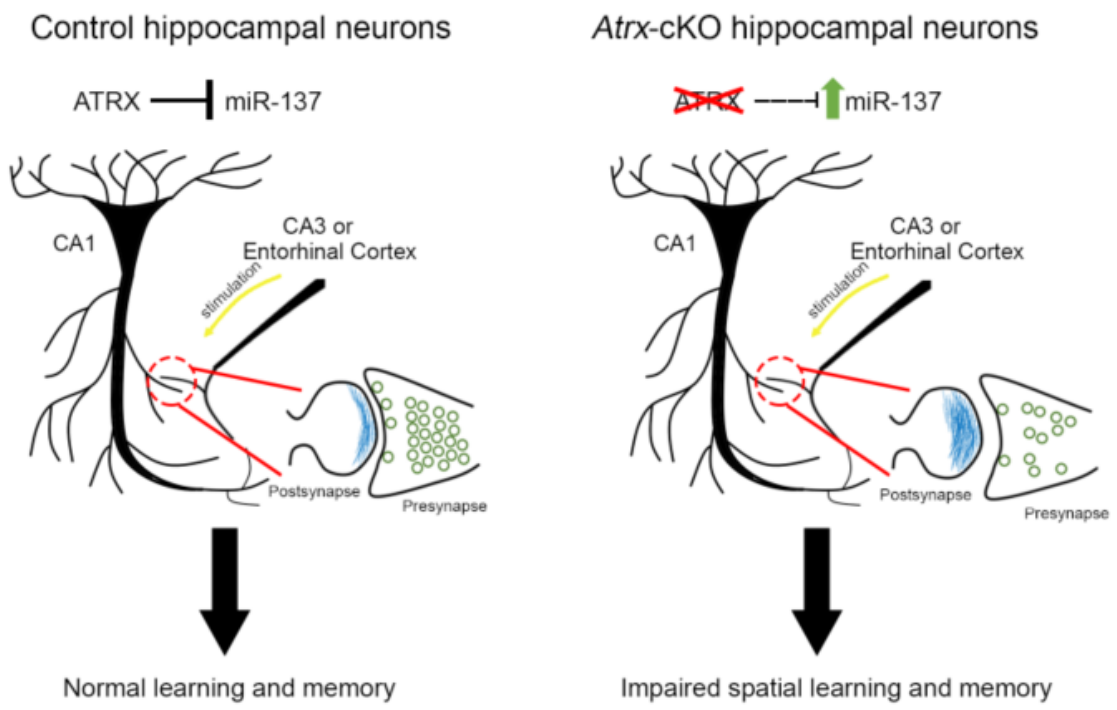

Figure 4-1 Proposed model of ATRX function in the hippocampus

(A) When present at normal levels, ATRX limits the expression of hippocampal miR-137 and alters target synaptic gene expression, thus preserving synaptic ultrastructural morphology and spatial learning and memory. (B) Loss of ATRX in forebrain glutamatergic neurons leads to increased hippocampal miR-137 expression in male mice, accompanied by ultrastructural synaptic defects, leading to sexually dimorphic defects in spatial learning and memory.

density, and number of docked vesicles in addition to a widened synaptic cleft and increased postsynaptic density size, leading to impaired hippocampal-dependent learning and memory.

4.7 Concluding remarks

The identification of ATRX as a sex-specific regulator of miRNA expression was an unexpected finding but investigating this phenomenon has uncovered a model by which ATRX may be able to regulate hippocampal-dependent learning and memory. Through its regulation of miR-137, ATRX loss affects many synaptic transcripts, which could explain the ultrastructural changes to the hippocampal synapses. However, ATRX loss appears to have a protective effect in females by reducing the levels of miR-137. We also identified gross morphological changes within the male hippocampal stratum radiatum/stratum lacunosum, which may have dire consequences for synaptic signaling. Certainly, a number of other details remain to be addressed before we fully understand how ATRX regulates miRNA expression and the resulting changes to synaptic signaling, but it is clear now that ATRX has many functions within the nervous system, during development and in the mature brain, and other biological roles may still be discovered in the future. By understanding these molecular mechanisms, we will better understand how *ATRX* mutations lead to disease and help to develop potential treatments to aid in patients with ATR-X syndrome and non-syndromic ID.

4.8 References

Adhikari, A., Topiwala, M. A., & Gordon, J. A. (2010). Synchronized activity between the ventral hippocampus and the medial prefrontal cortex during anxiety. *Neuron, 65*(2), 257-269. doi: 10.1016/j.neuron.2009.12.002

Agostini, M., Tucci, P., Steinert, J. R., Shalom-Feuerstein, R., Rouleau, M., Aberdam, D., . . . Melino, G. (2011). microRNA-34a regulates neurite outgrowth, spinal morphology, and function. *Proc Natl Acad Sci U S A, 108*(52), 21099-21104. doi: 10.1073/pnas.1112063108

Andersen, P., Bliss, T. V., Lomo, T., Olsen, L. I., & Skrede, K. K. (1969). Lamellar organization of hippocampal excitatory pathways. *Acta Physiol Scand, 76*(1), 4A-5A.

Aou, S., Li, X. L., Li, A. J., Oomura, Y., Shiraishi, T., Sasaki, K., . . . Wayner, M. J. (2003). Orexin-A (hypocretin-1) impairs Morris water maze performance and CA1-Schaffer collateral long-term potentiation in rats. *Neuroscience, 119*(4), 1221-1228.

Balamotis, M. A., Tamberg, N., Woo, Y. J., Li, J., Davy, B., Kohwi-Shigematsu, T., & Kohwi, Y. (2012). Satb1 ablation alters temporal expression of immediate early genes and reduces dendritic spine density during postnatal brain development. *Mol Cell Biol, 32*(2), 333-347. doi: 10.1128/MCB.05917-11

Betel, D., Wilson, M., Gabow, A., Marks, D. S., & Sander, C. (2008). The microRNA.org resource: targets and expression. *Nucleic Acids Res, 36*(Database issue), D149-153. doi: 10.1093/nar/gkm995

Bhat-Nakshatri, P., Wang, G., Collins, N. R., Thomson, M. J., Geistlinger, T. R., Carroll, J. S., . . . Nakshatri, H. (2009). Estradiol-regulated microRNAs control estradiol response in breast cancer cells. *Nucleic Acids Res, 37*(14), 4850-4861. doi: 10.1093/nar/gkp500

Brandstatter, J. H., Dick, O., & Boeckers, T. M. (2004). The postsynaptic scaffold proteins ProSAP1/Shank2 and Homer1 are associated with glutamate receptor complexes at rat retinal synapses. *J Comp Neurol, 475*(4), 551-563. doi: 10.1002/cne.20194

Chapleau, C. A., Calfa, G. D., Lane, M. C., Albertson, A. J., Larimore, J. L., Kudo, S., . . . Pozzo-Miller, L. (2009). Dendritic spine pathologies in hippocampal pyramidal neurons from Rett syndrome brain and after expression of Rett-associated MECP2 mutations. *Neurobiol Dis, 35*(2), 219-233. doi: 10.1016/j.nbd.2009.05.001

Chen, T., Cai, S. L., Li, J., Qi, Z. P., Li, X. Q., Ye, L. C., . . . Zhong, Y. S. (2017). Mecp2-mediated Epigenetic Silencing of miR-137 Contributes to Colorectal Adenoma-Carcinoma Sequence and Tumor Progression via Relieving the Suppression of c-Met. *Sci Rep, 7*, 44543. doi: 10.1038/srep44543

Cheng, Y., Wang, Z. M., Tan, W., Wang, X., Li, Y., Bai, B., . . . Jin, P. (2018). Partial loss of psychiatric risk gene Mir137 in mice causes repetitive behavior and impairs sociability and learning via increased Pde10a. *Nat Neurosci, 21*(12), 1689-1703. doi: 10.1038/s41593-018-0261-7

Cohen, J. E., Lee, P. R., Chen, S., Li, W., & Fields, R. D. (2011). MicroRNA regulation of homeostatic synaptic plasticity. *Proc Natl Acad Sci U S A, 108*(28), 11650-11655. doi: 10.1073/pnas.1017576108

Cole, A. J., Saffen, D. W., Baraban, J. M., & Worley, P. F. (1989). Rapid increase of an immediate early gene messenger RNA in hippocampal neurons by synaptic NMDA receptor activation. *Nature, 340*(6233), 474-476. doi: 10.1038/340474a0

Cross-Disorder Group of the Psychiatric Genomics, Consortium. (2013). Identification of risk loci with shared effects on five major psychiatric disorders: a genome-wide analysis. *Lancet, 381*(9875), 1371-1379. doi: 10.1016/S0140-6736(12)62129-1

Davidson, R. J. (2002). Anxiety and affective style: role of prefrontal cortex and amygdala. *Biol Psychiatry, 51*(1), 68-80.

Dergai, O., Novokhatska, O., Dergai, M., Skrypkina, I., Tsyba, L., Moreau, J., & Rynditch, A. (2010). Intersectin 1 forms complexes with SGIP1 and Reps1 in clathrin-coated pits. *Biochem Biophys Res Commun, 402*(2), 408-413. doi: 10.1016/j.bbrc.2010.10.045

Dobrunz, L. E., & Stevens, C. F. (1997). Heterogeneity of release probability, facilitation, and depletion at central synapses. *Neuron, 18*(6), 995-1008.

Fombonne, E. (2009). Epidemiology of pervasive developmental disorders. *Pediatr Res, 65*(6), 591-598. doi: 10.1203/PDR.0b013e31819e7203

Gibbons, R. J., Suthers, G. K., Wilkie, A. O., Buckle, V. J., & Higgs, D. R. (1992). X-linked alpha-thalassemia/mental retardation (ATR-X) syndrome: localization to Xq12-q21.31 by X inactivation and linkage analysis. *Am J Hum Genet, 51*(5), 1136-1149.

Grishanin, R. N., Kowalchyk, J. A., Klenchin, V. A., Ann, K., Earles, C. A., Chapman, E. R., . . . Martin, T. F. (2004). CAPS acts at a prefusion step in dense-core vesicle exocytosis as a PIP2 binding protein. *Neuron, 43*(4), 551-562. doi: 10.1016/j.neuron.2004.07.028

Guan, J. S., Haggarty, S. J., Giacometti, E., Dannenberg, J. H., Joseph, N., Gao, J., . . . Tsai, L. H. (2009). HDAC2 negatively regulates memory formation and synaptic plasticity. *Nature, 459*(7243), 55-60. doi: 10.1038/nature07925

Harrison, F. E., Hosseini, A. H., & McDonald, M. P. (2009). Endogenous anxiety and stress responses in water maze and Barnes maze spatial memory tasks. *Behav Brain Res, 198*(1), 247-251. doi: 10.1016/j.bbr.2008.10.015

Hjorth-Simonsen, A., & Jeune, B. (1972). Origin and termination of the hippocampal perforant path in the rat studied by silver impregnation. *J Comp Neurol, 144*(2), 215-232. doi: 10.1002/cne.901440206

Jacquemont, S., Coe, B. P., Hersch, M., Duyzend, M. H., Krumm, N., Bergmann, S., . . . Eichler, E. E. (2014). A higher mutational burden in females supports a "female

protective model" in neurodevelopmental disorders. *Am J Hum Genet, 94*(3), 415-425. doi: 10.1016/j.ajhg.2014.02.001

Joels, M., & Baram, T. Z. (2009). The neuro-symphony of stress. *Nat Rev Neurosci, 10*(6), 459-466. doi: 10.1038/nrn2632

Kaksonen, M., Pavlov, I., Voikar, V., Lauri, S. E., Hienola, A., Riekki, R., . . . Rauvala, H. (2002). Syndecan-3-deficient mice exhibit enhanced LTP and impaired hippocampus-dependent memory. *Mol Cell Neurosci, 21*(1), 158-172.

Kallarackal, A. J., Kvarta, M. D., Cammarata, E., Jaberi, L., Cai, X., Bailey, A. M., & Thompson, S. M. (2013). Chronic stress induces a selective decrease in AMPA receptor-mediated synaptic excitation at hippocampal temporoammonic-CA1 synapses. *J Neurosci, 33*(40), 15669-15674. doi: 10.1523/JNEUROSCI.2588-13.2013

Kamiya, H., & Zucker, R. S. (1994). Residual Ca2+ and short-term synaptic plasticity. *Nature, 371*(6498), 603-606. doi: 10.1038/371603a0

Kernohan, K. D., Jiang, Y., Tremblay, D. C., Bonvissuto, A. C., Eubanks, J. H., Mann, M. R., & Berube, N. G. (2010). ATRX partners with cohesin and MeCP2 and contributes to developmental silencing of imprinted genes in the brain. *Dev Cell, 18*(2), 191-202. doi: 10.1016/j.devcel.2009.12.017

Kernohan, K. D., Vernimmen, D., Gloor, G. B., & Berube, N. G. (2014). Analysis of neonatal brain lacking ATRX or MeCP2 reveals changes in nucleosome density, CTCF binding and chromatin looping. *Nucleic Acids Res, 42*(13), 8356-8368. doi: 10.1093/nar/gku564

Klemmer, P., Meredith, R. M., Holmgren, C. D., Klychnikov, O. I., Stahl-Zeng, J., Loos, M., . . . Li, K. W. (2011). Proteomics, ultrastructure, and physiology of hippocampal synapses in a fragile X syndrome mouse model reveal presynaptic phenotype. *J Biol Chem, 286*(29), 25495-25504. doi: 10.1074/jbc.M110.210260

Koenig, J. H., Kosaka, T., & Ikeda, K. (1989). The relationship between the number of synaptic vesicles and the amount of transmitter released. *J Neurosci, 9*(6), 1937-1942.

Kuokkanen, S., Chen, B., Ojalvo, L., Benard, L., Santoro, N., & Pollard, J. W. (2010). Genomic profiling of microRNAs and messenger RNAs reveals hormonal regulation in microRNA expression in human endometrium. *Biol Reprod, 82*(4), 791-801. doi: 10.1095/biolreprod.109.081059

Kushner, S. A., Elgersma, Y., Murphy, G. G., Jaarsma, D., van Woerden, G. M., Hojjati, M. R., . . . Silva, A. J. (2005). Modulation of presynaptic plasticity and learning by

the H-ras/extracellular signal-regulated kinase/synapsin I signaling pathway. *J Neurosci, 25*(42), 9721-9734. doi: 10.1523/JNEUROSCI.2836-05.2005

Lagos-Quintana, M., Rauhut, R., Yalcin, A., Meyer, J., Lendeckel, W., & Tuschl, T. (2002). Identification of tissue-specific microRNAs from mouse. *Curr Biol, 12*(9), 735-739.

Lambert, T. J., Storm, D. R., & Sullivan, J. M. (2010). MicroRNA132 modulates short-term synaptic plasticity but not basal release probability in hippocampal neurons. *PLoS One, 5*(12), e15182. doi: 10.1371/journal.pone.0015182

Langosch, D., Becker, C. M., & Betz, H. (1990). The inhibitory glycine receptor: a ligand-gated chloride channel of the central nervous system. *Eur J Biochem, 194*(1), 1-8.

Lee, H. S., Ghetti, A., Pinto-Duarte, A., Wang, X., Dziewczapolski, G., Galimi, F., . . . Heinemann, S. F. (2014). Astrocytes contribute to gamma oscillations and recognition memory. *Proc Natl Acad Sci U S A, 111*(32), E3343-3352. doi: 10.1073/pnas.1410893111

Levy, M. A., Kernohan, K. D., Jiang, Y., & Berube, N. G. (2015). ATRX promotes gene expression by facilitating transcriptional elongation through guanine-rich coding regions. *Hum Mol Genet, 24*(7), 1824-1835. doi: 10.1093/hmg/ddu596

Li, H., Zhong, X., Chau, K. F., Williams, E. C., & Chang, Q. (2011). Loss of activity-induced phosphorylation of MeCP2 enhances synaptogenesis, LTP and spatial memory. *Nat Neurosci, 14*(8), 1001-1008. doi: 10.1038/nn.2866

McGill, B. E., Barve, R. A., Maloney, S. E., Strickland, A., Rensing, N., Wang, P. L., . . . Milbrandt, J. (2018). Abnormal Microglia and Enhanced Inflammation-Related Gene Transcription in Mice with Conditional Deletion of Ctcf in Camk2a-Cre-Expressing Neurons. *J Neurosci, 38*(1), 200-219. doi: 10.1523/JNEUROSCI.0936-17.2017

Mead, J. R., Irvine, S. A., & Ramji, D. P. (2002). Lipoprotein lipase: structure, function, regulation, and role in disease. *J Mol Med (Berl), 80*(12), 753-769. doi: 10.1007/s00109-002-0384-9

Meng, Y., Zhang, Y., Tregoubov, V., Janus, C., Cruz, L., Jackson, M., . . . Jia, Z. (2002). Abnormal spine morphology and enhanced LTP in LIMK-1 knockout mice. *Neuron, 35*(1), 121-133.

Michod, D., Bartesaghi, S., Khelifi, A., Bellodi, C., Berliocchi, L., Nicotera, P., & Salomoni, P. (2012). Calcium-dependent dephosphorylation of the histone chaperone DAXX regulates H3.3 loading and transcription upon neuronal activation. *Neuron, 74*(1), 122-135. doi: 10.1016/j.neuron.2012.02.021

Minatohara, K., Akiyoshi, M., & Okuno, H. (2015). Role of Immediate-Early Genes in Synaptic Plasticity and Neuronal Ensembles Underlying the Memory Trace. *Front Mol Neurosci, 8*, 78. doi: 10.3389/fnmol.2015.00078

Moore, R. Y., Halaris, A. E., & Jones, B. E. (1978). Serotonin neurons of the midbrain raphe: ascending projections. *J Comp Neurol, 180*(3), 417-438. doi: 10.1002/cne.901800302

Morgan, C. P., & Bale, T. L. (2011). Early prenatal stress epigenetically programs dysmasculinization in second-generation offspring via the paternal lineage. *J Neurosci, 31*(33), 11748-11755. doi: 10.1523/JNEUROSCI.1887-11.2011

Nan, X., Hou, J., Maclean, A., Nasir, J., Lafuente, M. J., Shu, X., . . . Bird, A. (2007). Interaction between chromatin proteins MECP2 and ATRX is disrupted by mutations that cause inherited mental retardation. *Proc Natl Acad Sci U S A, 104*(8), 2709-2714. doi: 10.1073/pnas.0608056104

Nithianantharajah, J., McKechanie, A. G., Stewart, T. J., Johnstone, M., Blackwood, D. H., St Clair, D., . . . Saksida, L. M. (2015). Bridging the translational divide: identical cognitive touchscreen testing in mice and humans carrying mutations in a disease-relevant homologous gene. *Sci Rep, 5*, 14613. doi: 10.1038/srep14613

Nogami, T., Beppu, H., Tokoro, T., Moriguchi, S., Shioda, N., Fukunaga, K., . . . Kitajima, I. (2011). Reduced expression of the ATRX gene, a chromatin-remodeling factor, causes hippocampal dysfunction in mice. *Hippocampus, 21*(6), 678-687. doi: 10.1002/hipo.20782

Olde Loohuis, N. F., Ba, W., Stoerchel, P. H., Kos, A., Jager, A., Schratt, G., . . . Aschrafi, A. (2015). MicroRNA-137 Controls AMPA-Receptor-Mediated Transmission and mGluR-Dependent LTD. *Cell Rep, 11*(12), 1876-1884. doi: 10.1016/j.celrep.2015.05.040

Poon, V. Y., Gu, M., Ji, F., VanDongen, A. M., & Fivaz, M. (2016). miR-27b shapes the presynaptic transcriptome and influences neurotransmission by silencing the polycomb group protein Bmi1. *BMC Genomics, 17*(1), 777. doi: 10.1186/s12864-016-3139-7

Ripke, S., O'Dushlaine, C., Chambert, K., Moran, J. L., Kahler, A. K., Akterin, S., . . . Sullivan, P. F. (2013). Genome-wide association analysis identifies 13 new risk loci for schizophrenia. *Nat Genet, 45*(10), 1150-1159. doi: 10.1038/ng.2742

Ryan, B., Joilin, G., & Williams, J. M. (2015). Plasticity-related microRNA and their potential contribution to the maintenance of long-term potentiation. *Front Mol Neurosci, 8*, 4. doi: 10.3389/fnmol.2015.00004

Sando, R., 3rd, Gounko, N., Pieraut, S., Liao, L., Yates, J., 3rd, & Maximov, A. (2012). HDAC4 governs a transcriptional program essential for synaptic plasticity and memory. *Cell, 151*(4), 821-834. doi: 10.1016/j.cell.2012.09.037

Sarma, K., Cifuentes-Rojas, C., Ergun, A., Del Rosario, A., Jeon, Y., White, F., . . . Lee, J. T. (2014). ATRX directs binding of PRC2 to Xist RNA and Polycomb targets. *Cell, 159*(4), 869-883. doi: 10.1016/j.cell.2014.10.019

Schmid, S. L. (1997). Clathrin-coated vesicle formation and protein sorting: an integrated process. *Annu Rev Biochem, 66*, 511-548. doi: 10.1146/annurev.biochem.66.1.511

Schratt, G. (2009). microRNAs at the synapse. *Nat Rev Neurosci, 10*(12), 842-849. doi: 10.1038/nrn2763

Sheng, M., & Kim, E. (2000). The Shank family of scaffold proteins. *J Cell Sci, 113 (Pt 11)*, 1851-1856.

Shioda, N., Beppu, H., Fukuda, T., Li, E., Kitajima, I., & Fukunaga, K. (2011). Aberrant calcium/calmodulin-dependent protein kinase II (CaMKII) activity is associated with abnormal dendritic spine morphology in the ATRX mutant mouse brain. *J Neurosci, 31*(1), 346-358. doi: 10.1523/JNEUROSCI.4816-10.2011

Shioda, N., Yabuki, Y., Yamaguchi, K., Onozato, M., Li, Y., Kurosawa, K., . . . Fukunaga, K. (2018). Targeting G-quadruplex DNA as cognitive function therapy for ATR-X syndrome. *Nat Med, 24*(6), 802-813. doi: 10.1038/s41591-018-0018-6

Siegel, G., Obernosterer, G., Fiore, R., Oehmen, M., Bicker, S., Christensen, M., . . . Schratt, G. M. (2009). A functional screen implicates microRNA-138-dependent regulation of the depalmitoylation enzyme APT1 in dendritic spine morphogenesis. *Nat Cell Biol, 11*(6), 705-716. doi: 10.1038/ncb1876

Siegert, S., Seo, J., Kwon, E. J., Rudenko, A., Cho, S., Wang, W., . . . Tsai, L. H. (2015). The schizophrenia risk gene product miR-137 alters presynaptic plasticity. *Nat Neurosci, 18*(7), 1008-1016. doi: 10.1038/nn.4023

Smrt, R. D., Szulwach, K. E., Pfeiffer, R. L., Li, X., Guo, W., Pathania, M., . . . Zhao, X. (2010). MicroRNA miR-137 regulates neuronal maturation by targeting ubiquitin ligase mind bomb-1. *Stem Cells, 28*(6), 1060-1070. doi: 10.1002/stem.431

Stayton, C. L., Dabovic, B., Gulisano, M., Gecz, J., Broccoli, V., Giovanazzi, S., . . . et al. (1994). Cloning and characterization of a new human Xq13 gene, encoding a putative helicase. *Hum Mol Genet, 3*(11), 1957-1964.

Szulwach, K. E., Li, X., Smrt, R. D., Li, Y., Luo, Y., Lin, L., . . . Jin, P. (2010). Cross talk between microRNA and epigenetic regulation in adult neurogenesis. *J Cell Biol, 189*(1), 127-141. doi: 10.1083/jcb.200908151

Wahlsten, D., Metten, P., Phillips, T. J., Boehm, S. L., 2nd, Burkhart-Kasch, S., Dorow, J., . . . Crabbe, J. C. (2003). Different data from different labs: lessons from studies of gene-environment interaction. *J Neurobiol, 54*(1), 283-311. doi: 10.1002/neu.10173

Walters, B. J., Hallengren, J. J., Theile, C. S., Ploegh, H. L., Wilson, S. M., & Dobrunz, L. E. (2014). A catalytic independent function of the deubiquitinating enzyme USP14 regulates hippocampal synaptic short-term plasticity and vesicle number. *J Physiol, 592*(4), 571-586. doi: 10.1113/jphysiol.2013.266015

Wang, H., Ferguson, G. D., Pineda, V. V., Cundiff, P. E., & Storm, D. R. (2004). Overexpression of type-1 adenylyl cyclase in mouse forebrain enhances recognition memory and LTP. *Nat Neurosci, 7*(6), 635-642. doi: 10.1038/nn1248

Winston, F., & Carlson, M. (1992). Yeast SNF/SWI transcriptional activators and the SPT/SIN chromatin connection. *Trends Genet, 8*(11), 387-391.

Woolley, C. S., & McEwen, B. S. (1992). Estradiol mediates fluctuation in hippocampal synapse density during the estrous cycle in the adult rat. *J Neurosci, 12*(7), 2549-2554.

Xian, X., Liu, T., Yu, J., Wang, Y., Miao, Y., Zhang, J., . . . Chui, D. (2009). Presynaptic defects underlying impaired learning and memory function in lipoprotein lipase-deficient mice. *J Neurosci, 29*(14), 4681-4685. doi: 10.1523/JNEUROSCI.0297-09.2009

Xiao, M., Xu, L., Laezza, F., Yamada, K., Feng, S., & Ornitz, D. M. (2007). Impaired hippocampal synaptic transmission and plasticity in mice lacking fibroblast growth factor 14. *Mol Cell Neurosci, 34*(3), 366-377. doi: 10.1016/j.mcn.2006.11.020

Xu, T. L., & Gong, N. (2010). Glycine and glycine receptor signaling in hippocampal neurons: diversity, function and regulation. *Prog Neurobiol, 91*(4), 349-361. doi: 10.1016/j.pneurobio.2010.04.008

Zhou, Z., Hong, E. J., Cohen, S., Zhao, W. N., Ho, H. Y., Schmidt, L., . . . Greenberg, M. E. (2006). Brain-specific phosphorylation of MeCP2 regulates activity-dependent Bdnf transcription, dendritic growth, and spine maturation. *Neuron, 52*(2), 255-269. doi: 10.1016/j.neuron.2006.09.037

Appendices

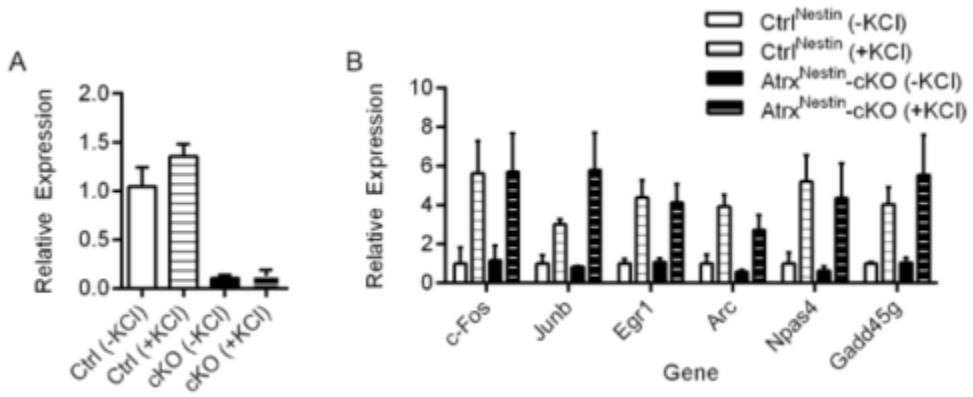

Appendix A ATRX loss does not affect expression of major immediate early genes.

(A) Expression of ATRX in Ctrl and Atrx^{Nestin}-cKO 10 DIV cultured E16.5 neurons before and after stimulation. (B) Expression of *c-Fos*, *Junb*, *Egr1*, *Arc*, *Npas4*, and *Gadd45g* in Ctrl and Atrx^{Nestin}-cKO cultured neurons before and after stimulation by potassium chloride (KCl).

Appendix B Permission to reproduce previously published work

The data and associated text in Chapter 2, sections 2.3.1-2.3.6 represent previously published data:

i

Tamming, R.J., Siu, J.R., Jiang, Y., Prado, M.A.M., Beier, F., and Berube, N.G. (2017) Mosaic inactivation of Atrx in the central nervous system causes memory deficits. Disease Models & Mechanisms: doi: 10.1242/dmm.027482.

The material is re-used here in accordance with the policy of *Disease Models and Mechanisms* CC-BY copyright provided that the source is attributed by citing doi.

Curriculum Vitae

Name:	Renee Tamming
Post-secondary Education and Degrees:	**The** University of Western Ontario London, Ontario, Canada 2009-2013 B.M.Sc. The University of Western Ontario London, Ontario, Canada 2013-2019 Ph.D.
Honours and Awards:	Province of Ontario Graduate Scholarship 2017 (Declined) Joshua & Jonathan Graduate Research Scholarship 2017 Western Graduate Research Scholarship 2013-2017 Paediatrics Research Scholarship 2015
Related Work Experience	Teaching Assistant The University of Western Ontario Biochemistry 4463G 2017 Biochemistry 4450A 2017

Publications:

Tamming, R.J., Siu, J.R., Jiang, Y., Prado, M.A.M., Beier, F., and Berube, N.G. (2017) Mosaic inactivation of Atrx in the central nervous system causes memory deficits. Disease Models & Mechanisms: doi: 10.1242/dmm.027482.

Tamming, R.J., Dumeaux, V., Langlois, L., Ellegood, J., Qiu, L.R., Jian, Y., Lerch, J.P., Berube, N.G. (2019) *Atrx* deletion in neurons leads to sexually-dimorphic dysregulation of miR-137 and spatial learning and memory deficits. In review, Cell Reports: doi: https://doi.org/10.1101/606442.